Pulvinar And Its Projections To Early Visual Cortical Areas In Primate

by

Keji Li

Dissertation

Submitted to the Faculty of the

Graduate School of Vanderbilt University

in partial fulfillment of the requirements

for the degree of

Doctor of Philosophy

in

Psychology

August, 2015

Nashville, Tennessee

Approved:

Vivien A. Casagrande, Ph.D.
Jon H. Kaas, Ph.D.
Anna W. Roe, Ph.D.
Mark T. Wallace, Ph.D.

ACKNOWLEDGEMENTS

Thanks to the institutions and grants that have supported my research: The Vanderbilt Vision Research Center, The Vanderbilt Brain Institute, The Vanderbilt Department of Psychology, The VUMC Cell Imaging Shared Resource, R01 EY01778, R01 EY008126, MH64913, EY007135, and HD15052.

Thanks to my mentor, Vivien Casagrande, for the support, for the experience and wisdom you imparted, for having my back and most of all for teaching me to be a scientist. It has been an honor to be your student.

Thanks to my committee: Jon Kaas, Anna Roe, and Mark Wallace for the frank critiques of my work and wise counsel on how to improve.

Thanks to my undergraduate mentor, Tiande Shou for leading me into the research of neuroscience.

Thanks to my lab manager, Julia Mavity-Hudson, for help with everything and thanks for making the lab a nice place to work in.

Thanks to my dear lab members: Ilya Khaytin, Gopathy Purushothaman, Roan Marion, Yaoguang Jiang, Brandon Moore and Dmitry Yampolsky for advice given and techniques taught, for nights worked, papers discussed and for cheering me up when life is hard.

Thanks to the undergrads who worked and studied with me: Samuel Budoff, Cesar Vargas, Jay Patel, Weston Eberbach, and Tara Welytok for experiments worked, slides mounted and data dutifully analysed.

Thanks to staff members past and present: Marie Rodriguez, Mary Feurtado, Mary Dawes, Maria Vinogradova and Janice Williams for many many questions answered and your great help with my experiments.

And finally, thanks to my loving parents, Ming Li and Yiping Gu, for being my role models and making me who I am today.

TABLE OF CONTENTS

Page

1. ACKNOWLEDGEMENTS....ii
2. LIST OF TABLES....vi
3. LIST OF FIGURES....vii

Chapter

1. Introduction....1
References....3

2. A visual hierarchy in primate pulvinar....5
Traditional subdivisions....5
Major subdivisions....5
Inferior (PI) and ventral lateral (PLvl) pulvinar....6
Dorsal lateral (PLda/PLdp) and medial pulvinar (PM)....6
Summary....8
Connections and functions of pulvinar subdivisions....10
Lateral maps....10
Medial inferior areas....14
PLdp, posterior dorsal PL....15
PLda, anterior dorsal PL....15
PLd/LP....16
PM....16
The general organization....17
Reference for connection table....19
Output of the pulvinar....19
Input to the pulvinar....21
References....24
Notes on prosimian pulvinar....30
References for notes on prosimian pulvinar....32

3. Retinotopic maps in the pulvinar of bush baby (*Otolemur garnettii*)....33
Introduction....33
Methods....34
Animal Preparation....34
Recording....34
Histology and Tissue Reconstruction....35
Data Analysis....37
Results....37
Architecture of the visual pulvinar....38
Visual Responses of Cells in PI and PL....40
Dorsal and Ventral Retinotopic Maps....40
The Horizontal Meridian Representation....44
The Vertical Meridian Representation....44
Overall Model....44
Receptive Field Sizes in the Dorsal and Ventral Maps....50

Area Medial to the Two Maps....50
Discussion....52
Architecture and Connections....52
Retinotopic Maps in Pulvinar and their connections with Visual Cortex....53
Prosimian and simian pulvinar....53
A New Model for Maps in Thalamic Nuclei....54
References....57

4. Pulvinar projections to V1 layer 1 in a primate....59
Introduction....59
Methods....60
Subjects....60
Surgery and Tracer Injections....60
Tissue processing and tracer visualization....61
Electron Microscopy....61
Bouton size quantification....61
Ultrastructural Analysis....62
Statistical Analysis....62
Results....62
Tracer Injections....62
Overview of the layer 1 projections from pulvinar....63
Comparison of bouton sizes in V1 and V2....68
Synapses and synaptic targets of pulvinar axons in V1 layer 1....68
Discussion....72
Axon distribution and morphology....72
Bouton Sizes....73
Anatomical Basis of pulvinar control of V1 output....73
References....75

5. The medial inferior pulvinar influences the middle temporal area (MT) output in primate....77
Introduction....77
Methods....78
Animals and Anesthesia....78
Electrophysiology....78
Receptive field mapping....78
Visual stimuli....79
Drug application....79
Histology....79
Data analysis....80
Results....80
Response properties of neurons in PIm....80
Injections in PIm....81
MT activity with PIm activation....81
MT activity after V1 inactivation....85
MT activity with PIm activation with V1 inactivation....85
Discussion....90
The impact of V1 suppression on MT activity....90
Different effects of direct and indirect pulvinar projections to MT....91
References....92

6. Summary and Conclusions.....94
The structure of primate pulvinar.....94
Pulvinar modulation of the cortex.....97
Strength and Diversity.....98
References.....100

LIST OF TABLES

Table Page

1. Output projections of the macaque pulvinar....11
2. Input to the macaque pulvinar....12
3. Antibodies Used....36

LIST OF FIGURES

Figure Page

1. Comparison of different pulvinar division schemes....9
2. Connections between pulvinar subdivisions and their cortical and subcortical targets....18
3. Chemoarchitecture of the bush baby pulvinar....39
4. Representative penetrations showing the reversals of receptive field progression....41
5. The Central and Peripheral Representation....42
6. The representation of the central-peripheral axis of the visual field....43
7. The upper and lower field representations of each of the maps....45
8. The representation of the horizontal meridian....46
9. The representation of the vertical meridian....47
10. Cross sections of the map model....48
11. Horizontal sections of the map model....49
12. Receptive field sizes vs. center eccentricity....51
13. Two types of mapping from 2D visual space to 3D brain structure....56
14. Tracer injection site in pulvinar....64
15. Pulvinar axon distribution in V1....65
16. High power confocal images of pulvinar axons in V1....66
17. High power confocal image of pulvinar axons in V2....67
18. Bouton sizes of some projections in early visual system....69
19. Example labeled pulvinar axons in V1 layer 1....70
20. Pulvinar axons in V1 target non-GABAergic profiles....71
21. Injection and recording site....82
22. MT activity increases with pulvinar activation....83
23. MT suppression with V1 blockade....86
24. MT activity decreases after pulvinar activation with V1 blockade....88
25. Comparisons of two interpretations of the parcellation of lateral pulvinar....95

CHAPTER 1

INTRODUCTION

The pulvinar is a thalamic complex heavily involved in visual processing and the integration of vision with other senses. Some progress has been made into revealing its roles in visual processing but pulvinar's exact functions are still unclear. The pulvinar is considered by some to be a higher order relay between visual cortical areas (Sherman, 2007; but see Anderson et al., 2004). It has been proposed to play important roles in attention (Petersen et al., 1987; Chalupa, 1991), both voluntary and involuntary (Van Essen, 2005), but also to respond to visual stimuli without attention (Smith et al., 2009). The pulvinar also has been proposed to act as a potential relay of saccade related motor information from the superior colliculus (SC) to the cortex (Robinson and Petersen, 1985; Robinson et al., 1986; Berman and Wurtz, 2011). Furthermore, the pulvinar strongly gates the visual information processing in the superficial layers of the primary visual cortex (V1) (Purushothaman et al., 2012). Pulvinar lesions may affect temporal discrimination and temporal binding (Arend et al., 2008), may cause spatial neglect (Wilke et al., 2010), or impair selection of targets for attention (Snow et al., 2009). Even more interesting potential functions of the pulvinar include mediating the influence of the emotional valence of visual stimuli in both visual processing and oculomotor control (West et al., 2011; Pessoa and Adolphs, 2010). Thus, the pulvinar complex has been implicated in a wide range of functions; these functions are primarily centered on vision but also include integration with other senses, as well as motor responses associated with visual guidance.

Although the pulvinar is extensively involved in the visual-related functions, there is relatively little understanding of its exact roles in vision. On the other hand, a lot has been discovered about visual processing in the cortex. The basic framework of visual processing in the cortex still follows that of a hierarchical model (Felleman and Van Essen, 1991). The idea of the sensory system working as a pipeline, streaming information through different areas and refining the information along the way, is ancient. Its modern incarnation came from the observations by Hubel and Wiesel (1965) that in cortical areas 17 (V1), 18 (V2) and 19, the higher order areas come with more complex receptive field properties. The idea of a visual hierarchy was introduced in primates (Van Essen and Maunsell, 1983) and more cortical areas were added (Felleman and Van Essen, 1991). In this scheme, information moves up and down between areas in an hierarchical order through feedforward and feedback pathways, respectively. Visual information enters the visual hierarchy at the level of V1, the root of the hierarchy. The receptive field structure of neurons, which reflect the format of visual information representation, is the simplest in the cortical areas at the bottom of this hierarchy, and takes several different (but all complex) forms in areas belonging to the different pathways in the intermediate levels of the hierarchy (Felleman and Van Essen, 1991).

The pulvinar has extensive connections with all visual cortical areas, both early and higher order, in primates. Therefore, the basic question remains: how does pulvinar fit within the hierarchical scheme so popular for representing the flow of visual information? Depending on the specific scheme used, the pulvinar can be divided into between 4 and 10 subdivisions (Gray et al., 1999; Gutierrez et al., 2000). Each of these subdivisions has different connection patterns with different visual cortical areas. Some subdivisions even have submodules with different connection patterns (Shipp, 2001, 2003). Different pulvinar subdivisions have cortical projections that focus on different parts of the cortical visual hierarchy, with some projecting to the early visual areas, some to the dorsal stream and some to the ventral stream (Kaas and Lyon, 2007; Shipp, 2003). As mentioned earlier, the projections from specific

pulvinar subdivisions to different cortical areas have been hypothesized to mediate higher order relays between cortical areas (Shipp, 2003; Sherman, 2012), synchronize cortical activity between cortical areas (Shipp, 2003; Saalmann et al., 2012), mediate conscious motion detection with V1 lesions (Barleben et al., 2014), and facilitate spatial attention (Anderson et al., 2004).

This thesis is a part of the larger effort to elucidate the role of pulvinar in visual processing. More specifically, this thesis addresses how pulvinar projections to the visual cortical areas affect the processing in those areas? In this thesis, the key focus is on pulvinar's functional influence on the early visual cortical areas, namely V1 and the middle temporal area (MT). The main aim was to determine what the effects of changing the activation level of pulvinar neuron has on the visual responses of neurons in V1 and MT, and also what the anatomical underpinnings of these effects are.

In the next chapter (chapter 2), the structure of the primate pulvinar is reviewed and a unified scheme of subdivisions is proposed. Additionally, the cortical connections and functions of individual pulvinar subdivisions is discussed. Given that a broader range of data is available for macaque monkey, chapter 2 focuses on this species. In subsequent chapters, however, the prosimian bush baby -- the species used for studies described in this thesis -- is the main focus. To provide a comparison between pulvinar data gathered in macaque monkey with that gathered in this thesis in bush baby, an appendix focusing on the organization of bush baby pulvinar has been added to chapter 2.

In the following chapter (chapter 3), a published electrophysiological study describing the two lateral retinotopic maps in the bush baby pulvinar is presented. In this chapter, the maps in bush baby also are compared and contrasted with similar maps in simian primate species. Additionally, a common pattern of lateral and medial inferior pulvinar organization in primates is proposed based on this comparison. A study partly based on the mapping in chapter 3 by this same lab was published shortly afterwards and not included in this thesis (Purushothaman et al., 2012). The study reported a strong excitatory impact of the lateral pulvinar maps on V1 visual response.

Chapter 4 considers the morphology of pulvinar projections to V1 in an effort to test several anatomical hypotheses to explain the unexpectedly strong impact of pulvinar's input to V1 output cells.

In chapter 5 the pulvinocortical projections are examined in another early visual cortical area, MT, where the functional effect of manipulating pulvinar activity on the activity of MT output cells is described.

Finally, in the last chapter, chapter 6, we summarize all of the findings and discuss their implications in regard to the larger picture of the pulvinar's functional role in mediating and modulating visual processing through the visual cortical hierarchy.

References

Anderson C, Van Essen D, Olshausen B. 2004. Directed visual attention and the dynamic control of information flow. In: Rees G, Tsotsos J, editors. Encylopedia of visual attention. Academic Press/Elsevier.

Arend I, Rafal R, Ward R. 2008. Spatial and temporal deficits are regionally dissociable in patients with pulvinar lesions. *Brain* **131**:2140–2152.

Barleben M, Stoppel C, Kaufmann J, Merkel C, Wecke T, Goertler M, Heinze H-J, Hopf J-M, Schoenfeld MA. 2014. Neural correlates of visual motion processing without awareness in patients with striate cortex and pulvinar lesions. *Human brain mapping* **36**:1585–1594.

Berman R, Wurtz R. 2011. Signals conveyed in the pulvinar pathway from superior colliculus to cortical area mT. *Journal of Neuroscience* **31**:373–384.

Chalupa L. 1991. Visual function of the pulvinar. In: The neural basis of visual function. CRC Press.

Felleman D, Van Essen D. 1991. Distributed hierarchical processing in the primate cerebral cortex. *Cerebral cortex* **1**:1–47.

Gray D, Gutierrez C, Cusick C. 1999. Neurochemical organization of inferior pulvinar complex in squirrel monkeys and macaques revealed by acetylcholinesterase histochemistry, calbindin and cat-301 immunostaining, and *wisteria floribunda* agglutinin binding. *Journal of Comparative Neurology* **409**:452–468.

Gutierrez C, Cola M, Seltzer B, Cusick C. 2000. Neurochemical and connectional organization of the dorsal pulvinar complex in monkeys. *Journal of Comparative Neurology* **419**:61–86.

Hubel D, Wiesel T. 1965. Receptive fields and functional architecture in two nonstriate visual areas (18 and 19) of the cat. *Journal of neurophysiology* **28**:229–289.

Kaas J, Lyon D. 2007. Pulvinar contributions to the dorsal and ventral streams of visual processing in primates. *Brain Research Reviews* **55**:285–296.

Pessoa L, Adolphs R. 2010. Emotion processing and the amygdala: From a'low road'to'many roads' of evaluating biological significance. *Nature Reviews Neuroscience* **11**:773–783.

Petersen S, Robinson D, Morris J. 1987. Contributions of the pulvinar to visual spatial attention. *Neuropsychologia* **25**:97–105.

Purushothaman G, Marion R, Li K, Casagrande V. 2012. Gating and control of primary visual cortex by pulvinar. *Nature Neuroscience* **15**:905–912.

Robinson D, Petersen S, Keys W. 1986. Saccade-related and visual activities in the pulvinar nuclei of the behaving rhesus monkey. *Experimental Brain Research* **62**:625–634.

Robinson D, Petersen S. 1985. Responses of pulvinar neurons to real and self-induced stimulus movement. *Brain Research* **338**:392–394.

Saalmann Y, Pinsk M, Wang L, Li X, Kastner S. 2012. The pulvinar regulates information transmission between cortical areas based on attention demands. *Science* **337**:753–756.

Sherman S. 2007. The thalamus is more than just a relay. *Current Opinion in Neurobiology* **17**:417–422.

Sherman S. 2012. Thalamocortical interactions. *Current opinion in neurobiology* **22**:575–579.

Shipp S. 2001. Corticopulvinar connections of areas v5, v4, and v3 in the macaque monkey: A dual model of retinal and cortical topographies. *Journal of Comparative Neurology* **439**:469–490.

Shipp S. 2003. The functional logic of cortico-pulvinar connections. *Philosophical Transactions of the Royal Society of London. Series B, Biological Sciences* **358**:1605–1624.

Smith A, Cotton P, Bruno A, Moutsiana C. 2009. Dissociating vision and visual attention in the human pulvinar. *Journal of Neurophysiology* **101**:917–925.

Snow J, Allen H, Rafal R, Humphreys G. 2009. Impaired attentional selection following lesions to human pulvinar: Evidence for homology between human and monkey. *Proceedings of the National Academy of Sciences* **106**:4054–4059.

Van Essen D, Maunsell J. 1983. Hierarchical organization and functional streams in the visual cortex. *Trends in neurosciences* **6**:370–375.

Van Essen D. 2005. Corticocortical and thalamocortical information flow in the primate visual system. *Progress in Brain Research* **149**:173–185.

West G, Al-Aidroos N, Susskind J, Pratt J. 2011. Emotion and action: The effect of fear on saccadic performance. *Experimental Brain Research* **209**:153–158.
Wilke M, Turchi J, Smith K, Mishkin M, Leopold D. 2010. Pulvinar inactivation disrupts selection of movement plans. *Journal of Neuroscience* **30**:8650–8659.

CHAPTER 2

A VISUAL HIERARCHY IN PRIMATE PULVINAR

In this background chapter we will focus on the structure of primate pulvinar and its connections with the cortex. We will primarily use the macaque monkey as the animal model, since macaque pulvinar is the most well-studied among primate species. Several models have been proposed for the ventral part of pulvinar, the part responsive to simple visual functions. A certain level of consensus has been reached in the organization of this area (Adams et al., 2000), and we will briefly compare the different models and discuss the consensus. Fewer studies have been done on the structure of the dorsal half of macaque pulvinar, but several attempts at a potential model have been made based on limited chemoarchitectonic information and connection patterns with various cortical areas. We will propose a tentative scheme of pulvinar subdivisions mainly based on electrophysiological and chemoarchitectonic literature. Through discussion of the respective connection patterns and functions of these subdivisions, we will confirm and extend an old hypothesis on pulvinar organizational logic: the pulvinar mirrors the information flow in a visual hierarchy proposed for the cortex (Felleman and Van Essen, 1991; Benevento and Davis, 1977; Dick et al., 1991).

Traditional subdivisions

Major subdivisions

The early subdivision schemes of the pulvinar were mainly based on architectonic features such as cell composition and fiber patterns (Olszewski, 1952). The pulvinar was first partitioned into 3 subdivisions, the lateral (PL), medial (PM) and inferior (PI) pulvinar (Figure 1A) (Walker, 1938). Later, oral or anterior pulvinar (PA) was included in pulvinar (Olszewski, 1952). PA lies at the rostral end of pulvinar, forming a small anterior protrusion. Its architectonic borders have not been clearly established (Olszewski, 1952). PA, however, has been implicated more in the processing of somatosensory information and will not be considered in this review, which is focused on visual processing. PL occupies the lateral portion of the pulvinar and features prominent fiber bundles running horizontally. PM includes the dorso-medial portion that is only lightly penetrated by fiber bundles. Compared to PL, PM is a more homogeneous structure, featuring evenly distributed and tightly packed cells (Olszewski, 1952).

On the ventral side, PI is wrapped dorsally and medially by the brachium of superior colliculus (brSC), separating it from both the dorsal portions of the pulvinar and the medial geniculate complex (MGC), limitans, and the posterior nucleus (Po). PI has mostly small, closely packed cells that stain darkly for Nissl, but also contains scattered large cells that stain particularly well for the calcium-binding protein calbindin (Cusick et al., 1993). The fiber rich PL extends below brSC at a relatively rostral level, wrapping around PI at lateral, ventral and posterior ends (Walker, 1938). In some studies all parts of pulvinar that are below and anterior to brSC are considered part of PI following Olszewski (1952). In this review we use PI in the more strict sense and consider the fiber-rich lateral area below brSC as a ventral part of PL (PLvl).

Inferior (PI) and ventral lateral (PLvl) pulvinar

PI is usually further divided into four parts. With immunostaining for calbindin, four differentially stained bands can be observed in macaque monkey PI: a calbindin-poor hole on the medial side, two dark regions on its medial and lateral borders, and an additional calbindin-light region on the lateral side. The lateral calbindin light region is shared between PL and PI. When stained for cytochrome oxidase (CO), the PI portion has sometimes been reported as slightly darker than the PL portion (Stepniewska and Kaas, 1997). In this way four subdivisions were defined in PI: posterior (PIp), medial (PIm), central medial (PIcm) and central lateral (PIcl) inferior pulvinar, from medial to lateral, with PLvl on the lateral border (Figure 1B) (Stepniewska and Kaas, 1997). In studies where the entire portion below brSC is considered PI, PIcl and PLvl were considered one unit and named PIl, and central PI (PIc) was used to refer to PIcm in the above scheme (Gutierrez et al., 1995). Staining for parvalbumin mostly complements the calbindin staining pattern (Stepniewska and Kaas, 1997). Additionally, in some reports, a shell region on the ventral lateral border of pulvinar (PL-s) can be identified by thick fiber bundles, as well as calbindin stained axons running parallel to the lateral surface (Gutierrez et al., 1995; Adams et al., 2000).

Multiple visuotopic maps exist in the ventral lateral and inferior pulvinar. Three visuotopic maps, P1, P2 and P3, were identified based on three distinct reciprocal connections between pulvinar and the middle temporal area (MT) (Ungerleider et al., 1984). P1 and P2 are highly topographical in their connections with MT (Ungerleider et al., 1984). P1 occupies PIcl and the medial part of PLvl, with a foveal representation on its rostro-dorso-lateral border, a ventro-lateral upper visual field and dorso-medial lower visual field representation. At the anterior end of PI/PL, on the P1 map is present. P2 lies lateral to the first map, wrapping around at its ventral, posterior, dorsal borders. P2 lies entirely in PL and has an adjoined foveal and vertical meridian representation with P1. P1 and P2 connect to similar cortical and subcortical areas (Kaas and Lyon, 2007; Ungerleider et al., 2014). These two anatomically defined maps were also identified electrophysiologically (Bender, 1981). The border between the electrophysiologically defined P1 and P2 lies in PL, and lacks a consistent chemoarchitectonic signature (Adams et al., 2000), with the potential exception of P2's correlation with a myelin-rich lateral portion of PL (Bender, 1981). P3 is anteromedial to P1, and has a more diffuse connection pattern with MT. The projection from P3 to MT reflects a rough visuotopy in this area (Ungerleider et al., 1984). This projection zone also appear to coincide with the chemoarchitectonically defined PIm (Adams et al., 2000).

The existence of PL-s is not generally agreed upon, as CO, CB and acetylcholinesterase (AChE) staining of this area is not consistent between studies (Gutierrez et al., 1995; Adams et al., 2000; Gray et al., 1999; Stepniewska and Kaas, 1997; Lysakowski et al., 1986). However, converging connectional evidence does point to a small lateral shell region of PLvl that neighbors the lateral geniculate nucleus (LGN). In Lyon et al. (2010), this area was named the lateral division of PI (PIl), and was found to send strong projections to MT and to the third visual cortical area (V3). A thin area on the lateral surface of ventral PL facing LGN with distinct connection patterns was identified in several other studies. SC provides separate projections to a shell region in ventral PL (Benevento and Standage, 1983; Lysakowski et al., 1986). MT has also been found to project back to this shell region (Shipp, 2001). This relay between SC and MT was confirmed electrophysiologically in the shell region as a concentration of SC to MT relay neurons (Berman and Wurtz, 2010, 2011).

Dorsal lateral (PLda/PLdp) and medial pulvinar (PM)

Gutierrez et al. (2000) proposed a comprehensive model for subdividing the dorsal pulvinar through a combination of connection and chemoarchitecture studies. A diagram of this scheme is provided in Figure 1C. Both AChE and parvalbumin reveal a darkly stained dorsal cap of pulvinar, named dorsal PL (PLd), which also stains lightly for calbindin (Gutierrez et al., 2000). PLd only covers a small portion of the dorsal PL and PM; the rest was divided into two parts. The dorsolateral portion of PM was named by

Gutierrez et al. (2000) as the lateral medial pulvinar (PMl), and the ventromedial portion of PM was named the medial PM (PMm) (Gutierrez et al., 2000). In this model by Gutierrez et al. (2000), PMl extends laterally into traditionally defined PL. Gutierrez et al. (2000) claimed although both PMm and PMl had patches of moderate stain for AChE and parvalbumin, PMl was overall more darkly stained than PMm. Parietal and superior temporal cortical projections to the pulvinar avoid each other, forming interdigitating patches in PMl. The superior temporal cortex also projects to PMm, and a small area inside PMm, named PMm core area (PMm-c), could be identified as a small patch always avoided by temporal cortical projections (Gutierrez et al., 2000).

An AChE rich PLd subdivision has also been reported by other groups (Lysakowski et al., 1986; Cavada et al., 1995), but is sometimes considered as a part of the lateral posterior nucleus (LP). PLd coincides with a dorsal cap of PL that is devoid of SC input but receives pretectal input (Benevento and Standage, 1983). Gutierrez et al. (2000) argued that this area belongs to pulvinar because it connects to both the posterior parietal cortex and the frontal eye field, and is likely to be involved in more basic visual functions compared to the supposedly more somatosensory dominated LP nucleus. The difficulty here is that the nuclei anterior to PLd (if this is indeed a separate nucleus), LP and the posterior superior lateral posterior nucleus (VLps), also have connections with posterior parietal cortex. The areas in LP and VLps that project to the posterior parietal cortex appear to be continuous with the parietal cortex projection zones in only the PLd area, but also anterior dorsal PL and the PL/PM border (Schmahmann and Pandya, 1990; Acuna et al., 1990). There also is functional evidence that supports the inclusion of PLd in the pulvinar complex. The comparable area in cebus monkey, named caudal LP (LPc) (Gattass et al., 1978a), was shown to have cells with multisensory visual/somatosensory responses (Gattass et al., 1978b), consistent with a role in integrating vision with other sensory modalities, a role proposed of the dorsal pulvinar by many researchers (Romanski et al., 1997; Romanski, 2007; Cappe et al., 2009).

In this model proposed by Gutierrez et al. (2000), PLd has a clear border with the rest of pulvinar. The chemoarchitectonic border between PMl and PMm, however, is less clear. Both areas were patchy when stained for AChE and parvalbumin (Gutierrez et al., 2000). Although there is a trend for the dorsomedial PM to be darker with these stains, the border between subdivisions, and indeed the number of subdivisions, cannot be determined by these stains alone. The connectional evidence for distinct PMl and PMm does not support a specific border between them, or even the existence of a clear border. The central part of superior temporal gyrus (STG), including the ventral parabelt areas, receives projections from both PMl and PMm, as does the posterior parietal cortex (PPC) (Gutierrez et al., 2000). STG projecting neurons dominate in PMm while PPC projecting neurons dominate in PMl, but both types of projection zones form patches in both PMl and PMm (Gutierrez et al., 2000). The patchiness may result from injections involving multiple cortical areas, or the existence of multiple small subdivisions or modules in PM.

The dorsal part of PL and the adjacent PL/PM border is distinct from the ventral PL/PIcl areas that have well organized retinotopic maps. Chemoarchitectonically, the dorsal border of PLvl (named PIl in the original paper) can be defined by a transition of calbindin staining from a light PLvl to a dark dorsal PL (Gutierrez et al., 1995). This dorsal border of PLvl is dorsal to brSC, consistent with connectionally and electrophysiologically defined lateral maps of P1/P2 (Gray et al., 1999; Adams et al., 2000). The two visuotopic maps P1 and P2 are capped by a more dorsal medial area with rough retinotopy and more complicated responses (Bender, 1981). Petersen et al. (1985) isolated this area and named it Pdm. Cells in this area showed very large receptive fields, covert attentional modulation, and longer and variable latencies (Petersen et al., 1985). This area occupies the anterior part of dorsal PL and the ventral PL/PM border, anterior to the posterior end of LGN and PIm (Figure 1D, also see definition of PLda below). Pdm shows up as a triangular area below PLd that is darkly stained for parvalbumin (Gutierrez et al., 2000). In a comparable triangular area in cebus monkey ($P_{\mu l}$ /P_{μ}), most of the neurons were found to be without robust visual response to simple visual stimuli, as contrasted to the visually responsive cells in ventral PL

(Gattass et al., 1978a; b). Further connectional evidence also supports the existence of this distinct subdivision, as we will discuss in more detail below.

The dark parvalbumin stain marking the anterior dorsal PL subdivision, however, does not extend to the posterior end of the pulvinar (Gutierrez et al., 2000). The posterior end of the dorsal PL and PL/PM border is only moderately stained for both parvalbumin and AChE (Gutierrez et al., 2000). A separate recipient zone of the superior SC was located in this area (Benevento and Standage, 1983). In fact, Rezak and Benevento (1979) divided PL into three parts, a ventral PLα that corresponds to PLvl, a posterior PLγ, and an antero-dorsal PLβ based on connection patterns. As will be discussed below, this area also has dense connections with the cortical areas in the ventral visual stream. Cells that respond to color-opponency and complex geometric shapes have also been found in dorsal PL and PL/PM border, although both anterior and posterior portions were probed and the results were not discussed separately (Benevento and Port, 1995).

Summary

There is ample evidence for several different sub-nuclei within the pulvinar, but also varying levels of dispute surrounding the number and organization of subdivisions. The three divisions of the medial inferior pulvinar (PIm, PIp and PIcm) are well supported by clear chemoarchitectonic features and connection patterns. The structure of PM and dorsal PL, on the other hand, has not been well studied, and what information is available is hampered by the complicated electrophysiological responses of cells in these areas and the lack of proper immuno-markers. Small areas like PL-s also pose technical difficulties as they are hard to access in electrophysiological and connectional studies. Keeping these difficulties in mind, we can still propose a single set of divisions for macaque pulvinar for the sake of clarity. This subdivision scheme is diagrammed in Figure 1D.

This set of divisions is based primarily on the schemes of Stepniewska and Kaas (1997) for the ventral pulvinar, and Gutierrez et al. (2000) for the dorsal pulvinar. Here we describe the divisions within the framework of the traditional macaque pulvinar areas, namely, PL, PI, and PM (Walker, 1938). The only exception to this rule is the proposal that the PL/PM border be moved medially to allow two areas to exist lateral to this border. PI can be divided into 4 parts, PIp, PIm, PIcm, PIcl, as proposed by Stepniewska and Kaas (1997). All four subdivisions extend slightly dorsal to brSC based on their respective chemoarchitectonic borders. The traditional PL can be divided into 5 parts. The shell region neighboring LGN is named PL-s, but does not show up at the most anterior-posterior levels of the pulvinar. PLvl encompasses all ventral PL areas outside of PL-s. PIcl and PLvl jointly cover the area occupied by the two lateral retinotopic maps (Adams et al., 2000). The dorsal border of PIcl and PLvl is thus defined by the dorsal end of these retinotopic maps. We keep the AChE rich cap at the dorsal end of the pulvinar, named PLd by Gutierrez et al. (2000), as a separate area. PLd extends into the traditional PM subdivision. We combine the part of PL that is dorsal to PLvl and ventral to PLd with its neighboring PL/PM border, and divide it into two areas: anterior dorsal PL (PLda), and posterior dorsal PL (PLdp). Tentatively, PLda is defined as the parvalbumin rich wedge on the anterior PL/PM border, neighboring PA anteriorly.

PM lacks clear chemoarchitectonic borders. Furthermore, PM projection zones to various cortical areas often overlap with each other (Romanski et al., 1997; Cappe et al., 2009; Rovo et al., 2012). In the following discussion, we will refer to the central parvalbumin/AChE light region as central PM (PMc), and the AChE dark area surrounding it dorsal (PMd), medial (PMm) and ventral (PMv) PM. Note that PMm here is not the same as defined by Gutierrez et al. (2000). These names, however, should not be considered to be names of distinct functional subdivisions of the medial pulvinar until more information is obtained.

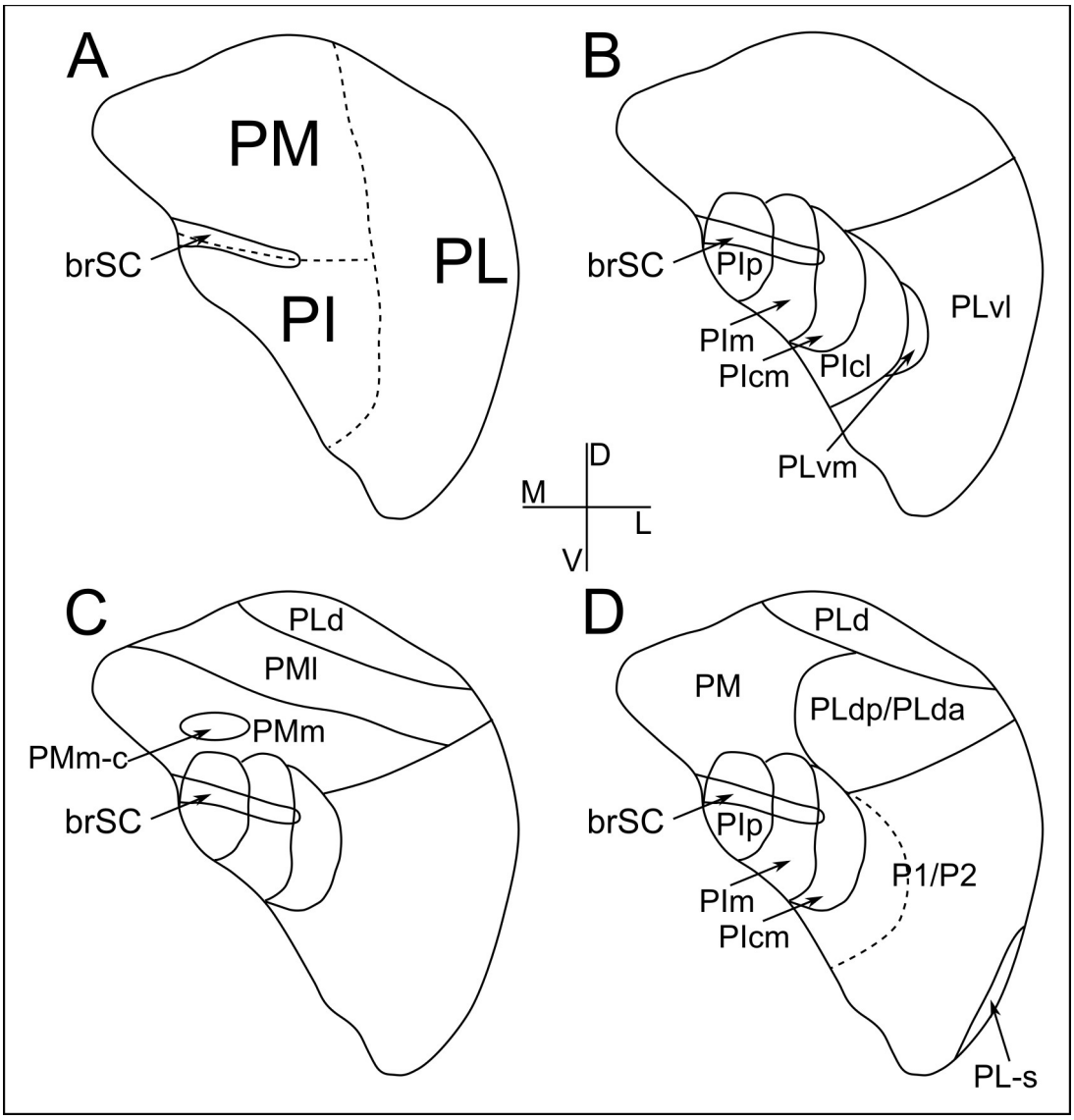

Figure 1: Comparison of different pulvinar division schemes

A-C coronal diagrams of different schemes for dividing the pulvinar. **A** pulvinar divided into the three traditional subdivisions. **B** ventral portions of the pulvinar divided according to the scheme in Adams et al., 2000. **C** dorsal portion of the pulvinar divided according to the scheme in Gutierrez et al., 2000. **D** A diagram of our proposed subdivisions of the pulvinar in the coronal plane. M: medial; D: dorsal; L: lateral; V: ventral. brSC: the brachium of superior colliculus. PM: medial pulvinar; PL: lateral pulvinar; PI: inferior pulvinar. PIp: posterior PI; PIm: medial PI; PIcm: central medial PI; PIcl: central lateral PI; PLvm: ventromedial PL; PLvl: ventrolateral PL. PLd: dorsal PL; PMl: lateral PM; PMm: medial PM; PMm-c: core region of medial PM. PL-s: shell of PL; PLdp: posterior dorsal PL; PLda: anterior dorsal PL.

Connections and functions of pulvinar subdivisions

We summarize the connections between pulvinar subdivisions and the cortical and subcortical areas of interest in Table 1 and Table 2. These connections are based on anatomical studies in macaque monkeys, as a representative of simian primates. After the tables we discuss the connections and functions of these listed pulvinar subdivisions individually.

Each row in the tables represents a brain area and each column a pulvinar subdivision. At each intersection the confidence of a one-way projection between the brain area and the pulvinar subdivision is marked. When two or more papers in macaque pulvinar support a projection the intersection is marked 'XX' to show high confidence in that projection. A single 'X' marks projections that are supported by only one paper in our reference list.

Table 1 shows output of the pulvinar, pulvinar projections to subcortical and cortical targets. Table 2 shows input of the pulvinar, including projections from the cortex to the pulvinar, and those from SC and the retina to the pulvinar. At the end of this chapter we provide a list of the papers referenced in the tables.

The connection patterns of the two lateral retinotopic maps are very similar. Different projections from these two maps have only been reported occasionally in prosimian bush babies (Glendenning et al., 1975; Raczkowski and Diamond, 1980; Wong et al., 2009). Therefore we combined the connections from the two maps, P1 and P2, in our tables for the sake of brevity. The dorsal cap region PLd has been considered a posterior extension of LP in some reports. At anterior-posterior levels where PL is present, we consider the dorsal area labeled LP in these reports as PLd. The corresponding column in the tables is named PLd/LP to reflect this nomenclature issue, as well as the difficulty in identifying an anterior border of PLd. Since it is often difficult to find correspondence between pulvinar subdivisions or cortical areas in macaque monkey and other primates, we restricted the tables to macaque, but discuss areas of correspondence in other primate species at the end of this chapter.

We also included the anterior pulvinar and the medial dorsal nuclei in the table, although we do not consider them a part of pulvinar in this chapter. Their cortical connections, however, closely mimic the pulvinar subdivisions neighboring them. The relationship that the dorsal pulvinar has with various neighboring thalamic nuclei suggests that the dorsal pulvinar may not only work with ventral part of pulvinar that focuses on visual processing, but also sensory information flow of other modalities.

Lateral maps

As mentioned earlier, PLvl and PIcl contain the two lateral anatomically defined retinotopic maps that Ungerleider et al. (1984) referred to as P1 and P2. These maps appear to correspond, at least in part, to the electrophysiologically identified inferior and lateral maps reported by Bender (1981) and Adams et al. (2000). These well-organized retinotopic maps are the main features that are evident in the ventral lateral part of the pulvinar. For simple visual stimuli, such as light spots and bars, P1 contains more responsive cells (90%) than P2 (74%) (Petersen et al., 1985). Receptive field sizes in P1 and P2 increase with eccentricity (Bender, 1982; Petersen et al., 1985; Berman and Wurtz, 2010; Li et al., 2013). For a given eccentricity the receptive fields of P1 and P2 are similar in size and somewhat larger than V1 receptive fields (Bender, 1982; Debruyn et al., 1993; Li et al., 2013; Petersen et al., 1985). Most cells in P1/P2 appear to be binocular with a minority of monocular cells (Bender, 1982; Li et al., 2013). These maps also have many cells that are selective for the orientation or direction of visual stimuli (Bender, 1982; Mathers and Rapisardi, 1973; Petersen et al., 1985; Robinson and Petersen, 1985).

	pulvinar subdivision	PI			PL					PM				PA	MD
brain area		PIp	PIm	PIcm	P1/P2	PLdp	PLda	PLd/LP	PL-s	PMd	PMm	PMv	PMc	PA	MD
subcortical	retina														
	superficial SC	x	x	x											
	deep SC														
occipital	V1		x	xx	xx										
	V2		x		xx										
ventral stream	V3/V4/DL	xx	xx	xx	xx	xx		x					x		
	TEO			x	xx	x									
	TE/TA				x	xx					xx	xx	xx		
dorsal stream	MT	x	xx	xx	x				xx						
	FST, MST		x	x			x								
	parietal						xx	xx		xx		x	xx	xx	x
other areas	belt/parabelt						x			x	xx	xx			
	frontal						x	x		xx	xx	xx	xx	x	xx
	posterior cingulate									xx	x				
	orbital frontal									x	xx	x	x		

Table 1: Output projections of the macaque pulvinar.

The projections from the pulvinar to SC and the retina, as well as those from the pulvinar to various cortical areas, are summarized. 'XX' shows projections confirmed in two or more studies and 'X' shows projections shown only once. SC superficial and SC deep are divided at the base of stratum opticum (SO). V3 and V4 are lumped together because many studies either did not differentiate them, or had injections that covered both. We also included studies for dorsal lateral cortical areas (DLc and DLr) and studies for central lateral area 19 in the row for V3/V4. We use 'frontal areas' in this table to mean areas 8a, 45 and 46, involving the frontal eye field (FEF) and other premotor areas. PI: inferior pulvinar; PIp: posterior PI; PIm: medial PI; PIcm: central medial PI; PL: lateral pulvinar; P1/P2: pulvinar retinotopic maps number 1 and 2, coextends central lateral PI (PIcl) and ventral lateral PL (PLvl); PLdp: posterior dorsal PL; PLda: anterior dorsal PL; PLd: dorsal cap of PL; LP: lateral posterior nucleus; PM: medial pulvinar; PMd: dorsal side of PM; PMm: medial side of PM; PMv: ventral side of PM; PMc: central part of PM; PA: anterior pulvinar; MD: the medial dorsal thalamic nucleus. TEO: posterior inferior temporal cortex; TE: anterior inferior temporal cortex; TA: anterior superior temporal cortex; MST: medial superior temporal area; FST: fundus of the superior temporal area. Other abbreviations see text above.

	pulvinar subdivision	PI			PL					PM				PA	MD
brain area		PIp	PIm	PIcm	P1/P2	PLdp	PLda	PLd/LP	PL-s	PMd	PMm	PMv	PMc	PA	MD
subcortical	retina	xx	xx									x			
	superficial SC	xx	xx	xx	xx				x						
	deep SC					xx				xx				x	
occipital	V1		xx		xx										
	V2				xx										
ventral stream	V3/V4/DL		x		xx	xx									
	TEO		x		xx	xx									
	TE/TA			x	xx	xx					xx		xx		
dorsal stream	MT	x	xx	x	xx	x			xx						
	FST, MST		xx		x										
	parietal						xx	xx		xx		x	x	xx	
other areas	belt/parabelt						x			x	x	x			
	frontal						x	x		x	xx		x		xx
	posterior cingulate	x	x					x		xx	x		xx		
	orbital frontal										xx				x

Table 2: Input to the macaque pulvinar.

The projections from the cortical areas to the pulvinar, as well as those from SC and the retina, are summarized. Conventions are the same as in Table 1.

These lateral maps have reciprocal connections with almost all visual cortical areas. Not only are they connected with the early visual cortices such as V1, V2 and MT, but with all of the cortical areas in the ventral stream including the anterior pole of the temporal cortex. The lateral maps also receive projections from MT, MST and FST but the organization of projections from P1 and P2 to these cortical areas remains less clear. It is likely that these dorsal stream areas receive their main pulvinar input from the medial inferior subdivisions (P3), but project back to the lateral maps (P1/P2), reflecting an integration of information between the dorsal and ventral streams in P1/P2. The superficial layers of SC also project to the lateral maps, providing an alternative source of visual information besides V1 and downstream cortical areas.

The retinotopic organization of the maps, however, does not do justice to the complex organization of the lateral pulvinar. Shipp (2003) argued for different functional submodules within the lateral pulvinar maps in macaque. In both pulvinar maps in PLvl and PIcl, the visual field is represented similarly on each sheet cut with an angle to the coronal plane. As a result, each point in the visual field is represented by a line of neurons in the pulvinar maps. These 'iso-representation lines' run roughly anterolateral-posteromedially (Bender, 1981). Based on the results of tracer injections into V1, V2, V3, V4 and MT, Shipp (2001) argued that V1-V4 all have their connections with P1/P2, but their projection zones are offset along the iso-representation axis, and ordered by their position on the visual hierarchy. The projection zones of MT, although partially overlapping with those of V1, are proposed to be displaced in a direction orthogonal to the iso-representation lines (Shipp, 2003). This arrangement would allow the P1/P2 maps to relay visual information along the ventral visual stream with dedicated portions of PLvl and PIcl that only partially overlap.

A recent study suggested that the P1/P2 maps work to facilitate the interaction between cortical visual areas (Saalmann et al., 2012). The wide array of connections that P1 and P2 have with cortical areas is consistent with such a role. In awake macaque monkeys, Saalmann et al. (2012) made simultaneous low frequency potential (LFP) recordings from V4, TEO, and the ventral lateral pulvinar. The animals were instructed to perform a task that required attending to a target after a cue and a delay. While the animals were attending to targets, there was an increase in the alpha band frequencies of the cross correlogram between the LFP of every pairwise combination of the three recorded areas. Further, there was an increase in the alpha band frequencies of the cross correlogram between the spikes in the PLvl and the LFPs in V4 and TEO. Finally, it was found based on Granger causality analysis that pulvinar activity caused enhanced synchrony between TEO and V4. The same causality was not found between V4 and PLvl/TEO, or between TEO and PLvl/V4 (Saalmann et al., 2012). Therefore, PLvl appeared to synchronize the activity in TEO and V4, but not the other way around.

With the exception of area V1, projections from pulvinar to all visual areas end densely in layers 3/4 with a few collaterals in layer 1 (Benevento and Rezak, 1976). This projection pattern has been considered to be the hallmark of feedforward driving projections (Felleman and Van Essen, 1991). Unlike extrastriate areas, pulvinar axons from PL and PI to V1 end in the superficial layers primarily in layer 1 (Carey et al., 1979; Ogren and Hendrickson, 1976; Rezak and Benevento, 1979; Marion et al., 2013). The lateral maps receive from cortical layers 5a and 6b (Conley and Raczkowski, 1990; Lund et al., 1975). From the model of Shipp (2003), this projection pattern is compatible with an area simultaneously relaying between neighboring visual areas in the hierarchy starting with V1. Thus the P1/P2 maps receive driving projection from all these visual areas, but also drive all these areas except for V1, because V1 is at the root of the cortical hierarchy (Felleman and Van Essen, 1991) and P1/P2 only relays between cortical visual areas.

Despite that fact that P1/P2 projections to V1 do not show driving characteristics, a recent report demonstrated that a net inhibition in V1 occurred following lateral pulvinar inactivation (Purushothaman et al., 2012). This net inhibition in layer 2/3 pyramidal cells was greatest at their preferred orientation, resulting in greater suppression of their responses below baseline firing rate at the preferred orientation while mismatches between retinotopic locals could cause either enhancement or suppression depending

on the arrangement (Purushothaman et al., 2012). This result suggests a bigger role of pulvinar lateral maps beyond visual information relay, as their modulatory projections also appeared to have major functional roles.

Medial inferior areas

As described above, the medial inferior pulvinar consists of PIcm, PIm and PIp. They provide input to V1, V4, and MT, but do not appear to interact with other areas in the ventral stream or dorsal stream. All three of these medial inferior pulvinar subnuclei appear to have different connection patterns, although the small size of PIp poses problems for connectional studies. Compared to PIcm, PIm receives more input, such as from V1 and FST/MST. These additional inputs may have to do with PIm's role in providing heavy input to MT (Stepniewska et al., 2000). Just as described for the ventral lateral pulvinar areas P1/P2, more pulvinar subdivisions appear to receive from more cortical areas than the cortical areas they project to. For example, all three subnuclei of medial PI receive clear V4 projections, but do not seem to project back to V4.

As mentioned above, P3 as defined by Ungerleider et al. (1984) is likely to be the same as PIm despite some controversies based on its connection patterns. Cusick et al. (1993) argued that PIm could be considered a 'core' nucleus, with PIp and PIcm serving as 'matrix' nuclei, as defined in Jones (1998). Jones (1998) defined a thalamic "core" nucleus as the nucleus that sends the main message to layer 4 of a cortical area, with "matrix" nuclei sending a more diffuse, presumably modulatory, projection to the superficial layers of the cortex. The original scheme was that SC to PIm to MT was to be the 'core' pathway while SC to PIcm/PIp to MT was to be the 'matrix' pathway. One piece of evidence in support this idea is that the majority of pulvinocortical projections land in layer 4 of the cortex, except for the projections to V1 (Lund et al., 1981; Ogren and Hendrickson, 1977; Rockland et al., 1999; Benevento and Rezak, 1976; Marion et al., 2013; Livingstone and Hubel, 1982; Trojanowski and Jacobson, 1976; Baleydier and Mauguiere, 1985). These projections to cortical layer 4 are, by the definition of Jones (1998), core projections. Other aspects of the anatomy of these pathways, however, do not support the original hypothesis. For example, it was demonstrated that PIm doesn't receive the majority of SC input in the pulvinar (Stepniewska et al., 1999; but see Lyon et al., 2010), contrary to what we would expect from a 'core' or 'lemniscal' pathway, which directly relay peripheral sensory input. On the other hand, PIcm does serve as a connectional (Stepniewska et al., 1999) and functional (Berman and Wurtz, 2010) relay between SC and MT, while PIm provides the major pulvinar projections to MT (Stepniewska et al., 1999). We also know that the PIcm relay to MT does not supply directional preference information to MT (Berman and Wurtz, 2011). Other 'core' and 'matrix' relay pairs can have separate inputs, as in MGC (Jones, 1998). A 'core'/'matrix' relation with different sources of input for PIm and PIcm/PIp, with LGN to V1 (or retina (O'Brien et al., 2001) to PIm) being the core pathway and SC to PIcm being the matrix pathway to MT, loosely defined, is still possible. In this scheme, the P3 map is not a single visuotopic nucleus but a subdivision made up of 2 or 3 closely related nuclei.

It has been suggested that following a V1 lesion, visual signals conveyed via SC and P3 might be responsible for the residual visual responses observed in MT, as well as the consequent visually guided behavior, which occurs without conscious visual perception, and is named blind sight (Rodman et al., 1989, 1990; Kaas, 2015; Leopold, 2012). As discussed above, there does not appear to be a direct relay from SC to MT through PIm. On one hand, PIcm and PIp may work as the relay instead of PIm (Stepniewska et al., 2000; Lyon et al., 2010; Berman and Wurtz, 2010; Kaas, 2015). On the other hand, LGN directly projects to MT via its koniocellular (K) neurons, and appears essential for blind sight (Schmid et al., 2010). Both PIp and PIm receive retinal input, and these retinal axons synapse directly on MT projecting cells in the pulvinar (Itaya and Van Hoesen, 1983; O'Brien et al., 2001; Cowey et al., 1994; Mizuno et al., 1982); however, these projections were minor outside of neonatal animals and animals with early V1 lesions (Warner et al., 2010; Kaas, 2015).

PLdp, posterior dorsal PL

PLdp shares reciprocal connections with V4, TEO and TE. Therefore it appears to be heavily involved in the ventral visual stream and its associated role of object recognition. This area also receives inputs from deep SC, raising an interesting question of what kind of multisensory information is needed for the computations in the ventral stream.

Several functional studies that discovered interesting response properties in the pulvinar have focused on this area. In one study, pulvinar neurons were tested with various face-like visual stimuli (Nguyen et al., 2013). On a population level, the pulvinar neurons showed differential responses between real faces, face-like cartoons, eyes and non-face pictures (Nguyen et al., 2013). Recorded neurons in this study were mostly found in PLdp, with some in P1/P2 and a few in PLda, P3 and ventral PM. The ability to distinguish between different types of complex visual stimuli is most likely attributable to PLdp neurons.

Komura et al. (2013) identified neurons in dorsal PL with activity correlated to the animals' confidence in a task to find the direction of a random dot motion. These confidence signaling cells showed similar responses regardless of the direction of motion, and only decreased in firing rate when the stimulus had low coherence and the animal was hesitant to answer (Komura et al., 2013). When the animal was given the choice to give up, more drop-outs were observed when these confidence neurons fired less. Furthermore, increased drop-outs were triggered by artificially silencing these areas in the pulvinar (Komura et al., 2013). The confidence signaling neurons were concentrated in posterior dorsal PL, which is also the area where local inhibition was effective at making animals give up (Komura et al., 2013). This study also defined a clear border between the dorsal PL and PLvl at posterior levels, as few confidence signaling neurons were found in ventral PL. This border is roughly consistent with a dorsal border of P1/P2 (Komura et al., 2013; Adams et al., 2000).

Benevento and Port (1995) made penetrations on the PL/PM border and found almost all visually responsive neurons to be selective to either color opponency or simple shapes, half of them selective to both. Unfortunately, the authors did not indicate at what anterior-posterior level in the pulvinar they found these neurons. Given that PLdp connects to ventral stream areas while PLda connects to the dorsal stream, we would predict that neurons in PLdp are more likely to display shape selective visual response properties.

PLda, anterior dorsal PL

The anterior dorsal PL is reciprocally connected with parietal cortical areas, as well as FEF and the auditory parabelt. With these connections, PLda appears to be a perfect place to coordinate orienting and spatial attention. As discussed above, this area indeed has been reported to have neurons with both covert attentional modulation and presaccadic activation, as contrasted with P1/P2 neurons that only showed presaccadic modulation when a saccade was actually made towards their receptive fields (Petersen et al., 1985). Thus, this area has been implicated in spatial attention and saccade control (Robinson and Petersen, 1985; Robinson et al., 1986).

The functional roles of PLda in orienting and attention have been studied using reversible blocking agents. Animals with PLda blockaded with a GABAa agonist showed attention biased to the ipsilesional side (Petersen et al., 1987; Wilke et al., 2010). In a saccade based cued reaction time task, monkeys made slower saccades to validly cued contralesional targets and faster saccades to invalidly cued ipsilesional targets. In other words, the animals were worse at following correct cues and resisting incorrect cues when the target was contralateral to the side of suppressed pulvinar (Petersen et al., 1987). In a more recent study these results were confirmed and the animals also showed faster saccades to ipsilesional targets, as well as a bias to saccade to the ipsilesional target when targets appeared on both hemifields

(Wilke et al., 2010). In addition, the use of upper limbs appeared to be hampered by the blockade of PLda, consistent with problems with the sensory motor transformation (Wilke et al., 2010).

The attention related visual processing in PLda not only follows a spatial framework, but also an object centered relative framework. In a human patient with a small lesion in the central portion of anterior dorsal pulvinar, performance in a visual search task was not only affected for target in the lower left quadrant of the visual field, but also the lower left element of search arrays presented anywhere in the visual field (Ward and Arend, 2007). The deficit demonstrated following a lesion to areas in the vicinity of PLda appeared to be in spatial processing (Ward and Arend, 2007).

Above, we have discussed various studies that find different connection patterns, response properties and functional roles for the anterior and posterior parts of the dorsal PL. When interpreting these results, however, we have to bear in mind that PLda and PLdp does not appear to have a clear border. Rather, a structure similar to that of P1/P2 maps in the more ventral parts of PL may also exist in dorsal PL where the posterior parietal projections of PLda are gradually replaced by ventral stream connections of PLdp. To determine the exact structure of dorsal PL, a study with multiple tracer injections in various parietal and inferior temporal areas, as well as careful reconstruction of the dorsal lateral pulvinar will be needed.

PLd/LP

The dorsal cap of PL, PLd, reciprocally connects with various parietal cortical areas. This connection pattern is similar to that of the areas neighboring PLd, in particular PA and LP. Additionally, this dorsal cap region is the only part of pulvinar receiving input from the pretectum, suggesting at a visuomotor related function of PLd (Benevento and Standage, 1983). Despite pretectum's lack of cholinergic neurons, its projection zone in the pulvinar is AChE positive (Lysakowski et al., 1986). This heavy AChE expression found in the PLd region may indicate an overlap between pretectum projections and projections from cholinergic nuclei such as the dorsolateral tegmental nucleus, the pedunculopontine tegmental nucleus, and the parabigeminal nucleus (Lysakowski et al., 1986), although the parabigeminal nucleus has been reported to project to the P1/P2 maps and not to the dorsal cap of PL (Diamond et al., 1992). The anterior border between PLd and LP is not clear. PLd is a distinct subdivision from LP since it appears to have different projection patterns to areas in the parietal cortex (Gutierrez et al., 2000). PLd connects with the posterior parietal cortex while LP connects with area 5 located in the anterior parietal cortex (Pons and Kaas, 1985; Yeterian and Pandya, 1985). It is interesting to note that PMd and PLd connect with parietal areas (caudal inferior parietal lobule (PG) and caudalmost cingulate sulcus (PEci), respectively) that are higher in the somatosensory hierarchy (Pandya and Seltzer, 1982) than areas that connect with LP and PA (superior parietal lobule (PE) and caudal superior parietal lobule (PEc)). In other words, the lower order somatosensory areas connect with thalamic nuclei near the pulvinar that specialize in that sensory modality, while higher order somatosensory areas connect with pulvinar subdivisions that have inputs from multiple sensory processing streams.

PM

As discussed above, there does not appear to be discrete subdivision within PM and we only refer to areas within PM by their relative locations. The projection pattern of PM is consistent with this lack of solid subdivisions. The projection zones to various areas heavily overlap, but are also displaced from one another. Besides the frontal areas involving mostly premotor regions, each group of cortical areas projects densely to only one side of PM. TE focuses on medial PM, just as parietal areas focus on dorsal PM, auditory areas ventral PM, and orbital frontal areas medial PM. In a hypothetical experiment that has multiple precise injections in various cortical areas and a precise reconstruction of PM, we would expect to see each PM connected cortical area occupying a projection zone in PM that focuses on its own corner of PM, while all of these projection zones overlap in the central part of PM.

With the limited data currently available, some basic organizational principles of PM may be inferred. Cappe et al. (2009) offered a picture of the dorsal pulvinar based on connection patterns. They injected three areas with two tracers for each area: a dorsal and a lateral injection for the premotor cortex; a rostral and a caudal injection for the auditory belt and parabelt, respectively; a dorsal and a ventral injection into the superior parietal regions of PE and the upper bank of the intraparietal sulcus (PEa). Their results agreed with the Gutierrez et al. (2000) in that the parietal cortex receives mainly from the antero-dorso-lateral part of PM, and that auditory belt and parabelt mainly receive from the postero-ventro-medial part (Cappe et al., 2009). They showed that the premotor cortex is connected to the dorso-medial area of PM, covering its dorsal surface, with some sparse connections that extend into PLd (Cappe et al., 2009). A similar connection pattern can been seen in many earlier studies (dorso-lateral pulvinar to posterior parietal cortex: Yeterian and Pandya (1985), Baleydier and Morel (1992), Morecraft et al. (1993), Cavada et al. (1995), Romanski et al. (1997), Matsuzaki et al. (2004); medial PM to premotor areas: Huerta et al. (1986), Stanton et al. (1988), Morecraft et al. (1993); and STG/STS (superior temporal sulcus) to ventral PM: Romanski et al. (1997)). Thus, the three corners of PM each relate to a different function, namely the function that is related to the neighboring thalamic nuclei outside of pulvinar. Ventral PM is physically close to the auditory complex of MGC. In fact, with posterior parabelt injection, a continuous line of labeled cells was observed that extended from MGC to ventral PM, through Po and limitans (De La Mothe et al., 2012). Antero-dorso-lateral PM is close to PLd, PA and LP, all areas related to somatosensory processing or visuo-somatosensory integration. Medial PM borders MD, which is heavily connected with prefrontal areas and related to working memory (Cappe et al., 2009), as well as the related function of motor planning (Granon and Poucet, 1995).

Of course, these are not the only types of information that are integrated in PM. TE in the ventral stream also projects to the medial PM, potentially adding object recognition information into the fray. Consistent with this connection with TE, a group of neurons in macaque PM was found to differentiate human faces (Maior et al., 2010). A minority of these cells even coded for the emotional content of human faces (Maior et al., 2010).

The general organization

Although much remains unknown, we can make the following general conclusion. Each main pulvinar area appears to have its own distinct connection patterns and functional roles. Some pulvinar subdivisions, particularly the mapped area of PL, or P1/P2, and PM, have finer internal subdivisions. Put together, however, a global pattern emerges in pulvinar's relationship with the cortex. The pulvinar has a hierarchical pattern similar to that of the cortex. The visual information flow in pulvinar roughly follows an axis that runs from its ventrolateral end to its dorsomedial end, with P1/P2 at its root. In the cortex the visual information flow follows a posterior to anterior axis (Felleman and Van Essen, 1991), with V1 at its root. This flow in the cortex is split into dorsal and ventral streams after V1, with both feeding eventually into frontal association areas. In the pulvinar, P3 subdivisions are connected with MT and surrounding cortical areas, while PLda and PLd are connected with posterior parietal areas. As such, subdivisions closely connected with the dorsal stream areas are dorsomedial to P1/P2, and are at the anterior end of the pulvinar. Similarly, both the posterior end of P1/P2 and PLdp are closely related to the ventral stream. Finally, PM, which sits at the dorsomedial end of the pulvinar, receives inputs from multiple modalities and potentially functions as a multisensory integration area. This organization is illustrated in a diagram of pulvinocortical projections in Figure 2.

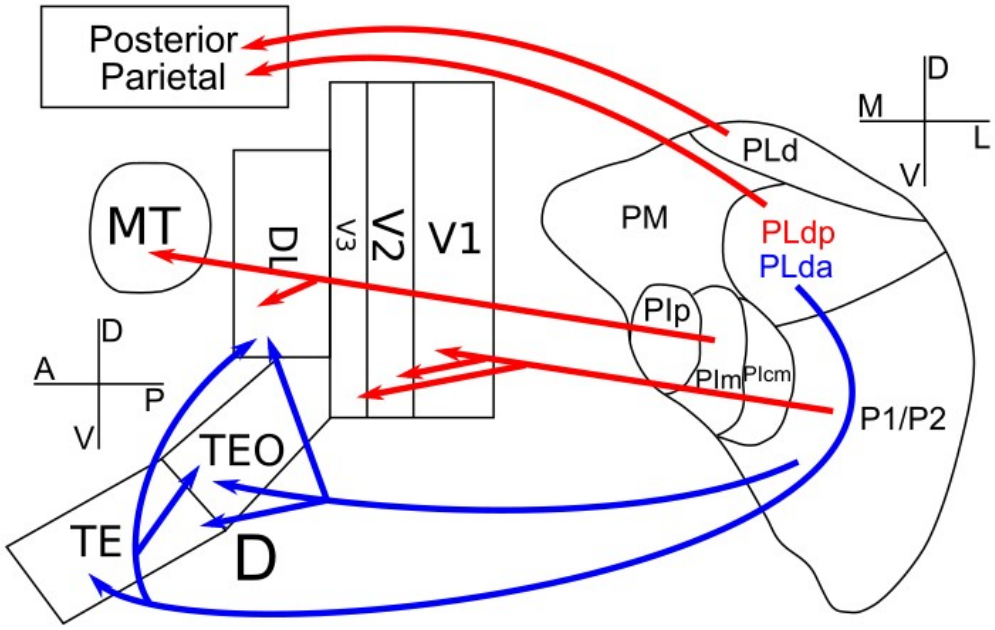

Figure 2: Connections between pulvinar subdivisions and their cortical and subcortical targets

A diagram of the pulvinar is on the right side, a diagram of the cortex is on the left side. Note the orientations are different for the two diagrams. Red letters and arrows show anterior areas and projections from anterior pulvinar subdivisions. Blue letters and arrows show posterior areas and projections from posterior pulvinar subdivisions.

The idea of a hierarchy in the pulvinar has been proposed several times before. In both macaque (Benevento and Davis, 1977) and marmoset (Dick et al., 1991), researchers have suggested that higher order visual areas connect with more dorsomedial regions in the pulvinar. However, these observations were only based on the connection patterns between the ventrolateral pulvinar and early visual cortices from V1-V3 (Benevento and Davis, 1977; Dick et al., 1991). There was no guarantee that such a hierarchy would extrapolate beyond the early visual cortices and the ventrolateral pulvinar. In this review we have expanded this hierarchy in the pulvinar, and identified the pulvinal correlates of the two visual streams in the cortex. Several other studies proposed a potential geometric correspondence between the thalamus and the cortex in general. In both rodents and primates, thalamocortical projections map the medial side of the thalamus to the anterior part of the cortex, while the lateral side of the thalamus is mapped to the posterior part of the cortex (Hohl-Abrahao and Creutzfeldt, 1991; Shipp, 2003). Adams et al. (1997) further argued that the mapping between the thalamus and the cortex, where the cardinal axes in the thalamus, the lateral-medial axis and the posterior-anterior axis, map to the posterior-anterior axis and lateral-medial axis in the cortex, respectively. The spatial transformation of this mapping coincides with the mapping between individual thalamic and cortical areas, for example, as transformation of retinotopic maps in V1 and LGN in cat and ferret (Adams et al., 1997). The mapping between this pulvinar hierarchy and the cortical visual hierarchy follows the same spatial transformation, in that the ventrolateral pulvinar maps to the posterior cortex, while the dorsomedial pulvinar maps to the anterior cortex.

This hierarchy we have identified is compatible with two previous proposal regarding the distribution of functional roles between pulvinar subdivisions. Kaas and Lyon (2007) proposed that the ventrolateral and dorsolateral portions of the pulvinar provide relays for the ventral stream, while P3 subdivisions in the medial inferior pulvinar provides relays for the dorsal stream areas. Compared the model of Kaas and Lyon (2007), our model shares the same early segments. The separation of anterior and posterior dorsal PL based on chemoarchitecture, function and connection patterns allowed us to fit the pulvinar connections to parietal areas into this pulvinar hierarchical model, and find the geometric similarity between the cortical and pulvinal hierarchies. As discussed above, Shipp (2003) identified a hierarchy within the subdivision of P1/P2 that mirrors the ventral stream hierarchy. The main pulvinar area that is connected only with the later ventral stream, PLdp, is a distinct area from P1/P2 and cannot be seen as a part of the hierarchy proposed by Shipp (2003). The hierarchy of the pulvinar subdivisions we discussed here is different from the hierarchy of submodules within a single pulvinar subdivision.

Reference for connection table

Papers referenced in making the connection tables are arranged here by connected brain area outside of pulvinar and the pulvinar subdivision involved. Although we did not use the results in connection studies for non-macaque primates when making the connection tables, we include them below for the sake of completeness. A plus sign marks studies that specifically involve the pulvinar of macaque monkeys, including studies using all macaque species, such as *macaca mulatta*, *macaca fascicularis*, *macaca fuscata*, etc.

Output of the pulvinar

- superficial SC: SGS and SO
  - PIm: +Berman and Wurtz (2011), +Berman and Wurtz (2010)
  - PIp: +Berman and Wurtz (2011), +Berman and Wurtz (2010)
  - PIcm: +Berman and Wurtz (2011), +Berman and Wurtz (2010)
- V1

    - P1/P2: Raczkowski and Diamond (1978), +Ogren and Hendrickson (1976), +Adams et al. (2000), Cooper et al. (1979), +Rezak and Benevento (1979), +Benevento and Rezak (1976), Wong et al. (2009), Dick et al. (1991), Kaske et al. (1991), +Lysakowski et al. (1988), Marion et al. (2013), Ogren and Hendrickson (1977), Soares et al. (2001), +Livingstone and Hubel (1982), +Kaas and Lyon (2007), Raczkowski and Diamond (1980)
    - P1: Wong et al. (2009)
    - PIm: Wong et al. (2009), +Lysakowski et al. (1988)
    - PIcm: +Lysakowski et al. (1988), +Kaas and Lyon (2007)
- V2
    - P1/P2: Wong et al. (2009), +Adams et al. (2000), +Benevento and Rezak (1976), Wong-Riley (1977), Dick et al. (1991), Kaske et al. (1991), +Levitt et al. (1995), +O'Brien et al. (2002), +Mizuno et al. (1983), +Lund et al. (1981), Marion et al. (2013), Ogren and Hendrickson (1977), +Rockland et al. (1999), Soares et al. (2001), +Livingstone and Hubel (1982), Kaas and Lyon (2007), +Lyon et al. (2010), Raczkowski and Diamond (1980)
    - PLdp: Dick et al. (1991)
    - PIm: +Mizuno et al. (1983)
    - PIcm: Kaas and Lyon (2007)
- V3/V4/DL
    - P1/P2: +Adams et al. (2000), +Benevento and Rezak (1976), +O'Brien et al. (2002), +Baleydier and Morel (1992), +Rockland et al. (1999), Soares et al. (2001), +Lyon et al. (2010)
    - PIcm: +Adams et al. (2000), Cusick et al. (1993), +Baleydier and Morel (1992), +Lysakowski et al. (1988), +Gray et al. (1999), +Shipp (2001)
    - PIm: +Lysakowski et al. (1988), +Lyon et al. (2010), +Shipp (2001)
    - PIp: +Adams et al. (2000), Cusick et al. (1993), +Baleydier and Morel (1992), +Gray et al. (1999)
    - PLdp: Cusick et al. (1993), +Lysakowski et al. (1988), +Lyon et al. (2010), +Gray et al. (1999)
    - PLd/LP: +Lyon et al. (2010)
    - PMc: +Lysakowski et al. (1988)
- MT
    - P1/P2: Glendenning et al. (1975), Raczkowski and Diamond (1978), Wong et al. (2009), +Adams et al. (2000), Stepniewska et al. (1999), Wong et al. (2009), Soares et al. (2001), Kaas and Lyon (2007), Raczkowski and Diamond (1980)
    - PIm: Glendenning et al. (1975), Wong et al. (2009), Lin and Kaas (1980), +Adams et al. (2000), +Berman and Wurtz (2011), +Berman and Wurtz (2010), Stepniewska et al. (1999), +Stepniewska et al. (2000), Wong et al. (2009), +O'Brien et al. (2002), Cusick et al. (1993), +Maunsell and Van Essen (1983), Standage and Benevento (1983), Kaas and Lyon (2007), +Lyon et al. (2010), Raczkowski and Diamond (1980), +Gray et al. (1999), Warner et al. (2010), +Shipp (2001)
    - PIp: +Berman and Wurtz (2011), +Berman and Wurtz (2010)
    - PIcm: +Berman and Wurtz (2011), +Berman and Wurtz (2010), +Lyon et al. (2010)
    - PL-s: +Shipp (2001), +Lyon et al. (2010), +Berman and Wurtz (2010)
- FST/MST
    - PIcm: Glendenning et al. (1975), +Adams et al. (2000)
    - PLda: +Rezak and Benevento (1979)
    - PIm: +Boussaoud et al. (1992), Kaas and Lyon (2007)
- TEO
    - P1/P2: +Benevento and Rezak (1976), +Webster et al. (1993), Steele and Weller (1993), +Baleydier and Morel (1992)
    - PIp: Steele and Weller (1993)
    - PIcm: +Webster et al. (1993)
    - PLdp: +Webster et al. (1993)
    - PMv/PMm: Steele and Weller (1993)
- TE/TA
    - PLdp: +Baizer et al. (1993), +Webster et al. (1993), +Baleydier and Morel (1992), +Yeterian and Pandya (1989)

    - P1/P2: +Webster et al. (1993)
    - PMc: +Webster et al. (1993), Steele and Weller (1993), +Trojanowski and Jacobson (1977)
    - PMv/PMm: Steele and Weller (1993), +Yeterian and Pandya (1989), +Markowitsch et al. (1985)
- belt/parabelt
    - PMm: +Hackett et al. (1998), +Cappe et al. (2009), De La Mothe et al. (2012), +Baleydier and Mauguiere (1985)
    - PMv: +Hackett et al. (1998), +Cappe et al. (2009), De La Mothe et al. (2012), +Hackett et al. (2007)
    - PMd: +Hackett et al. (1998)
    - PLda: +Hackett et al. (1998)
- PE/PEc/PF/PFG/PG
    - PLd/LP: +Rezak and Benevento (1979), +Hardy and Lynch (1992), +Acuna et al. (1990), +Cappe et al. (2009), +Matsuzaki et al. (2004)
    - PLda: +Rezak and Benevento (1979), +Baizer et al. (1993), +Acuna et al. (1990), +Matsuzaki et al. (2004), +Schmahmann and Pandya (1990), +Baleydier and Morel (1992), +Cappe et al. (2009)
    - PMd: +Baleydier and Mauguiere (1987), +Hardy and Lynch (1992), +Matsuzaki et al. (2004), +Morecraft et al. (1993), +Cavada et al. (1995)
    - PMv: sparse+Morecraft et al. (1993)
    - PMc: +Schmahmann and Pandya (1990), +Trojanowski and Jacobson (1977)
    - PMm: +Baleydier and Mauguiere (1985)
    - MD: +Acuna et al. (1990)
    - PA: +Acuna et al. (1990), +Schmahmann and Pandya (1990)
- area 1/2/3
    - PA: Cusick and Gould Iii (1990), +Pons and Kaas (1985)
- posterior cingulate, parahippocampal gyrus
    - PMd: +Baleydier and Mauguiere (1987), +Baleydier and Mauguiere (1985)
    - PMm: +Baleydier and Mauguiere (1985)
- prefrontal(FEF, 8a, 45a, 45b)
    - PMd: +Trojanowski and Jacobson (1974), +Asanuma et al. (1985), +Cappe et al. (2009), +Baleydier and Mauguiere (1985)
    - PMv: +Trojanowski and Jacobson (1974), +Asanuma et al. (1985), +Huerta et al. (1986), +Cappe et al. (2009), +Trojanowski and Jacobson (1976)
    - PMm: sparse+Morecraft et al. (1993), +Trojanowski and Jacobson (1976)
    - PMc: +Trojanowski and Jacobson (1974), +Romanski et al. (1997), +Contini et al. (2010), sparse+Trojanowski and Jacobson (1977)
    - PLda: +Huerta et al. (1986)
    - MD: +Asanuma et al. (1985), +Huerta et al. (1986), +Cappe et al. (2009), +Contini et al. (2010)
    - PLd/LP: +Cappe et al. (2009)
    - PA: sparse+Contini et al. (2010)
- orbital frontal
    - PMm: +Romanski et al. (1997), +Cavada et al. (1995), +Trojanowski and Jacobson (1976)
    - PMv: +Trojanowski and Jacobson (1976)
    - PMd: +Cavada et al. (1995)
    - PMc: +Trojanowski and Jacobson (1977)

Input to the pulvinar

- Retina
    - PIm: +Itaya and Van Hoesen (1983), +O'Brien et al. (2001), Warner et al. (2010), +Cowey et al. (1994), +Mizuno et al. (1982)
    - PIp: +O'Brien et al. (2001), +Mizuno et al. (1982)
    - PIcm: Warner et al. (2010)
    - PMv: +Itaya and Van Hoesen (1983)
- superficial SC: SGS and SO

    - PIcm: Glendenning et al. (1975), Lin and Kaas (1979), +Benevento and Rezak (1976), +Harting et al. (1980), Baldwin et al. (2013), +Berman and Wurtz (2011), +Berman and Wurtz (2010), +Lysakowski et al. (1986), Stepniewska et al. (1999), Huerta and Harting (1983), +Partlow et al. (1977), +Stepniewska et al. (2000)
    - PIp: Lin and Kaas (1979), +Benevento and Fallon (1975), +Harting et al. (1980), +Berman and Wurtz (2011), +Berman and Wurtz (2010), +Lysakowski et al. (1986), Mathers (1971), Stepniewska et al. (1999), Huerta and Harting (1983), +Stepniewska et al. (2000)
    - PIm: +Berman and Wurtz (2011), +Berman and Wurtz (2010), +Lysakowski et al. (1986), Mathers (1971)
    - PL-s: +Berman and Wurtz (2011), +Berman and Wurtz (2010)
    - Pp: Baldwin et al. (2013)
    - PLdp: Glendenning et al. (1975), +Benevento and Rezak (1976)
    - PLda: +Benevento and Rezak (1976)
    - P1/P2: +Benevento and Standage (1983), +Benevento and Rezak (1976), +Lysakowski et al. (1986), Stepniewska et al. (1999), Huerta and Harting (1983), +Lyon et al. (2010)
- deep SC: below SO
    - PMd: +Benevento and Standage (1983), +Benevento and Fallon (1975), +Lysakowski et al. (1986)
    - PLdp: +Benevento and Standage (1983), +Harting et al. (1980)
    - PA: +Benevento and Fallon (1975)
- V1
    - P1/P2: Symonds and Kaas (1978), Raczkowski and Diamond (1978), Raczkowski and Diamond (1981), Lin and Kaas (1979), +Kennedy and Bullier (1985), +Ogren and Hendrickson (1976), Conley and Raczkowski (1990), Dick et al. (1991), +Gutierrez and Cusick (1997), Hollander (1974), +Ungerleider et al. (1983), +Lund et al. (1975), +Ogren and Hendrickson (1977), +Rockland (1998), Raczkowski and Diamond (1980)
    - PIm: Lin and Kaas (1979), +Ogren and Hendrickson (1976), +Rockland (1998)
- V2
    - P1/P2: Raczkowski and Diamond (1981), Lin and Kaas (1979), +Kennedy and Bullier (1985), Wong-Riley (1977), Dick et al. (1991), +Ogren and Hendrickson (1977), Raczkowski and Diamond (1980)
    - PIm: Lin and Kaas (1979)
    - PLdp: Dick et al. (1991), +Ungerleider et al. (2014)
- V3/V4/DL
    - P1/P2: Raczkowski and Diamond (1981), +Benevento and Davis (1977), +Yeterian and Pandya (1997), +Shipp (2001)
    - PIm: +Benevento and Davis (1977)
    - PIcm: Shipp (2001)
    - PLdp: +Benevento and Davis (1977), +Weller et al. (2002)
- MT
    - PIm: Raczkowski and Diamond (1981), Lin and Kaas (1979), +Stepniewska et al. (2000), Wong et al. (2009), +Ungerleider et al. (1984), +Lund et al. (1981), +Rockland (1998), Raczkowski and Diamond (1980), +Gray et al. (1999), +Shipp (2001)
    - PIp: +Berman and Wurtz (2011), +Berman and Wurtz (2010)
    - PIcm: +Berman and Wurtz (2011), +Berman and Wurtz (2010)
    - P1/P2: Lin and Kaas (1979), Wong et al. (2009), +Ungerleider et al. (1984), +Rockland (1998), Raczkowski and Diamond (1980), +Gray et al. (1999)
    - PLdp: +Rockland (1998)
    - PL-s: +Maunsell and Van Essen (1983), +Shipp (2001), +Berman and Wurtz (2011), +Berman and Wurtz (2010)
- FST/MST
    - PIm: +Boussaoud et al. (1992), +Gutierrez et al. (2000)
    - P1/P2: +Gutierrez et al. (2000)
- TEO

    - PLdp: +Benevento and Davis (1977), +Romanski et al. (1997), +Webster et al. (1993), +Rockland (1996), +Yeterian and Pandya (1991)
    - PIm: +Rockland (1996)
    - P1/P2: +Webster et al. (1993), +Rockland (1996)
    - PMc: Steele and Weller (1993)
    - PMv/PMm: Steele and Weller (1993)
- TE/TA
    - PMm: +Romanski et al. (1997), Steele and Weller (1993), +Yeterian and Pandya (1988), +Yeterian and Pandya (1991)
    - PMv: Steele and Weller (1993)
    - PMc: +Webster et al. (1993), Steele and Weller (1993), +Rockland (1996), +Yeterian and Pandya (1991)
    - PLdp: +Webster et al. (1993), +Yeterian and Pandya (1991)
    - PIcm: +Webster et al. (1993)
    - P1/P2: +Webster et al. (1993), +Rockland (1996)
- belt/parabelt
    - PMm +Gutierrez et al. (2000), De La Mothe et al. (2012)
    - PMd: +Gutierrez et al. (2000)
    - PMv: +Gutierrez et al. (2000)
    - PLda: +Gutierrez et al. (2000)
- parietal
    - P1/P2: Lin and Kaas (1979)
    - PIm: Lin and Kaas (1979)
    - PLd/LP: Graham et al. (1979), +Benevento and Davis (1977), +Asanuma et al. (1985), +Gutierrez et al. (2000), +Asanuma et al. (1985), +Yeterian and Pandya (1985)
    - PLda: +Benevento and Davis (1977), +Gutierrez et al. (2000), +Yeterian and Pandya (1985)
    - PA: +Asanuma et al. (1985), +Pons and Kaas (1985), +Yeterian and Pandya (1985)
    - PMc: +Asanuma et al. (1985)
    - PMd: +Asanuma et al. (1985), +Yeterian and Pandya (1985), +Gutierrez et al. (2000), +Cavada et al. (1995)
    - PMv: +Asanuma et al. (1985)
- area 1/2/3
    - PA: Cusick and Gould Iii (1990), +Pons and Kaas (1985)
- posterior cingulate, parahippocampal
    - PMm: +Rockland (1996)
    - PMd: +Yeterian and Pandya (1988), +Rockland (1996), +Yeterian and Pandya (1988), +Baleydier and Mauguiere (1985), +Baleydier and Mauguiere (1985)
    - PMc: +Rockland (1996), +Yeterian and Pandya (1988)
    - PLd/LP: +Yeterian and Pandya (1988)
    - PIm: +Rockland (1996)
    - PIp: +Rockland (1996)
- prefrontal/FEF/8a/45a/45b/46
    - PMd: +Gutierrez et al. (2000)
    - PMm: +Stanton et al. (1988), +Gutierrez et al. (2000)
    - PMc: +Contini et al. (2010)
    - PLda: +Stanton et al. (1988)
    - MD: +Gutierrez et al. (2000), +Contini et al. (2010)
    - PLd: +Gutierrez et al. (2000)
- orbital frontal
    - PMm/PMd: +Cavada et al. (1995), +Yeterian and Pandya (1988)
    - MD: +Yeterian and Pandya (1988)

References

Acuna C, Cudeiro J, Gonzalez F, Alonso J, Perez R. 1990. Lateral-posterior and pulvinar reaching cells—comparison with parietal area 5a: A study in behaving *macaca nemestrina* monkeys. *Experimental Brain Research* **82**:158–166.

Adams M, Hof P, Gattass R, Webster M, Ungerleider L. 2000. Visual cortical projections and chemoarchitecture of macaque monkey pulvinar. *Journal of Comparative Neurology* **419**:377–393.

Adams N, Lozsadi D, Guillery R. 1997. Complexities in the thalamocortical and corticothalamic pathways. *European Journal of Neuroscience* **9**:204–209.

Asanuma C, Andersen R, Cowan W. 1985. The thalamic relations of the caudal inferior parietal lobule and the lateral prefrontal cortex in monkeys: Divergent cortical projections from cell clusters in the medial pulvinar nucleus. *The Journal of comparative neurology* **241**:357–381.

Baizer J, Desimone R, Ungerleider L. 1993. Comparison of subcortical connections of inferior temporal and posterior parietal cortex in monkeys. *Visual Neuroscience* **10**:59.

Baldwin M, Balaram P, Kaas J. 2013. Projections of the superior colliculus to the pulvinar in prosimian galagos (*otolemur garnettii*) and vGLUT2 staining of the visual pulvinar. *Journal of Comparative Neurology* **521**:1664–1682.

Baleydier C, Mauguiere F. 1985. Anatomical evidence for medial pulvinar connections with the posterior cingulate cortex, the retrosplenial area, and the posterior parahippocampal gyrus in monkeys. *Journal of Comparative Neurology* **232**:219–228.

Baleydier C, Mauguiere F. 1987. Network organization of the connectivity between parietal area 7, posterior cingulate cortex and medial pulvinar nucleus: A double fluorescent tracer study in monkey. *Experimental Brain Research* **66**:385–393.

Baleydier C, Morel A. 1992. Segregated thalamocortical pathways to inferior parietal and inferotemporal cortex in macaque monkey. *Visual Neuroscience* **8**:391–405.

Bender D. 1981. Retinotopic organization of macaque pulvinar. *Journal of Neurophysiology* **46**:672–693.

Bender D. 1982. Receptive-field properties of neurons in the macaque inferior pulvinar. *Journal of Neurophysiology* **48**:1–17.

Benevento L, Davis B. 1977. Topographical projections of the prestriate cortex to the pulvinar nuclei in the macaque monkey: An autoradiographic study. *Experimental Brain Research* **30**:405–424.

Benevento L, Fallon J. 1975. The ascending projections of the superior colliculus in the rhesus monkey (*macaca mulatta*). *Journal of Comparative Neurology* **160**:339–361.

Benevento L, Port J. 1995. Single neurons with both form/color differential responses and saccade-related responses in the nonretinotopic pulvinar of the behaving macaque monkey. *Visual Neuroscience* **12**:523–544.

Benevento L, Rezak M. 1976. The cortical projections of the inferior pulvinar and adjacent lateral pulvinar in the rhesus monkey (*macaca mulatta*): An autoradiographic study. *Brain Research* **108**:1–24.

Benevento L, Standage G. 1983. The organization of projections of the retinorecipient and nonretinorecipient nuclei of the pretectal complex and layers of the superior colliculus to the lateral pulvinar and medial pulvinar in the macaque monkey. *Journal of Comparative Neurology* **217**:307–336.

Berman R, Wurtz R. 2010. Functional identification of a pulvinar path from superior colliculus to cortical area mT. *Journal of Neuroscience* **30**:6342–6354.

Berman R, Wurtz R. 2011. Signals conveyed in the pulvinar pathway from superior colliculus to cortical area mT. *Journal of Neuroscience* **31**:373–384.

Boussaoud D, Desimone R, Ungerleider L. 1992. Subcortical connections of visual areas mST and fST in macaques. *Visual neuroscience* **9**:291–302.

Cappe C, Morel A, Barone P, Rouiller E. 2009. The thalamocortical projection systems in primate: An anatomical support for multisensory and sensorimotor interplay. *Cerebral Cortex* **19**:2025–2037.

Carey R, Fitzpatrick D, Diamond I. 1979. Layer i of striate cortex of *tupaia glis* and *galago senegalensis*: Projections from thalamus and claustrum revealed by retrograde transport of horseradish peroxidase. *Journal of Comparative Neurology* **186**:393–437.

Cavada C, Hernandez-Gonzalez A, Reinoso-Suarez F. 1995. Acetylcholinesterase histochemistry in the macaque thalamus reveals territories selectively connected to frontal, parietal and temporal association cortices. *Journal of chemical neuroanatomy* **8**:245–257.
Conley M, Raczkowski D. 1990. Sublaminar organization within layer vI of the striate cortex in galago. *Journal of Comparative Neurology* **302**:425–436.
Contini M, Baccarini M, Borra E, Gerbella M, Rozzi S, Luppino G. 2010. Thalamic projections to the macaque caudal ventrolateral prefrontal areas 45A and 45B. *European Journal of Neuroscience* **32**:1337–1353.
Cooper H, Kennedy H, Magnin M, Vital-Durand F. 1979. Thalamic projections to area 17 in a prosimian primate, microcebus murinus. *Journal of Comparative Neurology* **187**:145–167.
Cowey A, Stoerig P, Bannister M. 1994. Retinal ganglion cells labelled from the pulvinar nucleus in macaque monkeys. *Neuroscience* **61**:691–705.
Cusick C, Gould Iii H. 1990. Connections between area 3b of the somatosensory cortex and subdivisions of the ventroposterior nuclear complex and the anterior pulvinar nucleus in squirrel monkeys. *Journal of Comparative Neurology* **292**:83–102.
Cusick C, Scripter J, Darensbourg J, Weber J. 1993. Chemoarchitectonic subdivisions of the visual pulvinar in monkeys and their connectional relations with the middle temporal and rostral dorsolateral visual areas, mT and dLr. *Journal of Comparative Neurology* **336**:1–30.
De La Mothe LA, Blumell S, Kajikawa Y, Hackett T. 2012. Thalamic connections of auditory cortex in marmoset monkeys: Lateral belt and parabelt regions. *The Anatomical Record* **295**:822–836.
Debruyn E, Casagrande V, Beck P, Bonds A. 1993. Visual resolution and sensitivity of single cells in the primary visual cortex (v1) of a nocturnal primate (bush baby): Correlations with cortical layers and cytochrome oxidase patterns. *Journal of Neurophysiology* **69**:3–18.
Diamond I, Fitzpatrick D, Conley M. 1992. A projection from the parabigeminal nucleus to the pulvinar nucleus in galago. *Journal of Comparative Neurology* **316**:375–382.
Dick A, Kaske A, Creutzfeldt O. 1991. Topographical and topological organization of the thalamocortical projection to the striate and prestriate cortex in the marmoset (callithrix jacchus). *Experimental Brain Research* **84**:233–253.
Felleman D, Van Essen D. 1991. Distributed hierarchical processing in the primate cerebral cortex. *Cerebral cortex* **1**:1–47.
Gattass R, Oswaldo-Cruz E, Sousa A. 1978a. Visuotopic organization of the cebus pulvinar: A double representation of the contralateral hemifield. *Brain Research* **152**:1–16.
Gattass R, Pb Sousa A, Oswaldo-Cruz E. 1978b. Single unit response types in the pulvinar of the cebus monkey to multisensory stimulation. *Brain Research* **158**:75–87.
Glendenning K, Hall J, Diamond I, Hall W. 1975. The pulvinar nucleus of *galago senegalensis*. *Journal of Comparative Neurology* **161**:419–457.
Graham J, Lin C, Kaas J. 1979. Subcortical projections of six visual cortical areas in the owl monkey, *aotus trivirgatus*. *Journal of Comparative Neurology* **187**:557–580.
Granon S, Poucet B. 1995. Medial prefrontal lesions in the rat and spatial navigation: Evidence for impaired planning. *Behavioral Neuroscience* **109**:474–484.
Gray D, Gutierrez C, Cusick C. 1999. Neurochemical organization of inferior pulvinar complex in squirrel monkeys and macaques revealed by acetylcholinesterase histochemistry, calbindin and cat-301 immunostaining, and *wisteria floribunda* agglutinin binding. *Journal of Comparative Neurology* **409**:452–468.
Gutierrez C, Cola M, Seltzer B, Cusick C. 2000. Neurochemical and connectional organization of the dorsal pulvinar complex in monkeys. *Journal of Comparative Neurology* **419**:61–86.
Gutierrez C, Cusick C. 1997. Area v1 in macaque monkeys projects to multiple histochemically defined subdivisions of the inferior pulvinar complex. *Brain Research* **765**:349–356.
Gutierrez C, Yaun A, Cusick C. 1995. Neurochemical subdivisions of the inferior pulvinar in macaque monkeys. *Journal of Comparative Neurology* **363**:545–562.
Hackett T, De La Mothe LA, Ulbert I, Karmos G, Smiley J, Schroeder CE. 2007. Multisensory convergence in auditory cortex, iI. thalamocortical connections of the caudal superior temporal plane. *Journal of Comparative Neurology* **502**:924–952.
Hackett T, Stepniewska I, Kaas J. 1998. Thalamocortical connections of the parabelt auditory cortex in macaque monkeys. *The Journal of comparative neurology* **400**:271–286.

Hardy SP, Lynch J. 1992. The spatial distribution of pulvinar neurons that project to two subregions of the inferior parietal lobule in the macaque. *Cerebral Cortex* **2**:217–230.
Harting J, Huerta M, Frankfurter A, Strominger N, Royce G. 1980. Ascending pathways from the monkey superior colliculus: An autoradiographic analysis. *Journal of Comparative Neurology* **192**:853–882.
Hohl-Abrahao J, Creutzfeldt O. 1991. Topographical mapping of the thalamocortical projections in rodents and comparison with that in primates. *Experimental brain research* **87**:283–294.
Hollander H. 1974. Projections from the striate cortex to the diencephalon in the squirrel monkey (*saimiri sciureus*). a light microscopic radioautographic study following intracortical injection of h3 leucine. *Journal of Comparative Neurology* **155**:425–440.
Huerta M, Harting J. 1983. Sublamination within the superficial gray layer of the squirrel monkey: An analysis of the tectopulvinar projection using anterograde and retrograde transport methods. *Brain research* **261**:119–126.
Huerta M, Krubitzer L, Kaas J. 1986. Frontal eye field as defined by intracortical microstimulation in squirrel monkeys, owl monkeys, and macaque monkeys: I. subcortical connections. *Journal of Comparative Neurology* **253**:415–439.
Itaya SK, Van Hoesen GW. 1983. Retinal projections to the inferior and medial pulvinar nuclei in the old-world monkey. *Brain research* **269**:223–230.
Jones E. 1998. Viewpoint: The core and matrix of thalamic organization. *Neuroscience* **85**:331–345.
Kaas J, Lyon D. 2007. Pulvinar contributions to the dorsal and ventral streams of visual processing in primates. *Brain Research Reviews* **55**:285–296.
Kaas J. 2015. Blindsight: Post-natal potential of a transient pulvinar pathway. *Current Biology* **25**:R155–R157.
Kaske A, Dick A, Creutzfeldt O. 1991. The local domain for divergence of subcortical afferents to the striate and extrastriate visual cortex in the common marmoset (callithrix jacchus): A multiple labelling study. *Experimental Brain Research* **84**:254–265.
Kennedy H, Bullier J. 1985. A double-labeling investigation of the afferent connectivity to cortical areas v1 and v2 of the macaque monkey. *Journal of Neuroscience* **5**:2815–2830.
Komura Y, Nikkuni A, Hirashima N, Uetake T, Miyamoto A. 2013. Responses of pulvinar neurons reflect a subject's confidence in visual categorization. *Nature neuroscience* **16**:749–755.
Leopold D. 2012. Primary visual cortex, awareness and blindsight. *Annual review of neuroscience* **35**:91.
Levitt J, Yoshioka T, Lund J. 1995. Connections between the pulvinar complex and cytochrome oxidase-defined compartments in visual area v2 of macaque monkey. *Experimental Brain Research* **104**:419–430.
Li K, Patel J, Purushothaman G, Marion R, Casagrande V. 2013. Retinotopic maps in the pulvinar of bush baby (otolemur garnettii). *Journal of Comparative Neurology* **521**:3432–3450.
Lin C, Kaas J. 1979. The inferior pulvinar complex in owl monkeys: Architectonic subdivisions and patterns of input from the superior colliculus and subdivisions of visual cortex. *Journal of Comparative Neurology* **187**:655–678.
Lin C, Kaas J. 1980. Projections from the medial nucleus of the inferior pulvinar complex to the middle temporal area of the visual cortex. *Neuroscience* **5**:2219–2228.
Livingstone M, Hubel D. 1982. Thalamic inputs to cytochrome oxidase-rich regions in monkey visual cortex. *Proceedings of the National Academy of Sciences* **79**:6098–6101.
Lund J, Hendrickson A, Ogren M, Tobin E. 1981. Anatomical organization of primate visual cortex area vII. *Journal of Comparative Neurology* **202**:19–45.
Lund J, Lund R, Hendrickson A, Bunt AH, Fuchs AF. 1975. The origin of efferent pathways from the primary visual cortex, area 17, of the macaque monkey as shown by retrograde transport of horseradish peroxidase. *Journal of Comparative Neurology* **164**:287–303.
Lyon D, Nassi J, Callaway E. 2010. A disynaptic relay from superior colliculus to dorsal stream visual cortex in macaque monkey. *Neuron* **65**:270–279.
Lysakowski A, Standage G, Benevento L. 1986. Histochemical and architectonic differentiation of zones of pretectal and collicular inputs to the pulvinar and dorsal lateral geniculate nuclei in the macaque. *Journal of Comparative Neurology* **250**:431–448.
Lysakowski A, Standage G, Benevento L. 1988. An investigation of collateral projections of the dorsal lateral geniculate nucleus and other subcortical structures to cortical areas v1 and v4 in the macaque monkey: A double label retrograde tracer study. *Experimental brain research* **69**:651–661.

Maior R, Hori E, Tomaz C, Ono T, Nishijo H. 2010. The monkey pulvinar neurons differentially respond to emotional expressions of human faces. *Behavioural Brain Research* **215**:129–135.
Marion R, Li K, Purushothaman G, Jiang Y, Casagrande V. 2013. Morphological and neurochemical comparisons between pulvinar and v1 projections to v2. *Journal of Comparative Neurology* **521**:813–832.
Markowitsch HJ, Emmans D, Irle E, Streicher M, Preilowski B. 1985. Cortical and subcortical afferent connections of the primate's temporal pole: A study of rhesus monkeys, squirrel monkeys, and marmosets. *Journal of Comparative Neurology* **242**:425–458.
Mathers L, Rapisardi S. 1973. Visual and somatosensory receptive fields of neurons in the squirrel monkey pulvinar. *Brain research* **64**:65–83.
Mathers L. 1971. Tectal projection to the posterior thalamus of the squirrel monkey. *Brain Research* **35**:295–298.
Matsuzaki R, Kyuhou S, Matsuura-Nakao K, Gemba H. 2004. Thalamo-cortical projections to the posterior parietal cortex in the monkey. *Neuroscience Letters* **355**:113–116.
Maunsell J, Van Essen D. 1983. The connections of the middle temporal visual area (mT) and their relationship to a cortical hierarchy in the macaque monkey. *Journal of Neuroscience* **3**:2563–2586.
Mizuno N, Itoh K, Uchida K, Uemura-Sumi M, Matsushima R. 1982. A retino-pulvinar projection in the macaque monkey as visualized by the use of anterograde transport of horseradish peroxidase. *Neuroscience letters* **30**:199–203.
Mizuno N, Takahashi O, Itoh K, Matsushima R. 1983. Direct projections to the prestriate cortex from the retino-recipient zone of the inferior pulvinar nucleus in the macaque monkey. *Neuroscience letters* **43**:155–160.
Morecraft R, Geula C, Mesulam M. 1993. Architecture of connectivity within a cingulo-fronto-parietal neurocognitive network for directed attention. *Archives of Neurology* **50**:279–284.
Nguyen M, Hori E, Matsumoto J, Tran AH, Ono T, Nishijo H. 2013. Neuronal responses to face-like stimuli in the monkey pulvinar. *European Journal of Neuroscience* **37**:35–51.
Ogren M, Hendrickson A. 1976. Pathways between striate cortex and subcortical regions in *macaca mulatta* and *saimiri sciureus*: Evidence for a reciprocal pulvinar connection. *Experimental Neurology* **53**:780–800.
Ogren M, Hendrickson A. 1977. The distribution of pulvinar terminals in visual areas 17 and 18 of the monkey. *Brain Research* **137**:343–350.
Olszewski J ed. 1952. The thalamus of the *macaca mulatta*. an atlas for use with the stereotaxic instrument. Basle Switzerland: New York USA: S. Karger.
O'Brien B, Abel P, Olavarria J. 2001. The retinal input to calbindin-d28k-defined subdivisions in macaque inferior pulvinar. *Neuroscience Letters* **312**:145–148.
O'Brien B, Abel P, Olavarria J. 2002. Connections of calbindin-d28k-defined subdivisions in inferior pulvinar with visual areas v2, v4 and mT in macaque monkeys. *Thalamus & Related Systems* **1**:317–330.
Pandya D, Seltzer B. 1982. Intrinsic connections and architectonics of posterior parietal cortex in the rhesus monkey. *Journal of Comparative Neurology* **204**:196–210.
Partlow G, Colonnier M, Szabo J. 1977. Thalamic projections of the superior colliculus in the rhesus monkey, *macaca mulatta*. a light and electron microscopic study. *Journal of Comparative Neurology* **171**:285–317.
Petersen S, Robinson D, Keys W. 1985. Pulvinar nuclei of the behaving rhesus monkey: Visual responses and their modulation. *Journal of Neurophysiology* **54**:867–886.
Petersen S, Robinson D, Morris J. 1987. Contributions of the pulvinar to visual spatial attention. *Neuropsychologia* **25**:97–105.
Pons TP, Kaas J. 1985. Connections of area 2 of somatosensory cortex with the anterior pulvinar and subdivisions of the ventroposterior complex in macaque monkeys. *Journal of Comparative Neurology* **240**:16–36.
Purushothaman G, Marion R, Li K, Casagrande V. 2012. Gating and control of primary visual cortex by pulvinar. *Nature Neuroscience* **15**:905–912.
Raczkowski D, Diamond I. 1978. Connections of the striate cortex in *galago senegalensis*. *Brain Research* **144**:383–388.
Raczkowski D, Diamond I. 1980. Cortical connections of the pulvinar nucleus in galago. *Journal of Comparative Neurology* **193**:1–40.
Raczkowski D, Diamond I. 1981. Projections from the superior colliculus and the neocortex to the pulvinar nucleus in galago. *Journal of Comparative Neurology* **200**:231–254.

Rezak M, Benevento L. 1979. A comparison of the organization of the projections of the dorsal lateral geniculate nucleus, the inferior pulvinar and adjacent lateral pulvinar to primary visual cortex (area 17) in the macaque monkey. *Brain Research* **167**:19–40.
Robinson D, Petersen S, Keys W. 1986. Saccade-related and visual activities in the pulvinar nuclei of the behaving rhesus monkey. *Experimental Brain Research* **62**:625–634.
Robinson D, Petersen S. 1985. Responses of pulvinar neurons to real and self-induced stimulus movement. *Brain Research* **338**:392–394.
Rockland K, Andresen J, Cowie R, Robinson D. 1999. Single axon analysis of pulvinocortical connections to several visual areas in the macaque. *Journal of Comparative Neurology* **406**:221–250.
Rockland K. 1996. Two types of corticopulvinar terminations: Round (type 2) and elongate (type 1). *The Journal of comparative neurology* **368**:57–87.
Rockland K. 1998. Convergence and branching patterns of round, type 2 corticopulvinar axons. *Journal of Comparative Neurology* **390**:515–536.
Rodman H, Gross C, Albright T. 1989. Afferent basis of visual response properties in area mT of the macaque. i. effects of striate cortex removal. *The Journal of neuroscience* **9**:2033–2050.
Rodman H, Gross C, Albright T. 1990. Afferent basis of visual response properties in area mT of the macaque. iI. effects of superior colliculus removal. *The Journal of neuroscience* **10**:1154–1164.
Romanski L, Giguere M, Bates J, Goldman-Rakic P. 1997. Topographic organization of medial pulvinar connections with the prefrontal cortex in the rhesus monkey. *Journal of Comparative Neurology* **379**:313–332.
Romanski L. 2007. Representation and integration of auditory and visual stimuli in the primate ventral lateral prefrontal cortex. *Cerebral Cortex* **17**:61–69.
Rovo Z, Ulbert I, Acsady L. 2012. Drivers of the primate thalamus. *Journal of Neuroscience* **32**:17894–17908.
Saalmann Y, Pinsk M, Wang L, Li X, Kastner S. 2012. The pulvinar regulates information transmission between cortical areas based on attention demands. *Science* **337**:753–756.
Schmahmann J, Pandya D. 1990. Anatomical investigation of projections from thalamus to posterior parietal cortex in the rhesus monkey: A wGA-hRP and fluorescent tracer study. *Journal of Comparative Neurology* **295**:299–326.
Schmid M, Mrowka S, Turchi J, Saunders R, Wilke M. 2010. Blindsight depends on the lateral geniculate nucleus. *Nature* **466**:373–377.
Shipp S. 2001. Corticopulvinar connections of areas v5, v4, and v3 in the macaque monkey: A dual model of retinal and cortical topographies. *Journal of Comparative Neurology* **439**:469–490.
Shipp S. 2003. The functional logic of cortico-pulvinar connections. *Philosophical Transactions of the Royal Society of London. Series B, Biological Sciences* **358**:1605–1624.
Soares J, Gattass R, Souza A, Rosa M, Fiorani M, Brandao B. 2001. Connectional and neurochemical subdivisions of the pulvinar in cebus monkeys. *Visual Neuroscience* **18**:25–41.
Standage G, Benevento L. 1983. The organization of connections between the pulvinar and visual area mT in the macaque monkey. *Brain Research* **262**:288–294.
Stanton G, Goldberg M, Bruce C. 1988. Frontal eye field efferents in the macaque monkey: I. subcortical pathways and topography of striatal and thalamic terminal fields. *Journal of Comparative Neurology* **271**:473–492.
Steele G, Weller R. 1993. Subcortical connections of subdivisions of inferior temporal cortex in squirrel monkeys. *Visual Neuroscience* **10**:563.
Stepniewska I, Kaas J. 1997. Architectonic subdivisions of the inferior pulvinar in new world and old world monkeys. *Visual Neuroscience* **14**:1043–1060.
Stepniewska I, Qi H, Kaas J. 1999. Do superior colliculus projection zones in the inferior pulvinar project to mT in primates? *European Journal of Neuroscience* **11**:469–480.
Stepniewska I, Qi H, Kaas J. 2000. Projections of the superior colliculus to subdivisions of the inferior pulvinar in new world and old world monkeys. *Visual Neuroscience* **17**:529–549.
Symonds L, Kaas J. 1978. Connections of striate cortex in the prosimian, *galago senegalensis*. *Journal of Comparative Neurology* **181**:477–511.
Trojanowski J, Jacobson S. 1974. Medial pulvinar afferents to frontal eye fields in rhesus monkey demonstrated by horseradish peroxidase. *Brain Research* **80**:395–411.
Trojanowski J, Jacobson S. 1976. Areal and laminar distribution of some pulvinar cortical efferents in rhesus monkey. *Journal of Comparative Neurology* **169**:371–391.

Trojanowski J, Jacobson S. 1977. The morphology and laminar distribution of cortico-pulvinar neurons in the rhesus monkey. *Experimental brain research* **28**:51–62.
Ungerleider L, Desimone R, Galkin T, Mishkin M. 1984. Subcortical projections of area mT in the macaque. *Journal of Comparative Neurology* **223**:368–386.
Ungerleider L, Galkin T, Desimone R, Gattass R. 2014. Subcortical projections of area v2 in the macaque. *Journal of Cognitive Neuroscience*.
Ungerleider L, Galkin T, Mishkin M. 1983. Visuotopic organization of projections from striate cortex to inferior and lateral pulvinar in rhesus monkey. *Journal of Comparative Neurology* **217**:137–157.
Walker A ed. 1938. The primate thalamus. University of Chicago press.
Ward R, Arend I. 2007. An object-based frame of reference within the human pulvinar. *Brain* **130**:2462–2469.
Warner C, Goldshmit Y, Bourne J. 2010. Retinal afferents synapse with relay cells targeting the middle temporal area in the pulvinar and lateral geniculate nuclei. *Frontiers in Neuroanatomy* **4**:1–16.
Webster M, Bachevalier J, Ungerleider L. 1993. Subcortical connections of inferior temporal areas tE and tEO in macaque monkeys. *Journal of Comparative Neurology* **335**:73–91.
Weller R, Steele G, Kaas J. 2002. Pulvinar and other subcortical connections of dorsolateral visual cortex in monkeys. *Journal of Comparative Neurology* **450**:215–240.
Wilke M, Turchi J, Smith K, Mishkin M, Leopold D. 2010. Pulvinar inactivation disrupts selection of movement plans. *Journal of Neuroscience* **30**:8650–8659.
Wong P, Collins C, Baldwin M, Kaas J. 2009. Cortical connections of the visual pulvinar complex in prosimian galagos (*otolemur garnettii*). *Journal of Comparative Neurology* **517**:493–511.
Wong-Riley M. 1977. Connections between the pulvinar nucleus and the prestriate cortex in the squirrel monkey as revealed by peroxidase histochemistry and autoradiography. *Brain research* **134**:249–267.
Yeterian E, Pandya D. 1985. Corticothalamic connections of the posterior parietal cortex in the rhesus monkey. *Journal of Comparative Neurology* **237**:408–426.
Yeterian E, Pandya D. 1988. Corticothalamic connections of paralimbic regions in the rhesus monkey. *Journal of Comparative Neurology* **269**:130–146.
Yeterian E, Pandya D. 1989. Thalamic connections of the cortex of the superior temporal sulcus in the rhesus monkey. *Journal of Comparative Neurology* **282**:80–97.
Yeterian E, Pandya D. 1991. Corticothalamic connections of the superior temporal sulcus in rhesus monkeys. *Experimental brain research* **83**:268–284.
Yeterian E, Pandya D. 1997. Corticothalamic connections of extrastriate visual areas in rhesus monkeys. *Journal of Comparative Neurology* **378**:562–585.

The background chapter used macaque pulvinar as a representative model, to offer a general review on the structure, connections and function of the primate pulvinar. The experiments included in this thesis, however, used a prosimian species, bush baby (*Otolemur garnettii*), as an animal model, for the reasons discussed below. Therefore, in this appendix we briefly describe the structure and function of the bush baby pulvinar and compare and contrast its organization with the macaque pulvinar.

Compared to simians, prosimians have been proposed to more closely resemble the common ancestors of primates (Jerison, 1979). Therefore these primates can provide important information on how the structure of the pulvinar could have changed in different primate lines of decent. Additionally, outside of the macaque monkey, more is known about the bush baby pulvinar in terms of the numbers of studies, than any other primate species. Bush baby pulvinar, like its simian counterparts, sits on the caudo-dorso-lateral surface of thalamus. It is separated laterally from LGN and ventro-medially from the posterior nuclear group by fibers, but is difficult to separate from the more rostro-medial LP complex (Glendenning et al., 1975). Bush baby pulvinar can be divided into superior (PS) and inferior divisions (PI) as brSC runs horizontally between them, yet further division is not as easily based on chemoarchitecture. Horizontally running fibers can be found on the lateral side of PS, dividing PS into PL and PM. The PL/PM border is even harder to define than in simians, and sometimes PL was defined as lateral PS with a lighter CO stain and more tightly packed cells (Wong et al., 2009). As Glendenning et al. (1975) warned, we should not assume similarity between the similarly named subdivisions in bush baby pulvinar and simian pulvinar.

Bush baby pulvinar has a large area reciprocally connected with V1 straddling the brSC (Campos-Ortega, 1968). Similar to macaque pulvinar, two visuotopic maps can be identified in this lateral part of bush baby PI/PL based on V1 connection patterns, with the dorsal map mostly in PL and the ventral map mostly in PI. Both maps have a medial lower field representation and a lateral upper field representation, and a joined central field representation on the map border at its caudal medial end (Carey et al., 1979; Raczkowski and Diamond, 1980; Symonds and Kaas, 1978). These two maps, with adjoining central representations, as well as V1, V2 and MT connections (Raczkowski and Diamond, 1981; Wall et al., 1982), are similar to the P1/P2 maps in macaque monkey (Ungerleider et al., 1983, 1984). Cells in these mapped areas are responsive to simple visual stimuli (Li et al., 2013).

In bush baby, MT receives from at least two areas in PI, a larger area with sparser connections in central or lateral PI, and a smaller area in the caudo-medial part of PI (Raczkowski and Diamond, 1980; Wong et al., 2009; Wall et al., 1982). The medial MT projecting areas may also have a V1 projection without precise retinotopy (Raczkowski and Diamond, 1981). With connections with V1/V2/MT, a separate MT projection zone and a different V1 projection pattern, this caudo-medial PI area appears to be similar to PIm in macaque monkey.

As of yet, no areas similar to macaque Pdm have been identified in bush baby pulvinar. The border region between PL and PM receives projections from posterior temporal regions, similar to the dorsal medial PL in macaque (Raczkowski and Diamond, 1981; Rezak and Benevento, 1979). This area, however, does not receive projections from the intermediate layers of SC, unlike macaque PLdm (Raczkowski and Diamond, 1981; Benevento and Standage, 1983).

Pulvinar appears to have undergone a rotational shift both caudally and ventrally when pulvinar configuration of bush babies is compared to that of simians such as macaque, cebus, and owl monkeys. In bush baby pulvinar, the two visuotopic maps are at the lateral end of the pulvinar complex, with one map dorsal to the other, and a between-map border that runs horizontally. In macaque monkey the two maps are at the ventrolateral end of the pulvinar complex. The P2 map is lateral to P1, wrapping P1 ventrally and caudally. The relative positions of PIm also reflect this change. PIm moves from the caudo-medial end of PI in bush baby to covering the caudal half of the medial surface in owl monkey, to the rostro-

medial end of PI in macaque monkey (Wong et al., 2009; Stepniewska et al., 1999; Stepniewska and Kaas, 1997).

References for notes on prosimian pulvinar

Benevento L, Standage G. 1983. The organization of projections of the retinorecipient and nonretinorecipient nuclei of the pretectal complex and layers of the superior colliculus to the lateral pulvinar and medial pulvinar in the macaque monkey. *Journal of Comparative Neurology* **217**:307–336.

Campos-Ortega J. 1968. Descending subcortical projections from the occipital lobe of *galago crassicaudatus*. *Experimental Neurology* **21**:440–454.

Carey R, Fitzpatrick D, Diamond I. 1979. Layer i of striate cortex of *tupaia glis* and *galago senegalensis*: Projections from thalamus and claustrum revealed by retrograde transport of horseradish peroxidase. *Journal of Comparative Neurology* **186**:393–437.

Glendenning K, Hall J, Diamond I, Hall W. 1975. The pulvinar nucleus of *galago senegalensis*. *Journal of Comparative Neurology* **161**:419–457.

Jerison H. 1979. Brain, body and encephalization in early primates. *Journal of Human Evolution* **8**:615–635.

Li K, Patel J, Purushothaman G, Marion R, Casagrande V. 2013. Retinotopic maps in the pulvinar of bush baby (otolemur garnettii). *Journal of Comparative Neurology* **521**:3432–3450.

Raczkowski D, Diamond I. 1980. Cortical connections of the pulvinar nucleus in galago. *Journal of Comparative Neurology* **193**:1–40.

Raczkowski D, Diamond I. 1981. Projections from the superior colliculus and the neocortex to the pulvinar nucleus in galago. *Journal of Comparative Neurology* **200**:231–254.

Rezak M, Benevento L. 1979. A comparison of the organization of the projections of the dorsal lateral geniculate nucleus, the inferior pulvinar and adjacent lateral pulvinar to primary visual cortex (area 17) in the macaque monkey. *Brain Research* **167**:19–40.

Stepniewska I, Kaas J. 1997. Architectonic subdivisions of the inferior pulvinar in new world and old world monkeys. *Visual Neuroscience* **14**:1043–1060.

Stepniewska I, Qi H, Kaas J. 1999. Do superior colliculus projection zones in the inferior pulvinar project to mT in primates? *European Journal of Neuroscience* **11**:469–480.

Symonds L, Kaas J. 1978. Connections of striate cortex in the prosimian, *galago senegalensis*. *Journal of Comparative Neurology* **181**:477–511.

Ungerleider L, Desimone R, Galkin T, Mishkin M. 1984. Subcortical projections of area mT in the macaque. *Journal of Comparative Neurology* **223**:368–386.

Ungerleider L, Galkin T, Mishkin M. 1983. Visuotopic organization of projections from striate cortex to inferior and lateral pulvinar in rhesus monkey. *Journal of Comparative Neurology* **217**:137–157.

Wall J, Symonds L, Kaas J. 1982. Cortical and subcortical projections of the middle temporal area (mT) and adjacent cortex in galagos. *Journal of Comparative Neurology* **211**:193–214.

Wong P, Collins C, Baldwin M, Kaas J. 2009. Cortical connections of the visual pulvinar complex in prosimian galagos (*otolemur garnettii*). *Journal of Comparative Neurology* **517**:493–511.

CHAPTER 3

RETINOTOPIC MAPS IN THE PULVINAR OF BUSH BABY (*OTOLEMUR GARNETTII*)

The study described in this chapter was published and is reproduced below:
K. Li, J. Patel, G. Purushothaman, R.T. Marion & V.A. Casagrande (2013). Retinotopic maps in the pulvinar of bush baby (*Otolemur garnettii*). Journal of Comparative Neurology, 521(15), 3432-3450

Introduction

The primate pulvinar is located at the dorsal posterior end of the thalamus and at least three subdivisions, or equivalent areas (Gattass et al., 1978), of the pulvinar can be identified: the inferior (PI), lateral (PL), and medial pulvinar (PM) (Walker, 1938, P.48-56; Emmers et al., 1963; Huerta et al., 1986; Wong et al., 2009). Most cells recorded in PL and PI were reported to respond to simple visual stimuli (Bender, 1982; Petersen et al., 1985). PI and PL enjoy rich connections with the superior colliculus (SC), the parabigeminal nucleus and the primary visual cortex, as well as other early visual cortical areas of both the dorsal and ventral streams (Kaas and Lyon, 2007). Many functional roles have been proposed for these visual pulvinar subdivisions , including visual salience (Petersen et al., 1987), attention (Van Essen, 2005), visual stability (Robinson and Petersen, 1985; Berman and Wurtz, 2011), motion integration (Merabet et al., 1998), temporal binding (Arend et al., 2008) and as a relay between cortical visual areas (Sherman, 2007; Theyel et al., 2010), among others.

The number and organization of retinotopic maps in the visual pulvinar are of great interest because of pulvinar's wide connections with visual cortical areas and its various proposed functions. The visual pulvinar has been electrophysiologically surveyed in the Old World simian macaque (Bender, 1981) and the New World simian cebus (Gattass et al., 1978). Two retinotopic maps were identified in both species. The positions and the visual field representations of these maps, however, were reported to differ. In macaque, one map was reported in ventro-lateral PL and the other was described as straddling the PI/PL border (Bender, 1981), while one was found in ventral PI/PL and the other in dorsal PL in cebus (Gattass et al., 1978). The relationship between these observed pulvinar maps in macaque and cebus monkeys remains unclear: 1) the positions of homologous retinotopic maps may have shifted between Old World and New World simian species, 2) true differences between the reported maps may have developed between the species, or 3) maps may not have been detected in the study of one of these species.

Compared to simians, prosimians are considered to be closer to the common ancestors of modern primates (Jerison, 1979) and generally have a smaller and less differentiated pulvinar compared to simians (Raczkowski and Diamond, 1981). With knowledge of pulvinar retinotopy of a prosimian, the comparison between it and that of simians can help reveal the following: the common structure of primate pulvinar, the correspondence between reported pulvinar retinotopic maps in different primate species, and potentially, pulvinar features that have evolved solely in simians. Additionally, the functional features of simian pulvinar that are recently evolved are likely to have evolved separately for New and Old World simians, and may correlate with simians' expanded development of extrastriate cortex. The retinotopic organization of pulvinar, however, has not been electrophysiologically examined in any prosimian species. In this study we used bush babies (*Otolemur garnettii*) as a representative species of prosimians. We electrophysiologically examined the retinotopy of its visual pulvinar and constructed 3D models of the maps from data across cases. We also compared the resulting functional maps with the chemoarchitecture of each pulvinar subdivision.

Methods

Animal Preparation

Six bush babies (*Otolemur garnettii*) of both sexes weighing 0.77-1.1 kg were used in this study. All experiments were performed according to a protocol approved by the Vanderbilt University Institutional Animal Care and Use Committee (IACUC). Some of these animals were used in multi-day terminal recording sessions while others underwent a series of 1-day survival recording sessions before a final 1-day terminal recording session.

Anesthesia was first induced with 20-40 mg/kg ketamine and 0.4-0.5 mg/kg xylazine, and maintained with 1-3% isoflurane during surgery. During the first session an 8 mm craniotomy and durotomy were performed over LGN centered at the Horsley-Clarke coordinates of anterior-posterior +3 and medial-lateral 7. After surgery, isoflurane was replaced by urethane in terminal sessions and propofol/nitrous oxide in survival sessions. Urethane was given intra-peritoneally, induced with a dose of 1.25 mg/kg and maintained with 0.25 mg/kg boosters every 2 hours. For propofol/nitrous oxide anesthesia, the animal was given propofol intravenously at 2.5-6 mg/kg/hr first and then at 0.2-0.6 mg/kg/hr after the animal was stabilized. Once the animal was deeply anesthetized, it was given the muscle relaxant, vecuronium bromide, intravenously at 0.15 mg/kg/hr. While the animal was infused with vecuronium bromide, it was respired with 75% nitrous oxide in oxygen in the survival sessions, or room air in the terminal sessions. During the recording session the end tidal CO2 pressure was monitored and maintained between 35 and 50 mmHg. EEG and ECG were monitored to ensure a stable anesthetic plane, and the animals' toes were pinched periodically to help with ECG monitoring of anesthesia.

The animals' pupils were dilated with 1% topical atropine solution. The eyes were focused onto a tangent screen 57 cm away using contact lenses of appropriate size and power. A map of the blood vessel pattern was reflected back onto the tangent screen from the tapetum to locate the optic disks, which were used to infer the locations of the areae centralis.

A survival recording session usually lasted 10-12 hours, after which the brain opening was covered with Tecoflex (artificial dura) for protection. A specially molded plastic cap of appropriate size was glued with dental cement over the craniotomy window, and the scalp was sutured closed. First vecuronium bromide infusion and then propofol anesthesia was withdrawn and the animal was monitored until it was fully awake, at which point it was given treats and the analgesic buprenorphine 0.01 mg/kg. After a survival session an animal was allowed at least two weeks to recover before another survival session was performed. All pulvinar mapping was done on the left hemisphere. Some of these animals received tracer injections in the right pulvinar for a related study.

Recording

We recorded extracellular single and multi-unit activity using epoxylite-coated tungsten microelectrodes (FHC, Inc., Bowdoin, ME) with impedances ranging from 1 to 2.5MΩ at 1 kHz. The signal was amplified and digitized with a Plexon multichannel acquisition processor (Plexon, Inc., Dallas, TX), and fed to a speaker after filtering. The high impedance of these electrodes ensured that we could differentiate between background “hash” and neural spikes.

The central vision representation of bush baby pulvinar was found by first looking for the central vision representation of LGN near the Horsley-Clarke coordinates of AP +3 and ML 7, and then moving 1.5 to 2 mm medially. The electrode was initially lowered 7-7.5mm from the cortical surface, then advanced in steps of 100μm. At each location, we examined the visual responsiveness of cells using spots, bars and other light patterns projected on the tangent screen.

When we found any visual response with bright light spots, we used an ophthalmoscope to project confined light spots or light bars with clear borders and uniform luminance on the screen, to locate the

receptive field. Recorded units were classified as vague, moderate or brisk by their visual responses. A brisk unit showed large clear spikes and a clear response similar to the response of V1 cells, with either no adaptation or fast recovery. A moderate unit showed a defined receptive field, spikes clearly larger than background hash and consistent recovery from adaptation. A vague unit showed correlation between visual stimulation and activity but either was hard to localize, showed very slow recovery from fatigue, or had small spikes barely larger than background hash. For most non-vague units we also tested the ocularity of the receptive field. We hand plotted the receptive field centers of vague units, the accurate receptive fields of the non-vague units, and separate receptive fields for the two eyes when they deviated.

At the end of each penetration, one or two lesions were made by passing 5μA of current through the electrode tip for 10 seconds, with tip negative. Four to nine penetrations were made in each session. Penetrations were spaced 500μm apart.

Histology and Tissue Reconstruction

At the end of each terminal recording session the animal was overdosed with Nembutal (>120mg/kg) and perfused transcardially with a saline rinse followed by a fixative consisting of 3% paraformaldehyde, 0.1% glutaraldehyde and 0.2% picric acid (saturated solution, V/V) in 0.1M phosphate buffer (PB). Perfusions were done within five weeks of the first recording sessions so lesions left in the early sessions remained visible. The brain was blocked at AP +8 in the coronal plane in Horsley-Clarke coordinates. The thalamus was coronally sectioned frozen at 52μm. During the sectioning, needle probe marks were left in the thalamus perpendicular to the cutting plane to facilitate reconstruction.

Sections from the first three animals were stained for Nissl substance, cytochrome oxidase (CO), acetylcholinesterase (AChE) and calbindin, in series, to reveal pulvinar subdivisions. In later cases only some of the four stains were used to facilitate reconstruction. CO staining was used in all cases. We employed a CO staining protocol that used 0.02% diaminobenzidine (DAB), 0.03% cytochrome C, 0.015% catalase, 2% sucrose, 0.03% nickel-ammonium-sulphate and 0.03% cobalt-chloride in 0.05M PB of 7.4pH. This method is based on the one used by Boyd and Matsubara (1996), and it allowed better differentiation, sharper contrast and faster reactions compared to the original method (Wong-Riley, 1979). Our staining for AChE followed the procedure of Geneser-Jensen and Blackstad (1971).

For immunostaining for calbindin (see also Table 3), sections were first incubated with 1:5000 calbindin D28k rabbit-anti-rat antibody (Swant, Inc., Marly, Switzerland, Code No.: cb-38a, Lot No.: 9.03), then 1:500 biotin conjugated donkey anti-rabbit antibody (Millipore, Corporation, Billerica, MA, USA, Code No.: AP182B), and later ABC standard elite kit (Vector laboratories, Inc., Burlingame, CA). The immunostaining was visualized with 0.05% DAB, 0.04% nickel-ammonium-sulfate and 0.003% H_2O_2. Omission of the primary antibody in our control sections resulted in a completely lack of staining, demonstrating the specificity of the donkey anti-rabbit antibody we used. The primary antibody was a polyclonal and was produced against recombinant rat calbindin D-28k. In normal concentration, the antibody yields only a single band at 28kDa for primate brain tissue (manufacturer product description: http://www.swant.com/pfd/Rabbit%20anti%20Calbindin%20D-28k%20CB38.pdf). Additionally, the LGN of primates, including bush baby, has been shown to express calbindin D28k only in its koniocellular (K) layers but not in the magnocellular (M) or parvocellular (P) layers (Johnson and Casagrande, 1995; Hendry and Reid, 2000). This distribution pattern was perfectly reflected in our stained sections (see Figure 31D).

Antigen	Immunogen	Manufacturer	Species	Catelog No.	JCN antibody No.	Dilution
Calbindin	Recombinant rat Calbindin D-28k	Swant (Switzerland)	Rabbit polyclonal	CB38	10000340	1:5000

Table 3: Antibodies Used

Two additional bush baby hemispheres were used in this study and each was blocked and sectioned as in the other six cases, but without electrophysiological recording. Sections from one of these cases were stained in series for CO and myelin, the other CO, AChE, calbindin and myelin. We used the method of Gallyas (1979) for myelin staining. All photomicrographs of sections used in figures were enhanced in contrast. Photomicrographs of myelin sections were digitally stretched in our figures to compare with other sections, as the myelin stained sections tended to shrink more than the others.

In the cases with pulvinar recordings, LGN, pulvinar and pulvinar subdivisions were manually reconstructed along with the penetrations. Sections were aligned based on large blood vessels and marks placed during cutting. The penetrations were located using the electrolytic lesions. Shrinkage factors were calculated for each penetration from the distance between lesions measured during experiment and measured on sections. Penetrations in the same animals were found to show shrinkage factors within 10% of each other. In a few penetrations one of the lesions was not visible, in which case each of these penetrations was reconstructed assuming a shrinkage factor that equaled the average of other penetrations in the same animal. The sites of recorded units were deduced from their depths relative to the depths of the lesions.

Data Analysis

In our analysis the centers of recorded units' receptive fields were measured in a polar coordinate system, whose origin was on the contralateral *area centralis* (AC) and the unit vector of angle zero degrees horizontally pointed to the right. The coordinates for ipsilateral receptive fields were measured with a coordinate system centered on the ipsilateral AC. The shape of a receptive field was modeled as an ellipse with either a vertical or horizontal major axis. The eccentricity of receptive field centers' was translated from the distance on tangent screen to the angle from AC, and the area of receptive fields was translated accordingly.

The visual field representation at each recorded location of our penetrations was calculated as the gravity center of the centers of all receptive fields recorded at that location. For binocular units we did not include ipsilateral receptive fields, and at locations with many single units of different visual response qualities (see above), we only included receptive fields with response qualities of the tier highest at that location.

We mapped 365 multi- or single unit locations in the pulvinar of 6 animals. We focused our penetrations in PI and PL as previous studies showed that these areas are connected to V1 and V2 (Symonds and Kaas, 1978; Raczkowski and Diamond, 1980, 1981). In each penetration the electrode was lowered in steps of 100μm. At each depth, new units were identified based on differences in spike shapes and receptive field properties. Visual pulvinar was broadly surveyed in different animals, and data from all six cases were combined to construct the final maps. We observed ~250μm differences in the relative positions of LGN and pulvinar in different animals. A gross difference of about 500μm also was observed in the position of thalamus as a whole, presumably due to small differences in ear canal height or orbital tissue thickness that impact the head position in the stereotaxic apparatus. Nevertheless, we were able to align the reconstructed models from different animals by the shape of brachium of the superior colliculus (brSC) and PI. Consequently, residual variations in PL/PI shape and retinotopic organization within each pulvinar nucleus were quite small.

Results

In this section we first present the chemoarchitectonic subdivisions we identified in bush baby pulvinar, to provide a reference frame for the location of the retinotopic maps. Major map features will then be described, together with representative electrode penetrations that demonstrate these features. And

finally, we present an overall model that gives predictions of the receptive field progressions that should be seen in any given penetration based on this model.

Architecture of the visual pulvinar

We determined the pulvinar subdivisions using CO, myelin, AChE and calbindin staining to compare the architectonic subdivisions to the physiological maps (Figure 3). The three large subdivisions of the bush baby pulvinar, PL, PI and PM, were found on sections stained with any of the four methods. The brSC was easily recognized by its dark horizontally oriented fibers in myelin stained sections (Figure 3A), and as a lightly stained horizontal fiber bundle in sections stained with the other three methods (Figure 3B-D). This broad fiber bundle extended from the caudal end to the rostro-ventral border of pulvinar, separating PI from PL and PM. PI occupied the ventral half of pulvinar in the most posterior coronal sections, and became smaller in more anterior sections, disappearing at about the same anterior-posterior (AP) level as the middle of the LGN. PL could be distinguished from PM with its darker myelin staining. PL also showed darker CO staining while PM appeared patchy and generally lighter with CO staining (Figure 3B). About half of the pulvinar area above brSC could be considered PL. Anteriorly, the border between the lateral posterior nucleus (LP) and PL, as well as the border between anterior pulvinar and PM, were hard to define based on the staining methods we used.

Past studies have found the bush baby inferior pulvinar difficult to subdivide based on chemoarchitectonic features (Symonds and Kaas, 1978; Wong et al., 2009). At their medial end the dense fiber bundles of brSC grew wide and curved ventrally. These fibers clearly separated PI from PM. In this heavily myelinated area a darkly stained circle was found consistently in myelin stained sections (arrowhead, Figure 3A). This circle extended dorsally into the PM/PL border. CO and AChE stained sections revealed a dark patch in the same area (Figure 3BC). These features were very similar to those described in the medial inferior pulvinar in owl monkeys (Lin and Kaas, 1979; Stepniewska and Kaas, 1997). Therefore, bush baby PI can be divided into medial (PIm) and central (PIc) zones, with PIm at the PI/PM/PL junction, and PIc occupying the rest of PI.

Additionally, we found two distinct areas in bush baby PIc, a large lateral region that stained lightly for myelin and darkly for both CO and AChE, as well as a ventro-medial region which stained darkly for myelin and lightly for both CO and AChE. These features resembled those described for the lateral (PIcl) and medial (PIcm) portions of PIc in simian species (Stepniewska and Kaas, 1997; Gray et al., 1999). However, one salient feature of PIcl/PIcm/PIm in simians is the alternate dark and light bands revealed by immunostaining for the calcium binding protein calbindin (Stepniewska and Kaas, 1997), yet our calbindin staining (Figure 3D) showed only small differences between these subdivisions. In keeping with prior schemes, nevertheless, we refer to the three subdivisions of bush baby inferior pulvinar as PIcl, PIcm, and PIm, from lateral to medial. Lacking connectional data, however, we cannot be certain that these subdivisions are homologous to the simian pulvinar subdivisions with the same names.

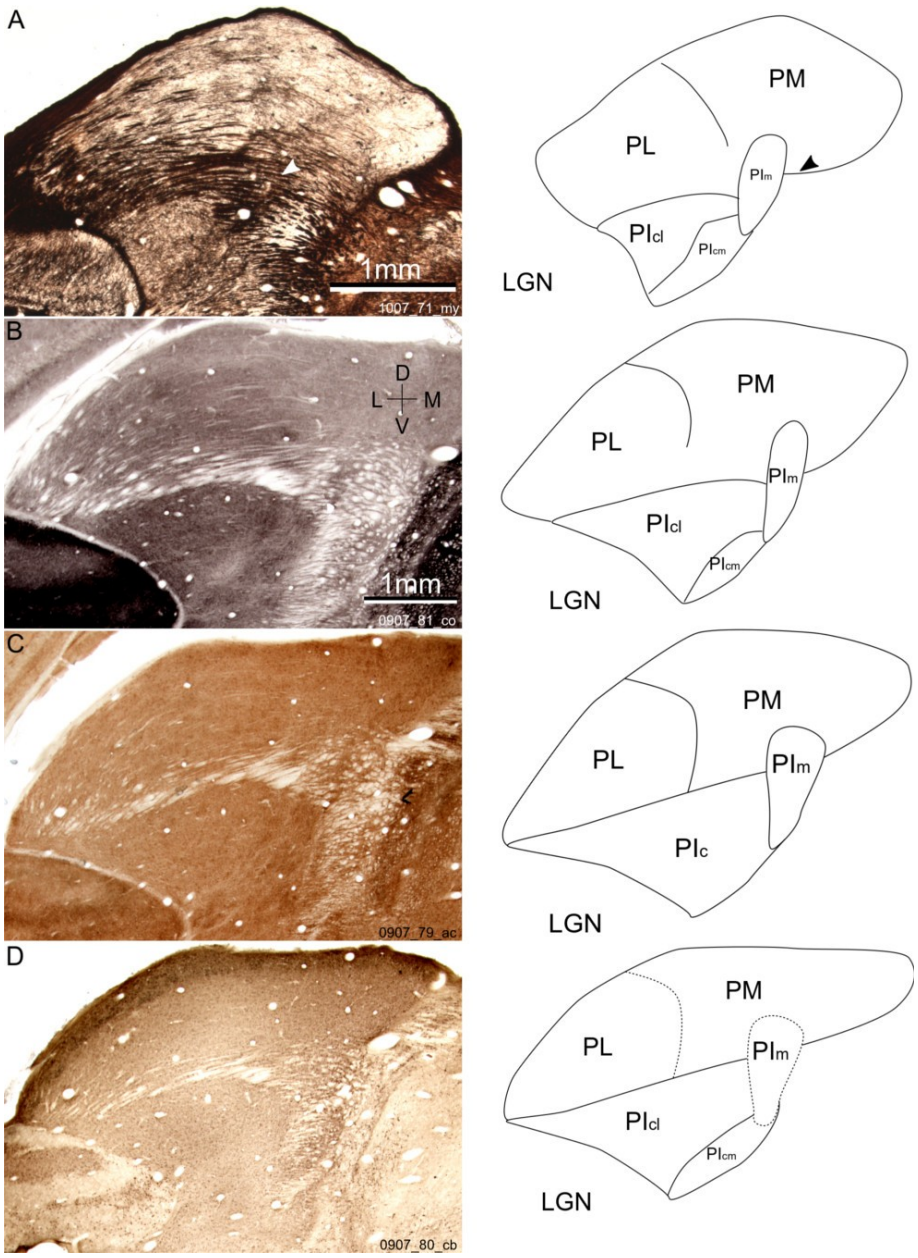

Figure 3: Chemoarchitecture of the bush baby pulvinar

A-D left: coronal sections of bush baby pulvinar in two animals at comparable anterior-posterior levels. The four sections are stained for myelin, cytochrome oxidase (CO), acetylcholinesterase (AChE), and calbindin (CB), respectively. The myelin section showed more shrinkage during staining and was digitally stretched to match with the other sections. **A-D** right: line drawings of subdivision borders visible in the sections on the left. Solid lines are clear borders between subdivisions, while dotted lines show borders not obvious with that staining. The arrowheads in A show the location of the myelin circle. D, dorsal; L, lateral; V, ventral; M, medial. Subdivisions: PL, lateral pulvinar; PM, medial pulvinar; PIm, medial inferior pulvinar; PIc, central inferior pulvinar; PIcl, lateral part of PIc; PIcm, medial part of PIc. LGN, lateral geniculate nucleus.

Visual Responses of Cells in PI and PL

Neurons in both PL and the lateral part of PI showed robust responses to simple visual stimuli. Almost all visually responsive cells showed localized receptive fields, but a few responded over wide areas of the visual field. Most cells were better driven by light spots than light bars. The majority of cells we found occurred to receive binocular input. Among the 126 cells we tested ocularity on, 73 are binocular, 22 are ipsilateral and 31 are contralateral. Additionally, 12 of the 73 binocular cells only respond when both eyes receive visual stimulation. Weak direction selectivity was observed for many neurons. Cells that responded either in a transient or a sustained manner to standing contrast were found in a mixed population in PI and PL. A majority of visually driven cells showed strong adaptation to repeated stimulation, but there also were cells with strong facilitation. Most, although not all, of the cells' receptive fields, were located in the contralateral visual field. Collectively the receptive fields of recorded cells covered more than 60 degrees of the contralateral visual field. The receptive field positions of pulvinar neurons shifted systematically through the visual field as the electrode advanced ventrally, showing well organized visual field representations in most of PI and PL.

Dorsal and Ventral Retinotopic Maps

One major feature of the receptive field progressions observed in electrode penetrations was the reversal of progression. As the electrode passed through the visual pulvinar, the recorded receptive fields first progressed towards the vertical meridian (VM), then turned sharply and progressed away from VM. The reversal of receptive field progression in each penetration occurred at similar dorsal-ventral depths in pulvinar. This reversal marked a border between two visual field representations (see Figure 4B, D and F). Both of the pulvinar areas above and below the region where progression reversals occurred showed precise retinotopy, with each area representing the full contralateral field. Double representations were clearly demonstrated in some penetrations, where receptive fields in the same area of the visual field appeared before and after the reversal (see Figure 4F). As such, these progressions can be considered as evidence for two distinct retinotopic maps.

3-D views of the dorsal (red) and ventral (blue) map

The model of the dorsal map contains all recorded units showing receptive fields that appeared before the progression reversals. Similarly, the model of the ventral map contains all recorded units after the receptive progression reversal. Both models were smoothed so a few ((< 5)) for each structure) recording sites are left out. A coronal view is shown in **panel A** and a parasagittal view is shown in **panel B**. Light gray shows the outline of the pulvinar. Dark gray shows the outline of the inferior pulvinar. D, dorsal; L, lateral; V, ventral; M, medial; A, anterior; P, posterior. Each arm of the compass is 0.5mm in the model.

For convenience we refer to these maps, henceforth, as the dorsal and the ventral maps based on their relative positions in pulvinar. We used a 3-D wire frame volume that contained all cells included in the receptive field progression towards VM to represent the dorsal retinotopic map, and another wire frame volume that contained all receptive fields progressing away from VM to represent the ventral map, as shown in Figure 5. The border between the two maps lay roughly on the PI/PL border at its posterior end, and extended anteriorly as a mostly horizontal sheet. In the anterior half of the maps, as PI became smaller, larger portions of the ventral map extended dorso-medially across brSC (Figure 5B). The visual field representation of the dorsal and ventral maps was roughly continuous across the map border, as the receptive fields moved smoothly near the progression reversals.

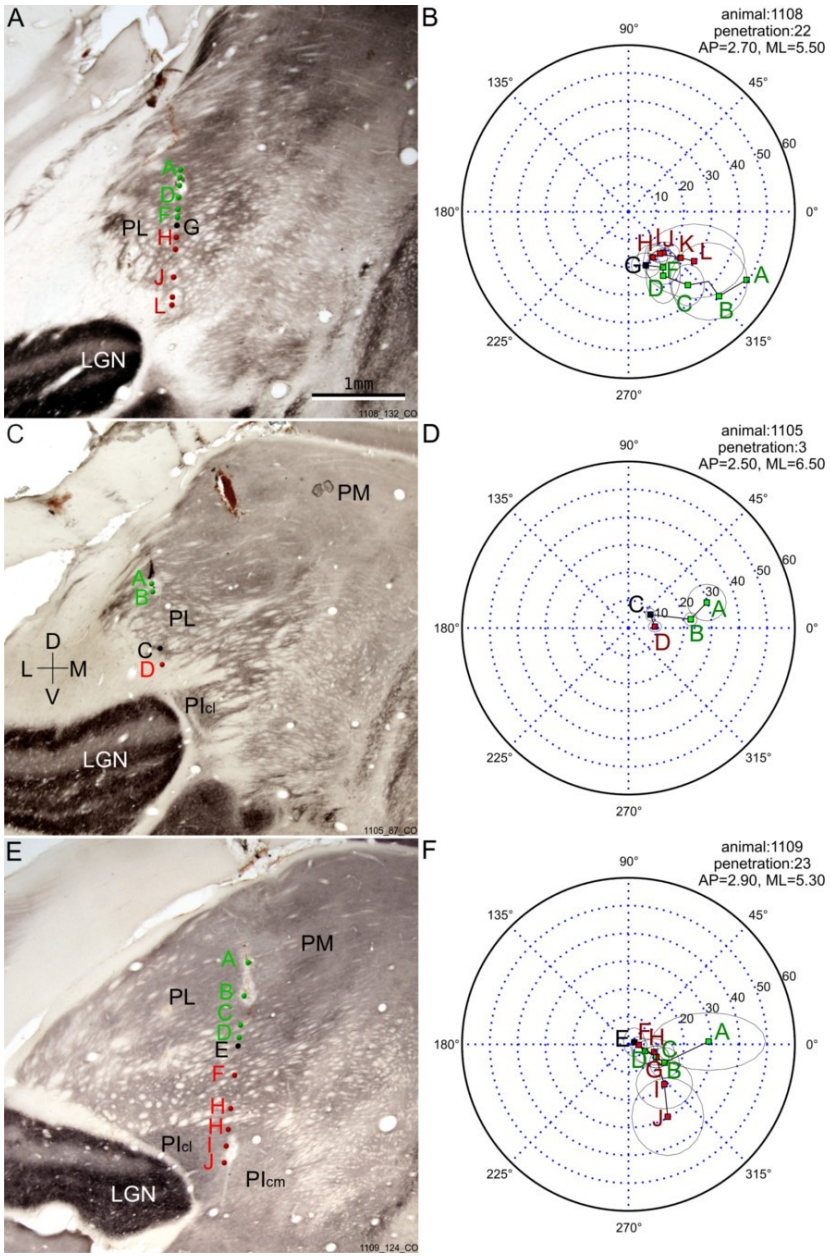

Figure 4: Representative penetrations showing the reversals of receptive field progression

A, C, E: reconstruction of 3 example penetrations from 3 different cases overlaid on coronal CO sections, with corresponding receptive field progression shown on the right in B, D, F. **B, D, F**: perimeter charts of penetrations with colored dots showing the receptive field centers of corresponding units whose locations in the brain are indicated in the sections on the left. Green dots and green letters indicate units dorsal to the reversal point while red dots and letters indicate units ventral to the reversal point. Black dots and letters label the reversal point. The top section is just anterior to PI while the other two sections are in the middle of PI. A trend for the receptive fields to shift gradually towards the vertical meridian(VM) then away from VM can be seen clearly. PL, lateral pulvinar; PI, inferior pulvinar; PM, medial pulvinar; LGN, lateral geniculate nucleus.

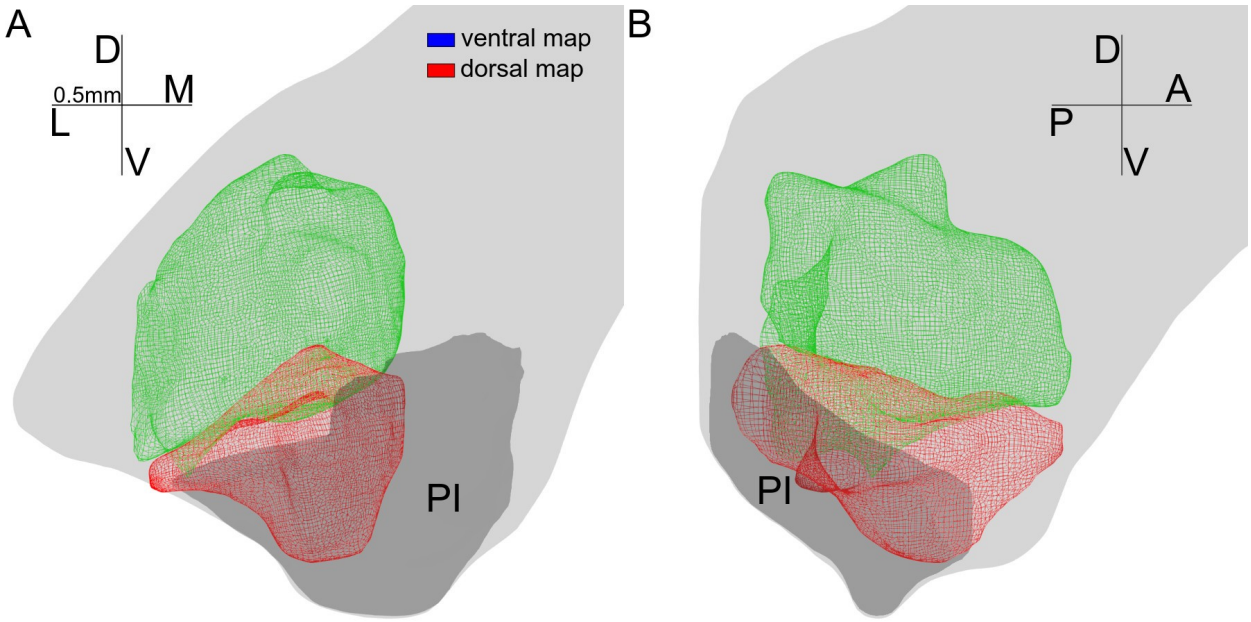

Figure 5: The Central and Peripheral Representation

The representation of the central-peripheral axis of the visual field is shown with colored eccentricity contour representations in Figure 6AB. These contours were modeled as 3D volumes that contained all but a few (<5) recorded cells with receptive fields within 5, 10, or 15 degrees of central vision. The two maps had adjoined central vision representations, located at the postero-medial end of both maps. Representative penetrations shown in Figure 6C-F demonstrated the two main features of the central-peripheral representation. First, in single penetrations cells closer to the border between the two maps had more central receptive fields, while cells on the dorsal surface of the dorsal map and the ventral surface of the ventral map had more peripheral receptive fields. Second, postero-medial penetrations had reversal points closer to central vision, and generally cells with more central receptive field than were found in antero-lateral penetrations at comparable depths.

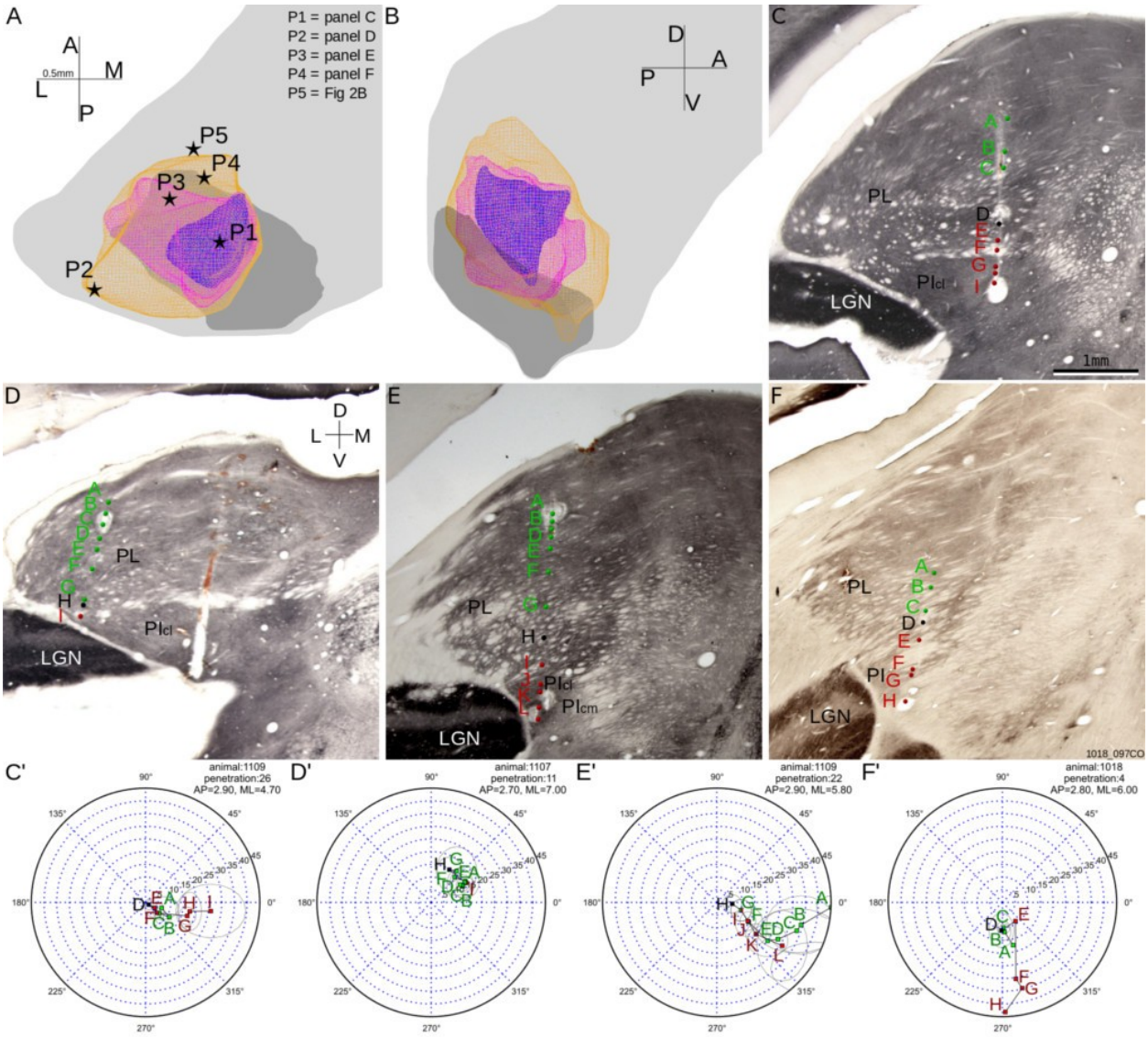

Figure 6: The representation of the central-peripheral axis of the visual field

A-B: Horizontal (panel A) and parasagittal (panel B) views of the representations of visual field areas within 5 degrees (blue), 10 degrees (green) and 15 degrees (red) of the area centralis. Same conventions as Figure 3. **C-F**: Example penetrations with locations shown in panel A, with same conventions as in Figure 2. Purple letters mark sites outside the two maps.

The Horizontal Meridian Representation

Both maps represented the upper field in their lateral half and the lower field in their medial half, as shown in Figure 7. We deduced the horizontal meridian (HM) representation from the borders between these two volumes representing the upper and lower fields in each map. HM was represented as a vertical sheet continuous between the dorsal and the ventral maps, as can be seen in Figure 7B, D and Figure 8AC. Indeed, receptive field progressions roughly near HM were found along the border between the representations of two quadrants (Figure 4F and Figure 8CD). Figure 8EF demonstrated that penetrations had lower field receptive fields medial to the sheet, and upper field receptive fields lateral to it.

There were two areas where the HM representation sheet was not flat. In the dorsal map the posterior end of the HM representation was convex toward the lateral side. This feature can be clearly seen from the overall shape of the border between the upper and lower field representations, as shown in Figure 8A. Individual penetrations showed the same feature, as posterior penetrations (see Figure 8C) had dorsal map receptive fields on both sides of HM but the receptive field progression showed strong fluctuations with elevation, while in more anterior penetrations receptive field progressions flattened out along HM (see Figure 4F and Figure 8D). In the ventral map the ventral end of the HM representation curved laterally. As a result, vertical penetrations often showed oblique receptive field progressions (see Figure 6E and Figure 8C) instead of horizontal progressions.

The Vertical Meridian Representation

The VM was represented as a curve on both the posterior and the medial edges of the border between the two maps. In the dorsal map, the representation of visual field areas near VM extended along the medial and ventral surfaces of the map. Similarly, in the ventral map, the representation of the visual field near-VM area extended along the dorsal and medial surfaces. In other words, an iso-azimuth contour (see Figure 9A inset) was represented as a rotated T shape on most coronal sections. Medial and posterior penetrations, like the ones shown in Figure 6E and Figure 9C, showed reversal points closer to VM than anterior and lateral penetrations, representative penetrations of which are shown in Figure 6F and Figure 9D. We observed some penetrations with receptive field progressions along VM in the ventral map. These observations were consistent with a curved medial border in the ventral map, where the ventral ends of iso-azimuth contours curve laterally together with the medial border (Figure 9A inset).

Overall Model

Coronal and horizontal cross-sections of the maps are shown in Figure 10 and Figure 11, respectively. The three coronal sections shown in Figure 10B-D are drawn directly from a model which combines the models of eccentricity and quadrant representations at three anterior-posterior levels marked in panel A. Hypothetical penetrations are marked on the coronal sections and their receptive field progressions, as predicted from the model, are shown in panels E-G.

At these anterior-posterior levels, both the representations of the upper and lower visual fields were present, so the 3 lateral hypothetical penetrations (I, IV, VII) were all in the upper field, and the 3 medial ones (III, VI, IX) were all in the lower field. The upper and lower field representations were not symmetrical in the coronal plane. A larger upper field representation was found in the more posterior part of map, while a larger lower field representation was found at more anterior levels (compare panels B and D). The curvature of the HM representation at its posterior end caused the two posterior penetrations (II, V) to approach HM from the lower field and move again into the lower field after the reversal. All of the penetrations at the posterior levels, and the medial penetrations at more anterior levels (I-III, VI, IX), had receptive fields close to the VM representation, and therefore had reversal points close to VM.

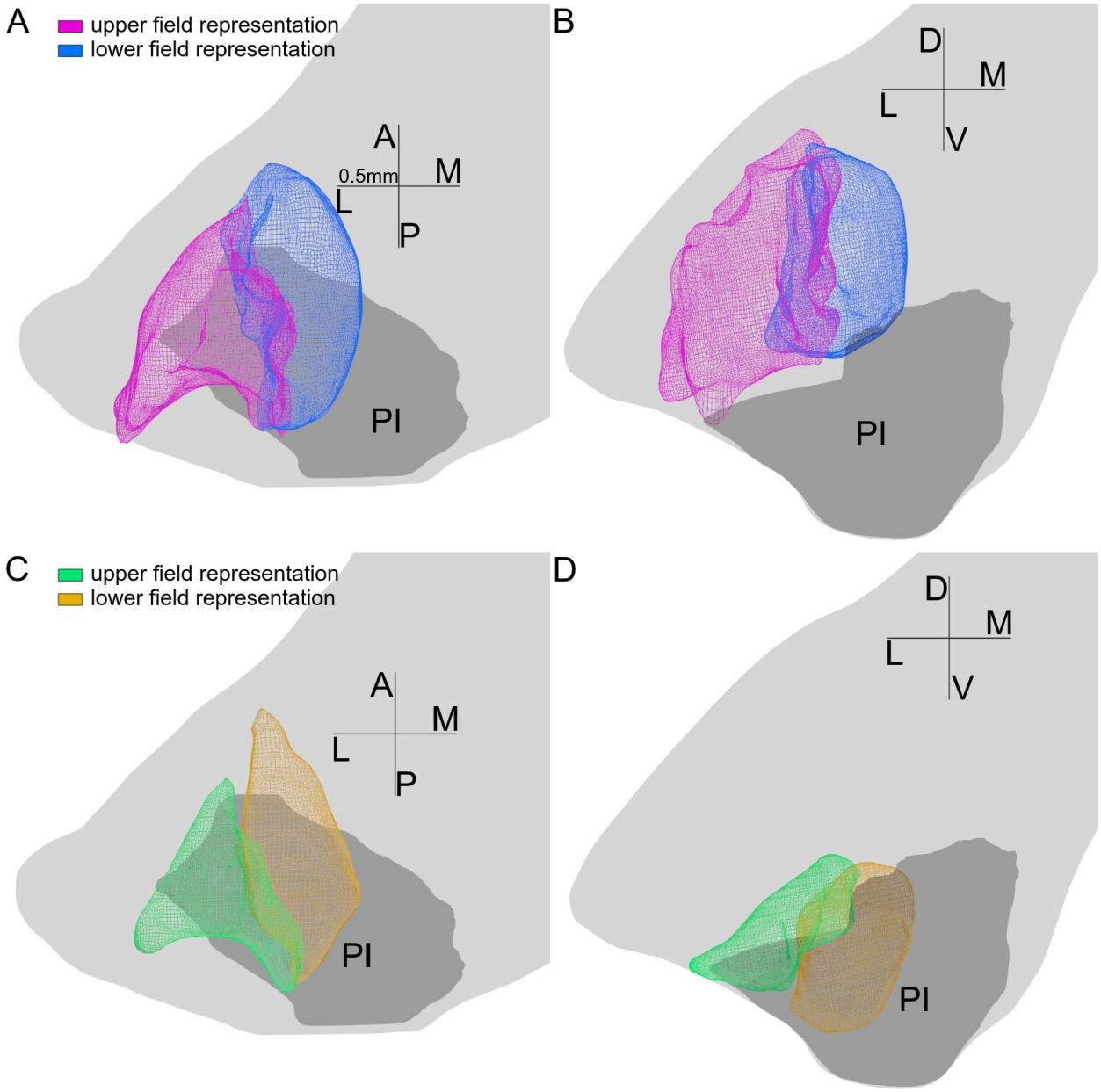

Figure 7: The upper and lower field representations of each of the maps

Same conventions as in Figure 3. **A, B**: horizontal and coronal views of the upper (purple) and lower (blue) field representations of the dorsal map. **C, D**: horizontal and coronal views of the upper (green) and lower (yellow) field representations of the ventral map. For both maps the upper field representations lie on the lateral side and the lower field representation lie on the medial side of the maps.

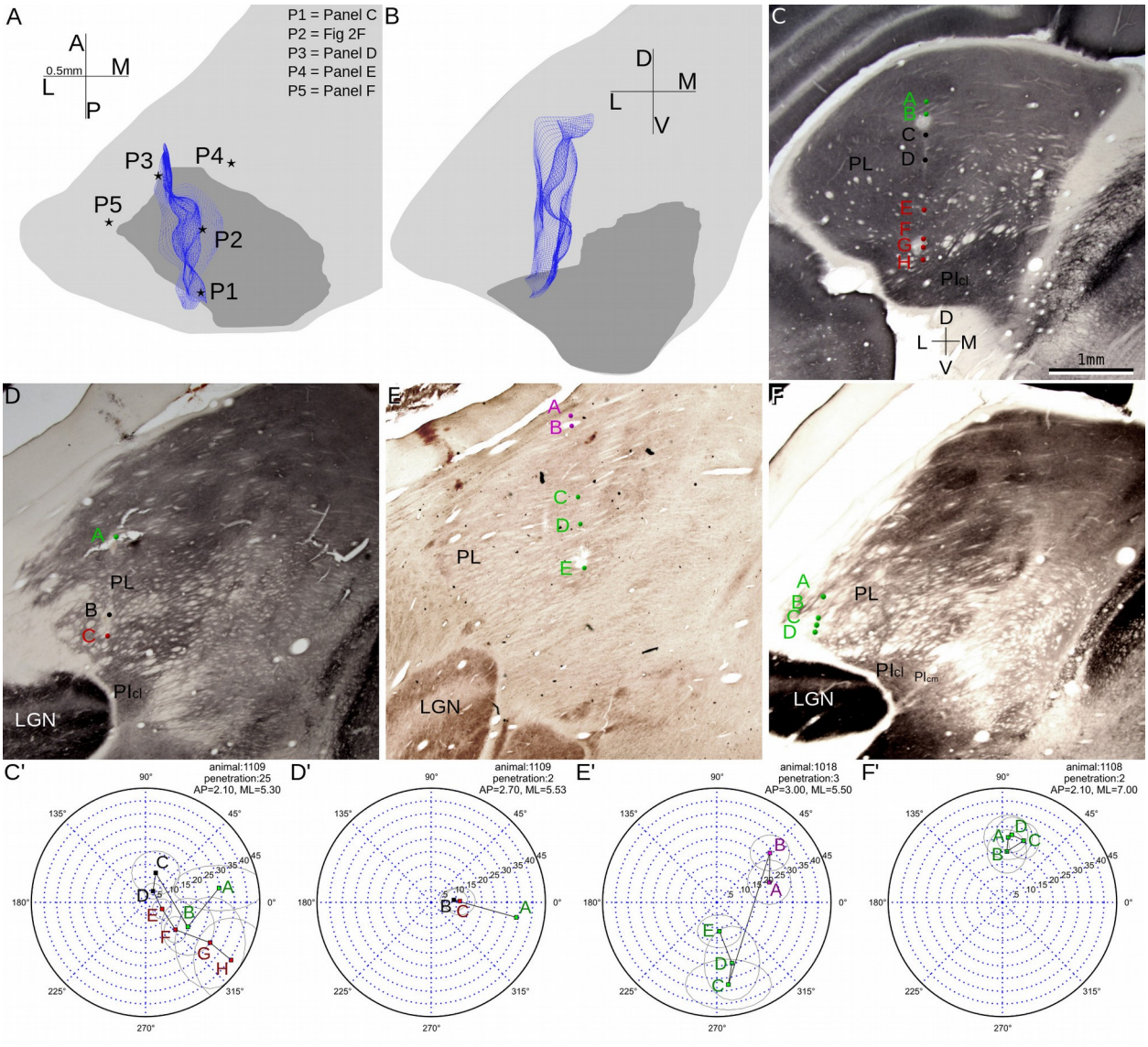

Figure 8: The representation of the horizontal meridian

A-B: Horizontal (panel A) and coronal (panel B) views of the horizontal meridian (HM) representation (in blue), with same conventions as in Figure 3. The horizontal meridian representation was modeled as the border between the upper and lower field representations of both maps. In panel A each star shows the location of a penetration whose receptive field progression is shown in another panel as indicated in top right table. **C-F**: Receptive field progressions of four penetrations that show features of the horizontal meridian, with same conventions as in Figure 2.

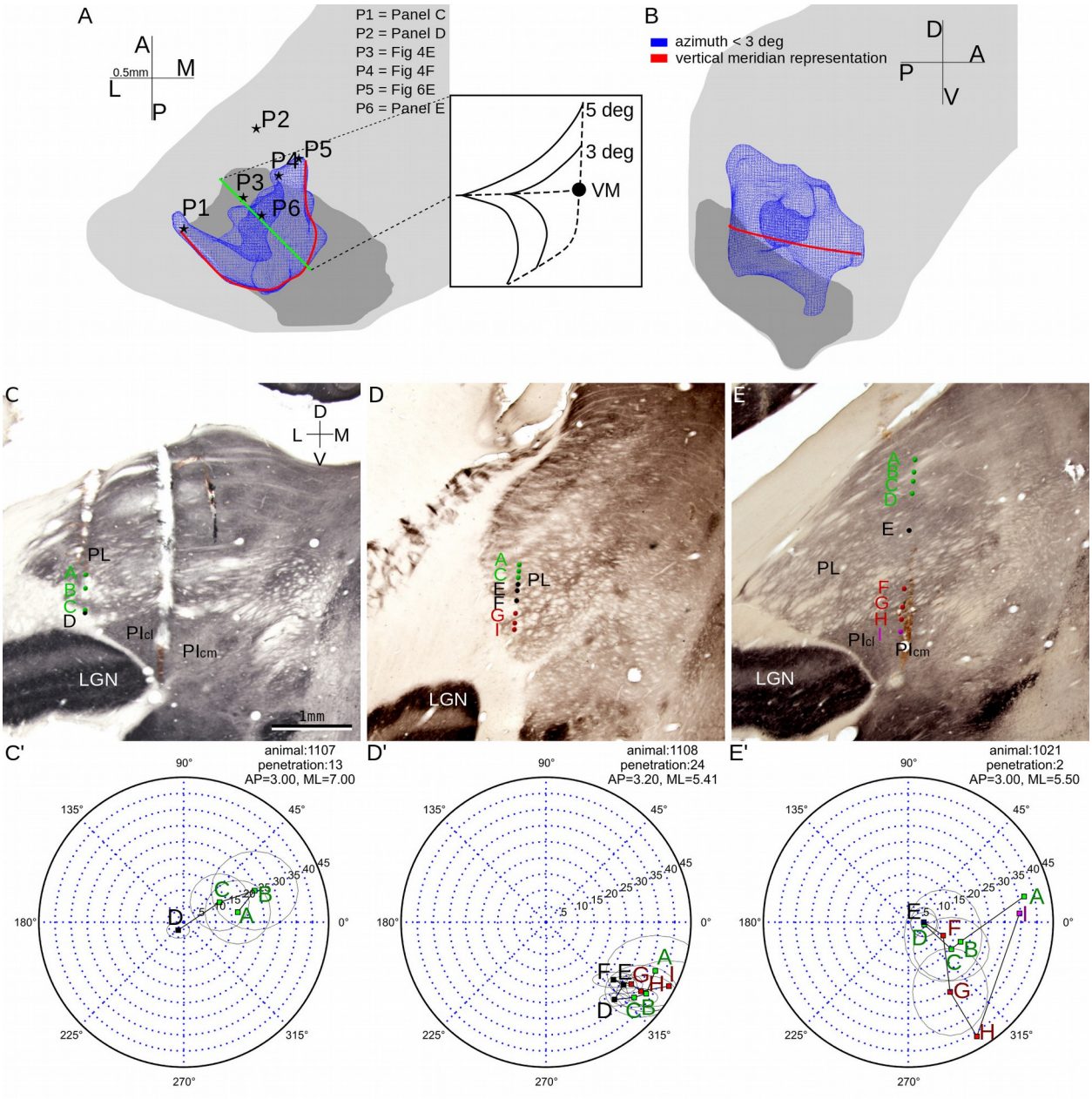

Figure 9: The representation of the vertical meridian

A-B: Horizontal (panel A) and coronal (panel B) views of the representation of the visual field area within 3 degrees of VM in blue. The red line shows the VM representation deduced from data. In panel A each star shows the location of a penetration shown in C-F. **Inset in A**: A diagram of iso-azimuth contours in the plane shown as a green line in panel A. Dashed lines show the borders of the dorsal and ventral maps. Solid lines show iso-azimuth contours of 3 and 5 degrees. Big solid dot show the VM representation. **C-D**: Receptive field progressions of penetrations shown in panel A, with same conventions as Figure 2.

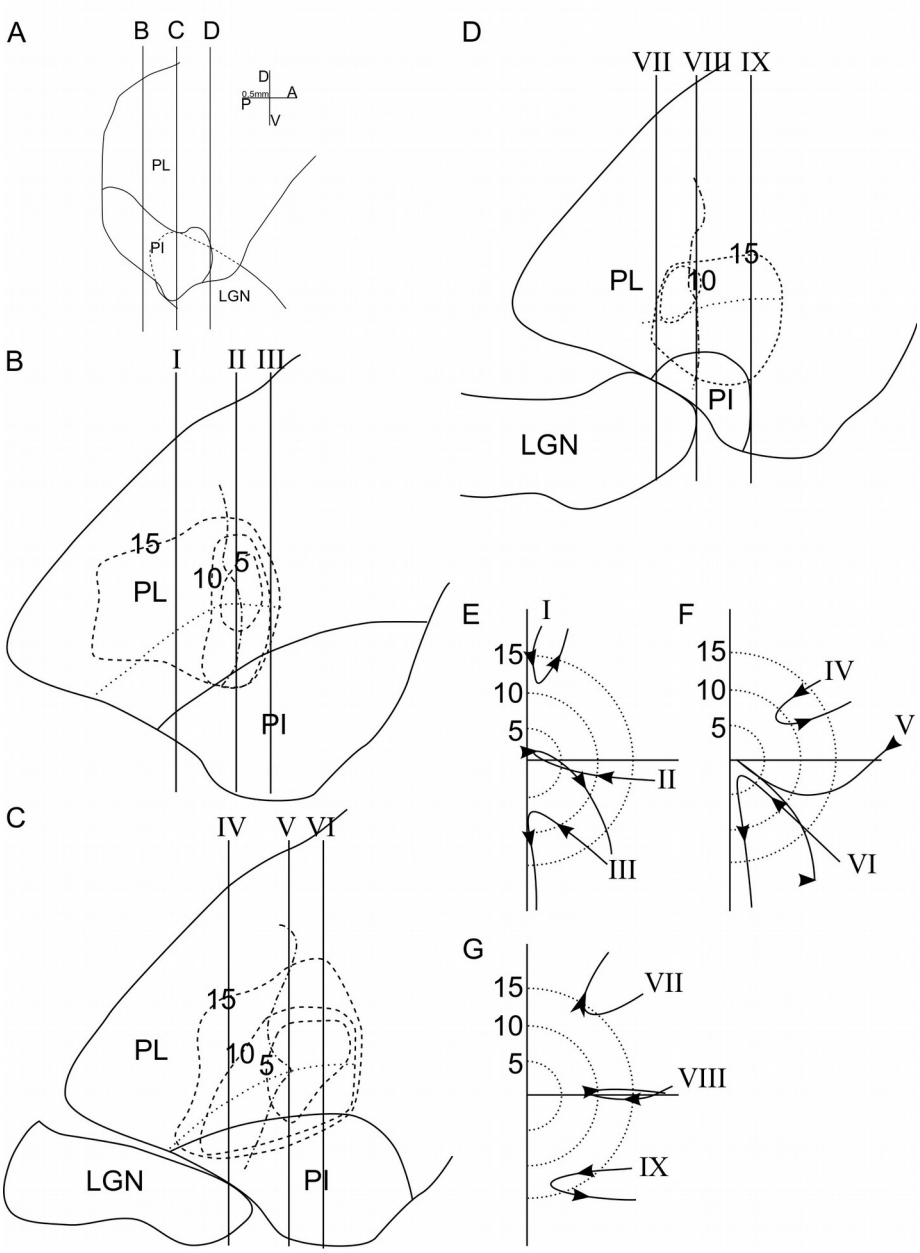

Figure 10: Cross sections of the map model

A: The location of coronal sections shown in panels B-D. **B-D**: three coronal sections through the pulvinar at different anterior-posterior levels. Solid lines show the outline of the pulvinar and the PI/PL border. Dotted lines show the border between the two maps. Dashed lines show the iso-eccentricity contours at 5, 10 and 15 degrees from the central vision, as indicated by the number on each contour. Dot-dash lines show the border between upper and lower visual field representations. The vertical lines with roman numerals indicate the location of hypothetical penetrations with predicted receptive field progressions shown in panels E-G. **E-G**: The receptive field progressions predicted from the map model for hypothetical penetrations shown in panels B-D.

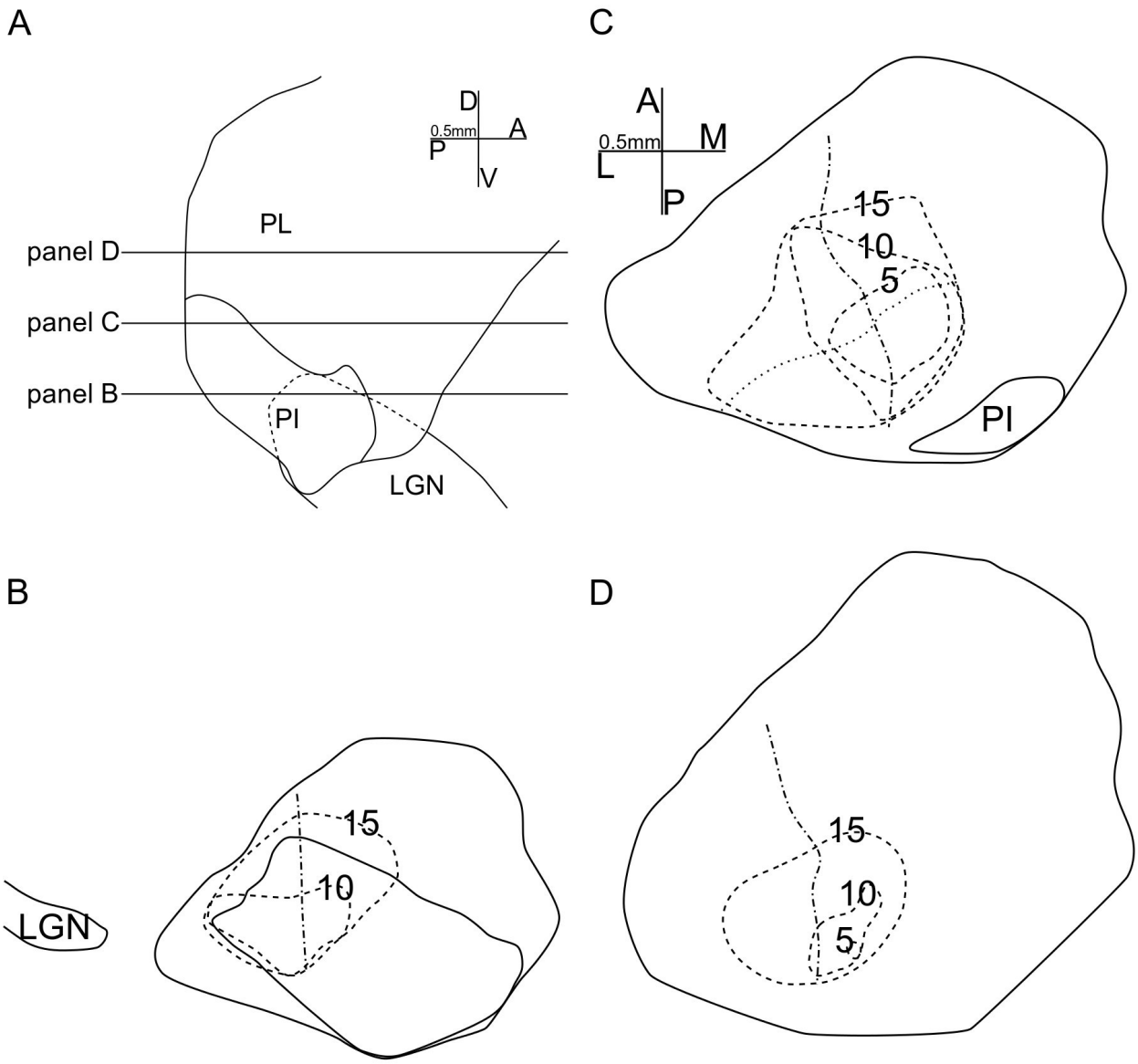

Figure 11: Horizontal sections of the map model

A: The location of the horizontal sections shown in B-D. **B-D**: Solid lines show the outline of pulvinar with inferior pulvinar and LGN separately. Other conventions as in Figure 8.

Horizontal cross-sections through this combined model (Figure 11) showed the retinotopic organization of the individual maps most clearly. The ventral cross-section (panel B) and the dorsal cross-section (panel D) showed the basic features of the ventral and the dorsal map, respectively. These features included a medio-posterior central vision representation, and an HM representation sheet that ran anterior-posteriorly. The cross-section in the middle (panel C) shows the transition between the dorsal and ventral maps. The border between the two maps was higher at its posterior end and lower at its anterior end. As a result, in horizontal cross-sections showing both maps, the dorsal map was anterior to the ventral map. The central vision representation fell between the maps and on the sheet representing HM.

Receptive Field Sizes in the Dorsal and Ventral Maps

It is of interest to determine if neurons in the two retinotopic maps have different receptive field sizes, as would be expected if the neurons in the two maps are dominated by different inputs or integrate information differently across the visual field. To test this hypothesis we chose penetrations with clear reversal points in their receptive field progressions, and assigned the units encountered before and after the reversal point to the two identified retinotopic maps. The receptive field areas of these units were compared to the eccentricity of their receptive field centers in Figure 12. As shown, more central receptive fields had smaller areas in both the dorsal and the ventral maps (Pearson r test, dorsal map: $r = 0.5194$, $p = 4.23E\text{-}4$; ventral map: $r = 0.5853$, $p = 5.18E\text{-}6$). Both maps showed similar slopes representing the increase in receptive field size with eccentricity. The receptive field sizes of dorsal map cells were slightly larger than those of the ventral map cells (t-test, $t = 2.056$, $p = 0.0426$).

Compared to the two maps of macaque monkey lateral pulvinar (Bender, 1981, Figure 10), the maps in bush baby pulvinar had neurons with larger receptive fields for the same eccentricities. These pulvinar cells also featured receptive field sizes comparable to cells in bush baby V2 (Allison and Casagrande, 1994), and larger receptive fields than found in bush baby V1 cells (Debruyn et al., 1993). The same relationship was found in macaque monkey, where pulvinar cell receptive fields were larger in size than V1 cells (Bender, 1981; Hubel and Wiesel, 1974), suggesting that if V1 provides the visual drive to these maps, there is convergence of input to pulvinar.

Area Medial to the Two Maps

A few penetrations suggested that more visual areas may exist medial to the two identified maps. In these medial penetrations, receptive fields were encountered that were in a drastically different location than would be predicted in a typical receptive field progression through the dorsal and ventral maps. Some of these receptive fields were encountered at the beginning of some penetrations, before we entered the dorsal map. The rest were encountered deep in penetrations below cells showing receptive field progressions typical for the ventral map. Among the cells encountered after the ventral map, some also displayed very large receptive fields, often encompassing the full contralateral visual field. Others showed receptive fields located well into the ipsilateral visual field, or extending over VM into the ipsilateral visual field. In each of the latter cases the location of the optic disks was rechecked to ensure that the eyes had not moved.

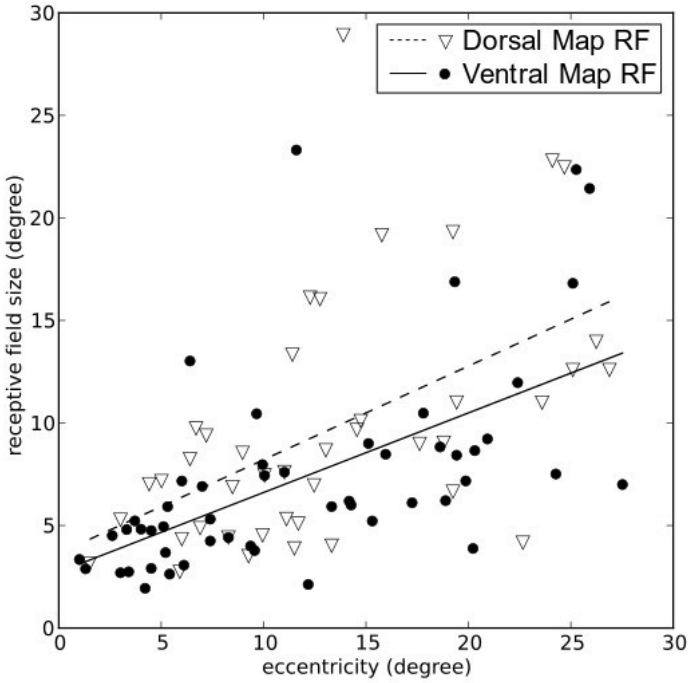

Figure 12: Receptive field sizes vs. center eccentricity

Only non-vague (moderate and brisk) units in penetrations showing clear reversals of RF progression were included in the analysis. Straight lines are linear regressions for the two classes of units. The eccentricities were translated from distance on the tangent screen to the view angle from area centralis and the receptive field sizes were calculated as the square root of the area of the ellipses used to model the receptive fields. The ratios between receptive field sizes and eccentricity were not significantly different for the two classes of units.

Discussion

In this study, we identified three architectonic subdivisions in bush baby PI. Two electrophysiologically defined retinotopic maps were found, one confined in PL and the other within ventral PL and PIcl, a new subdivision of PI that we were able to identify in this study. The central vision representations of both maps were found at the posterior end of the border between the two maps. We found that bush baby pulvinar receptive fields were slightly larger than those found in the macaque monkey, and they increased in size with eccentricity. We did not find qualitative differences in stimulus preferences between cells in the two maps. Below we discuss how the architectonic structure of bush baby PI and PL relate to their connection patterns and how their connections correlate with the retinotopic maps. We compare the retinotopic pulvinar maps in bush baby with those found in the New and Old World simian species, represented by macaque and cebus monkey, respectively. Finally, we propose two models of retinotopic organization that can account for bush baby pulvinar maps and the maps described previously in macaque monkey.

Architecture and Connections

With both architectonic and retinotopic information, we were able to establish subdivisions within bush baby PI that appear consistent with the subdivisions described in simian species (Stepniewska and Kaas, 1997; Gray et al., 1999). We used the nomenclature established in owl monkey since it appeared to fit best with the bush baby subdivisions (see Lin and Kaas (1979)). These subdivisions also bear similarity with PI subdivisions described in other simians. In owl monkey, PIm is defined uniquely by a dark myelin circle (Lin and Kaas, 1979). In macaque, CO staining of PI showed four bands demarcating PIcl, PIcm, PIm and PIp with alternating dark and light staining from lateral to medial (Gutierrez et al., 1995; Stepniewska and Kaas, 1997). In bush baby PIm showed a myelin circle, while PIcl, PIcm and PIm showed dark, light and dark alternating CO bands, suggesting homology with these subdivisions in simians.

A number of connectional studies in bush babies and macaques also support the chemoarchitectonic subdivisions we found in this study. In bush baby, both V1 and MT have been reported to employ two separate connections with the PI subdivisions that we defined as PIcl and PIm (Symonds and Kaas, 1978; Wall et al., 1982; Wong et al., 2009). Some connections with the temporal cortices have been found exclusively in PIcm among PI subdivisions (Raczkowski and Diamond, 1980, 1981). In macaque, PIcl and PIm also have been reported to have separate connections with MT (Ungerleider et al., 1984) and to receive separate inputs from V1 (Gutierrez and Cusick, 1997). Also, several studies showed that V2 projects to PIcl (Kennedy and Bullier, 1985; Raczkowski and Diamond, 1980) but not PIm (O'Brien et al., 2002; Raczkowski and Diamond, 1980) in both bush baby and macaque. Some interspecies differences, however, also have been reported to exist in the connection patterns between PI and higher visual areas. For example, the only PI subdivision that showed connections to DLr (the rostral dorsolateral visual area, considered to overlap with V4 in macaque) was PIm in bush baby (Raczkowski and Diamond, 1981), and PIcm in macaque (Kaas and Lyon, 2007).

PL and PI have been reported to receive inputs from several subcortical visual areas, including the superficial layers of the superior colliculus (SC) and the parabigeminal nucleus (Diamond et al., 1992). Parabigeminal projections appeared to be located within PL and PIcl (Diamond et al., 1992). The superficial layers of the superior colliculus have been shown to project to the posterior half of PI, and to a thin dorsal layer in PL (Diamond et al., 1992). Baldwin et al. (2011) further reported two chemoarchitectonic subdivisions at the caudal end of PI that receive from SC. These areas were identified by immunostaining for the vesicular glutamate transporter 2 (vGluT2). We were unable to correlate these areas with the chemoarchitectonic subdivisions identified in this study. More subdivisions may be found in bush baby PI and PL but different chemoarchitectonic methods will be required.

Retinotopic Maps in Pulvinar and their connections with Visual Cortex

The map features we found electrophysiologically were consistent with those observed in connectional studies. As expected from the connectional patterns, we found that a localized point in the paracentral visual field was represented as a curved strip of cells in the pulvinar, running roughly anterior-posterior, on a iso-eccentricity contour as seen in Figure 6B. The two strips curve toward the border between the two maps at their anterior ends, and meet at some point. Anatomical examples that match our maps can be seen in Symonds and Kaas (1978), showing V1 projections, and in the study by Carey et al. (1979), showing retrograde labeling from V1. In the latter study when a series of injections were made in V1 from the central to the peripheral representation, the strips of labeled pulvinar cells moved both anteriorly and away from the border between the dorsal and ventral maps (Carey et al., 1979). This pattern is consistent with a representation of central vision at the medio-posterior end of the border between the two visuotopic maps. Consistent with our findings concerning the upper and lower visual field representations, the lateral part of PI/PL has been reported to connect to lateral V1, which represents the upper visual field (Raczkowski and Diamond, 1981), while medial part of PI/PL has been reported to connect to medial V1, which represents the lower visual field (Raczkowski and Diamond, 1981; Conley and Raczkowski, 1990; Debruyn et al., 1993). The central-peripheral and upper-lower field axes in our maps are also consistent with those inferred from pulvinar-MT connections (see Wall et al. (1982); Wong et al. (2009)).

The two pulvinar visuotopic maps have cortical connections only with the early visual cortices. Both maps have major connections with V1, V2, V3, and to a lesser extent MT (Raczkowski and Diamond, 1981). Reciprocal connections with the temporal visual areas were reported to be restricted to either PM or the medial and ventral border of PI (Raczkowski and Diamond, 1980, 1981). Connections with the posterior parietal cortex were only found in PM (Glendenning et al., 1975; Raczkowski and Diamond, 1981).

Prosimian and simian pulvinar

The pulvinar of simians, particularly the pulvinar of anthropoid primates, is generally larger than that of studied prosimians (Chalfin et al., 2007). In the Old World simian macaque, the pulvinar is rotated laterally and posteriorly in comparison to that of the bush baby. Once these transformations have been accounted for, most architectonic and visuotopic map features appear to correspond nicely between these two species. In bush baby, the dorsal and ventral maps are found lateral to PIm, while in macaque they are found ventral, lateral and posterior to the MT recipient zone of PIm, consistent with an overall pulvinar rotation. The lateral map in macaque is analogous to the dorsal bush baby map we report here, and the inferior macaque map appears to correspond nicely to the ventral bush baby map. The upper field is represented laterally in both bush baby maps, and ventrally in both macaque maps. Under the same transformation the vertical sheet of HM representation in bush baby lies at a similar position in pulvinar as the mostly horizontal sheet of HM representation in macaque. Two major differences, however, exist between the two species. In macaque pulvinar, VM is represented on the border between the two maps, while in bush baby pulvinar VM is represented on the posterior and medial edges of that border. Additionally, in macaque the lateral map has a second order representation of the visual field, much like in V2, where the HM representation is split to form its anterior border. In bush baby, by contrast, both pulvinar visuotopic maps appear to have first order representations.

The two maps in bush baby pulvinar are similar in visual field representation to the ventrolateral map in the New World cebus pulvinar. The ventrolateral cebus map reported in Gattass et al. (1978) may, in fact, consist of two individual retinotopic maps. Cebus pulvinar is rotated laterally and posteriorly compared to bush baby pulvinar, as in the macaque. Instead of being located at the medio-posterior pole as in bush baby pulvinar maps, the central vision representation of the ventrolateral pulvinar map is

located on its latero-anterior border in cebus. If the bush baby pulvinar maps are rotated, most bush baby map features align nicely with those reported for the cebus ventrolateral map in pulvinar. These features include the shapes of both the VM and HM representations and their spatial relation (compare Figure 8A and Figure 9A of this paper to Figures 4C and 5 in Gattass et al. (1978)). Given its relation with the two bush baby pulvinar maps, the ventrolateral map in cebus pulvinar can be divided into two maps along the horizontal extension of the VM representation, where penetrations showed a reversal of receptive field progressions similar to the ones seen in bush baby. That border runs from the dorso-anterior end of the ventrolateral map to its ventro-posterior end. Since that border in cebus is not horizontal, however, double representations were not apparent in individual penetrations in that study. Instead, anterior penetrations can be predicted to encounter cells in the ventral visuotopic map with receptive fields adjacent to those belonging to posterior cells in the dorsal visuotopic map. Indeed, we can see examples of this double representation in the A+2 and A+0 penetrations in Figure 4 of Gattass et al. (1978), where the receptive fields in A+2, after the reversal, matched the receptive fields in A+0 before the reversal. Additionally, the cebus dorso-medial map appeared to be located in the equivalent position to dorsal medial PL (Pdm) in macaque (Petersen et al., 1985), which might correspond to a separate map dorso-anterior to the dorsal map in bush baby. The latter would require more data to confirm, however.

The second order representation reported in the lateral map of macaque pulvinar appears not to be shared by either cebus or bush baby. Given the orientation of the maps in bush baby, for the dorsal map to have a second order representation, most vertical penetrations should have started with receptive fields near HM, yet only a small part of our observed penetrations showed this feature. The cebus ventrolateral pulvinar map is reported as having straight, parallel iso-elevation contours (Gattass et al., 1978). Regardless of whether the cebus ventrolateral pulvinar map consists of one or two maps, this result suggests that there is no second order map in this area. The second order representation reported in macaque pulvinar map is thus specific to this species and suggests that this organization evolved separately in Old World simians.

A New Model for Maps in Thalamic Nuclei

The visual field is mapped onto the two dimensional sheet on the retina but is represented in a three dimensional volume in structures such as the pulvinar. Although the visual field is roughly represented the same way in different primates there are significant differences in detail. At least two models of visual field mapping exist in primate thalamus.

In the maps reported in macaque pulvinar, the VM representation covers half the surface of the map. Both HM and VM are represented as curved sheets. Central vision is represented as a long curve on the intersection between the HM and VM representations. Map features like the representations of VM, HM and the central vision are one dimension higher than the visual field features they represent: central vision, a point, is represented as a curve, and VM, a line, is represented as a sheet. There exist perfect iso-projection curves for each of the two macaque pulvinar maps such that each point on the same curve represents the same location in the visual field (Bender, 1981). In other words, when sliced perpendicular to local iso-projection curves, each slab of the map contains the full representation of the contralateral visual field. The way the pulvinar maps represent the visual field as described in macaque is similar to that of V1 and LGN. In both of these areas, the visual field is mapped onto one surface, with a column made of cells from different layers representing the same point in the visual field. With this organization, different visual functions could potentially be carried out in different slabs of the same map. One such hypothesis concerning pulvinar states that more anterior slabs relay visual signals between V1 and V2, while more posterior slabs relay signals between gradually higher levels in the visual hierarchy (Shipp, 2003, Figures 5-6).

In contrast to the macaque pulvinar maps, central vision is represented as a single point in both bush baby pulvinar maps, and VM is represented as a curve in both maps. In each of the maps, the

representation of the elevation axis is parallel to the VM representation, and the azimuth axis is represented on the polar axis of a polar coordinate system on planes perpendicular to the VM representation. This organization leaves the polar angle as the iso-projection axis. The iso-projection curves are roughly concentric to the central vision representation and parallel to the HM representation. Unlike the organization described in macaque pulvinar, there is no obvious way to subdivide such maps into divisions with full visual field representations. As a result, cells with different functions are more likely to be mixed in bush baby pulvinar rather than clustered. Indeed we found cells with different visual responses mixed in bush baby pulvinar.

These two different types of visuotopic organization are diagrammed in Figure 13. The left model represents the way the visual field is mapped in macaque pulvinar, while the right model shows how the visual field is mapped in the bush baby pulvinar. The difference in the shapes of certain map features, such as the central vision representation and VM, can be easily visualized. These models can be applied to other thalamic nuclei where 2-D sensory sheets are represented in a 3-D volume and where specific aspects of the sensory sheet are emphasized. For example, the map organization reflected in primate LGN conforms to the former model represented also by the macaque pulvinar. Cells with different functions achieve a higher level of clustering in the former model compared to the latter. This difference in pulvinar map organization may reflect the higher levels of differentiation in Old World simian pulvinar compared to both prosimian and New World simian pulvinar.

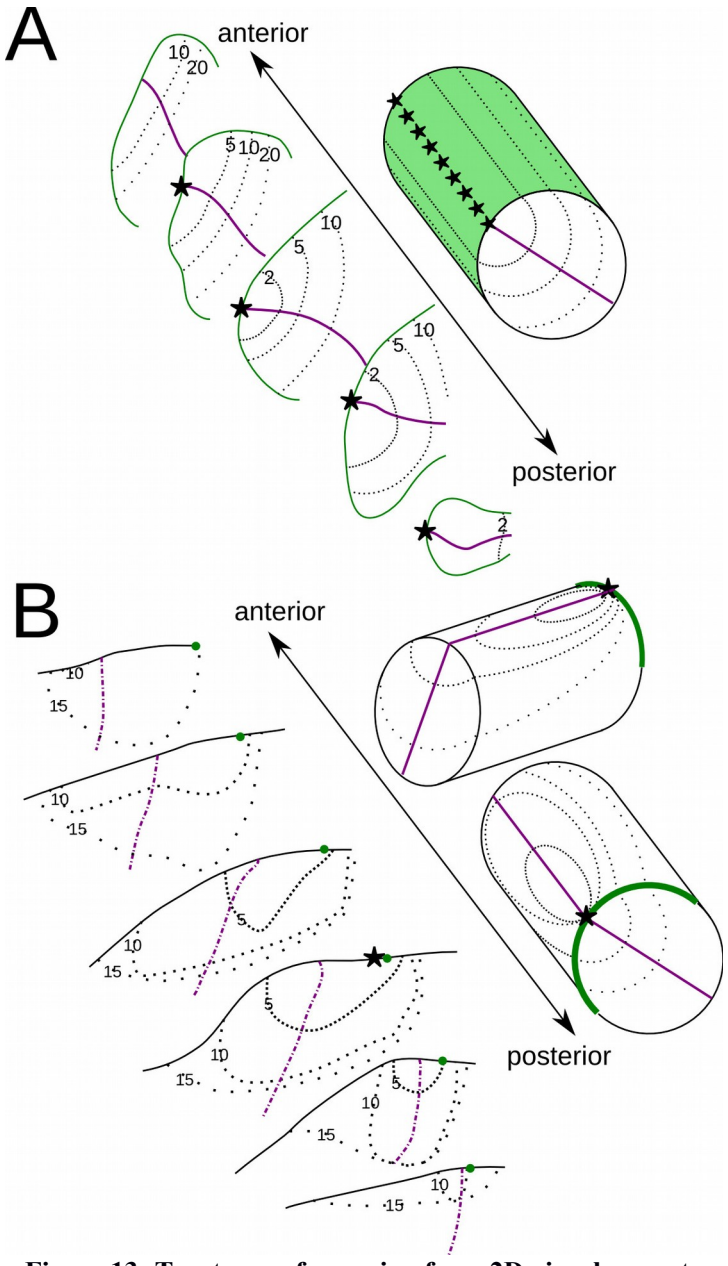

Figure 13: Two types of mapping from 2D visual space to 3D brain structure

Stars represent central vision. Thick dashed lines show the intersection of the horizontal meridian (HM) representations with the structure surface. The vertical meridian (VM) is shown as the gray surface in the left panel, and as a thick dotted line in the right panel. Note that most of the visible intersection between HM and the surface in the left panel is also the intersection between the HM and VM representations, and thus the central vision representation. Thin dotted lines and dashed lines are iso-azimuth and iso-elevation contours, respectively. The VM representation line in the right panel is only on the structure surface, in contrast to all other lines representing the intersection between a plane in the structure and the structure surface. The left configuration is analogous to the maps reported in macaque pulvinar by Bender (1981), the right analogous to the one found in bush baby pulvinar in this study.

References

Allison J, Casagrande V. 1994. Receptive field structure of v2 neurons in the prosimian primate *galago crassicaudatus*. In: Society of neuroscience annual meeting.

Arend I, Rafal R, Ward R. 2008. Spatial and temporal deficits are regionally dissociable in patients with pulvinar lesions. *Brain* **131**:2140–2152.

Baldwin M, Balaram P, Kaas J. 2011. Superior colliculus connections and vGLUT2 expression within visual thalamus of prosimian galagos (*otolemur garnettii*). In: Neuroscience meeting planner. Washington, DC: Society for Neuroscience.

Bender D. 1981. Retinotopic organization of macaque pulvinar. *Journal of Neurophysiology* **46**:672–693.

Bender D. 1982. Receptive-field properties of neurons in the macaque inferior pulvinar. *Journal of Neurophysiology* **48**:1–17.

Berman R, Wurtz R. 2011. Signals conveyed in the pulvinar pathway from superior colliculus to cortical area mT. *Journal of Neuroscience* **31**:373–384.

Boyd J, Matsubara J. 1996. Laminar and columnar patterns of geniculocortical projections in the cat: Relationship to cytochrome oxidase. *Journal of Comparative Neurology* **365**:659–682.

Carey R, Fitzpatrick D, Diamond I. 1979. Layer i of striate cortex of *tupaia glis* and *galago senegalensis*: Projections from thalamus and claustrum revealed by retrograde transport of horseradish peroxidase. *Journal of Comparative Neurology* **186**:393–437.

Chalfin B, Cheung D, Muniz J, De Lima Silveira L, Finlay B. 2007. Scaling of neuron number and volume of the pulvinar complex in new world primates: Comparisons with humans, other primates, and mammals. *Journal of Comparative Neurology* **504**:265–274.

Conley M, Raczkowski D. 1990. Sublaminar organization within layer vI of the striate cortex in galago. *Journal of Comparative Neurology* **302**:425–436.

Debruyn E, Casagrande V, Beck P, Bonds A. 1993. Visual resolution and sensitivity of single cells in the primary visual cortex (v1) of a nocturnal primate (bush baby): Correlations with cortical layers and cytochrome oxidase patterns. *Journal of Neurophysiology* **69**:3–18.

Diamond I, Fitzpatrick D, Conley M. 1992. A projection from the parabigeminal nucleus to the pulvinar nucleus in galago. *Journal of Comparative Neurology* **316**:375–382.

Emmers R, Akert K, Woolsey C eds. 1963. A stereotaxic atlas of the brain of the squirrel monkey (*saimiri sciureus*). 1st ed. University of Wisconsin Press Madison.

Gallyas F. 1979. Silver staining of myelin by means of physical development. *Neurological Research* **1**:203–209.

Gattass R, Oswaldo-Cruz E, Sousa A. 1978. Visuotopic organization of the cebus pulvinar: A double representation of the contralateral hemifield. *Brain Research* **152**:1–16.

Geneser-Jensen F, Blackstad T. 1971. Distribution of acetyl cholinesterase in the hippocampal region of the guinea pig. *Cell and Tissue Research* **114**:460–481.

Glendenning K, Hall J, Diamond I, Hall W. 1975. The pulvinar nucleus of *galago senegalensis*. *Journal of Comparative Neurology* **161**:419–457.

Gray D, Gutierrez C, Cusick C. 1999. Neurochemical organization of inferior pulvinar complex in squirrel monkeys and macaques revealed by acetylcholinesterase histochemistry, calbindin and cat-301 immunostaining, and *wisteria floribunda* agglutinin binding. *Journal of Comparative Neurology* **409**:452–468.

Gutierrez C, Cusick C. 1997. Area v1 in macaque monkeys projects to multiple histochemically defined subdivisions of the inferior pulvinar complex. *Brain Research* **765**:349–356.

Gutierrez C, Yaun A, Cusick C. 1995. Neurochemical subdivisions of the inferior pulvinar in macaque monkeys. *Journal of Comparative Neurology* **363**:545–562.

Hendry S, Reid R. 2000. The koniocellular pathway in primate vision. *Annual Review of Neuroscience* **23**:127–153.

Hubel D, Wiesel T. 1974. Uniformity of monkey striate cortex: A parallel relationship between field size, scatter, and magnification factor. *Journal of Comparative Neurology* **158**:295–305.

Huerta M, Krubitzer L, Kaas J. 1986. Frontal eye field as defined by intracortical microstimulation in squirrel monkeys, owl monkeys, and macaque monkeys: I. subcortical connections. *Journal of Comparative Neurology* **253**:415–439.

Jerison H. 1979. Brain, body and encephalization in early primates. *Journal of Human Evolution* **8**:615–635.
Johnson J, Casagrande V. 1995. Distribution of calcium-binding proteins within the parallel visual pathways of a primate (*galago crassicaudatus*). *Journal of Comparative Neurology* **356**:238–260.
Kaas J, Lyon D. 2007. Pulvinar contributions to the dorsal and ventral streams of visual processing in primates. *Brain Research Reviews* **55**:285–296.
Kennedy H, Bullier J. 1985. A double-labeling investigation of the afferent connectivity to cortical areas v1 and v2 of the macaque monkey. *Journal of Neuroscience* **5**:2815–2830.
Lin C, Kaas J. 1979. The inferior pulvinar complex in owl monkeys: Architectonic subdivisions and patterns of input from the superior colliculus and subdivisions of visual cortex. *Journal of Comparative Neurology* **187**:655–678.
Merabet L, Desautels A, Minville K, Casanova C. 1998. Motion integration in a thalamic visual nucleus. *Nature* **396**:265–268.
O'Brien B, Abel P, Olavarria J. 2002. Connections of calbindin-d28k-defined subdivisions in inferior pulvinar with visual areas v2, v4 and mT in macaque monkeys. *Thalamus & Related Systems* **1**:317–330.
Petersen S, Robinson D, Keys W. 1985. Pulvinar nuclei of the behaving rhesus monkey: Visual responses and their modulation. *Journal of Neurophysiology* **54**:867–886.
Petersen S, Robinson D, Morris J. 1987. Contributions of the pulvinar to visual spatial attention. *Neuropsychologia* **25**:97–105.
Raczkowski D, Diamond I. 1980. Cortical connections of the pulvinar nucleus in galago. *Journal of Comparative Neurology* **193**:1–40.
Raczkowski D, Diamond I. 1981. Projections from the superior colliculus and the neocortex to the pulvinar nucleus in galago. *Journal of Comparative Neurology* **200**:231–254.
Robinson D, Petersen S. 1985. Responses of pulvinar neurons to real and self-induced stimulus movement. *Brain Research* **338**:392–394.
Sherman S. 2007. The thalamus is more than just a relay. *Current Opinion in Neurobiology* **17**:417–422.
Shipp S. 2003. The functional logic of cortico-pulvinar connections. *Philosophical Transactions of the Royal Society of London. Series B, Biological Sciences* **358**:1605–1624.
Stepniewska I, Kaas J. 1997. Architectonic subdivisions of the inferior pulvinar in new world and old world monkeys. *Visual Neuroscience* **14**:1043–1060.
Symonds L, Kaas J. 1978. Connections of striate cortex in the prosimian, *galago senegalensis*. *Journal of Comparative Neurology* **181**:477–511.
Theyel B, Llano D, Sherman S. 2010. The corticothalamocortical circuit drives higher-order cortex in the mouse. *Nature Neuroscience* **13**:84–88.
Ungerleider L, Desimone R, Galkin T, Mishkin M. 1984. Subcortical projections of area mT in the macaque. *Journal of Comparative Neurology* **223**:368–386.
Van Essen D. 2005. Corticocortical and thalamocortical information flow in the primate visual system. *Progress in Brain Research* **149**:173–185.
Walker A ed. 1938. The primate thalamus. University of Chicago press.
Wall J, Symonds L, Kaas J. 1982. Cortical and subcortical projections of the middle temporal area (mT) and adjacent cortex in galagos. *Journal of Comparative Neurology* **211**:193–214.
Wong P, Collins C, Baldwin M, Kaas J. 2009. Cortical connections of the visual pulvinar complex in prosimian galagos (*otolemur garnettii*). *Journal of Comparative Neurology* **517**:493–511.
Wong-Riley M. 1979. Changes in the visual system of monocularly sutured or enucleated cats demonstrable with cytochrome oxidase histochemistry. *Brain Research* **171**:11–28.

CHAPTER 4

PULVINAR PROJECTIONS TO V1 LAYER 1 IN A PRIMATE

Introduction

Pulvinar is the largest thalamic nucleus in primates and connects extensively with various visual cortical areas. Despite decades of research, the exact functional role of pulvinar in vision remains unknown. Within the visual system, the pulvinar occupies the position of a "higher order" thalamic nucleus, receiving heavy projections from the primary visual cortex (Campos-Ortega, 1968; Raczkowski and Diamond, 1978, 1981; Hollander, 1974). The retinotopic maps in the lateral pulvinar (PL) appear to be downstream of V1 based on data showing the total loss of visual responses after V1 lesions in macaque in monkey (Bender, 1981, 1983). It has been proposed that, at least for some pathways, the pulvinar functions as a higher order relay between cortical areas (Sherman and Guillery, 2002) including between V1 and V2.

In a hierarchical model, the projections from the primary sensory nuclei to the cortex have been considered to carry the main sensory information to (or "drive") the cortex and their associated features have been described as characteristics of driving projections (Sherman and Guillery, 1998). Rockland and Pandya (1979), and subsequently Felleman and Van Essen (1991), argued that input to cortical layer 3/4 defined feedforward driving projections and that input above or below layer 3/4 defined feedback modulatory input in the cortex, as all primary sensory nuclei project to layer 3/4 of the cortex (Sherman and Guillery, 1998, 2006, pp 8–13; Jones, 1998) and feedback projections from higher order cortical areas to primary cortical areas avoid layer 4 (Felleman and Van Essen, 1991). Since pulvinar sends axons both to layer 1 of V1 and layer 3/4 of all extrastriate visual areas, how does it fit into this hierarchical model?

Primate pulvinar sends projections to layer 1 of cortex, terminating broadly in the occipital and temporal cortex, including the primary visual cortex (V1), secondary visual cortex (V2), visual area number three (V3), visual area number four (V4) and the middle temporal area (MT) (Rockland et al., 1999). In extrastriate areas, these layer 1 projections from pulvinar are always accompanied by much more robust layer 3/4 pulvinar projections (Rockland et al., 1999). In contrast, in area V1, pulvinar only projects to layers 1-3, and most robustly to layer 1 (Ogren and Hendrickson, 1977; Rezak and Benevento, 1979; Benevento and Rezak, 1976). This special thalamocortical projection from pulvinar to V1 that evades layer 4 and focuses on layer 1, raising a second question: how similar or dissimilar are pulvinar to layer 1 projections between V1 and extrastriate visual areas?

In a previous report, we discovered that net inhibition occurred in V1 layer 2/3 following pulvinar inactivation (Purushothaman et al., 2012). This net inhibition of layer 2/3 pyramidal cells was greatest when cells are stimulated with drifting gratings of their preferred orientation, sometimes resulting in below baseline response to visual stimulation at that preferred orientation. The functional contribution of pulvinar projections to V1 layer 2/3 cells also is retinotopically localized. Specifically, local pulvinar cell activation caused retinotopically matched enhancement of activity in V1, but suppression of activity in the surrounding cells in V1 (Purushothaman et al., 2012). Pulvinar activation was even able to evoke V1 neuron activity when LGN input to V1 was blocked (Purushothaman et al., 2012). This result suggests that pulvinar projections to V1 have very strong functional impact, since the layer 2/3 pyramidal cells are normally under strong inhibition (Holmgren et al., 2003). Furthermore, in layer 1, local gamma-aminobutyric acid (GABA) expressing interneurons have been found to only co-innervate target spines with thalamocortical input that express vesicular glutamate transporter 2 (vGluT2), but not cortico-cortical input that express vGluT1 (Kubota et al., 2007). This specific inhibition puts thalamocortical

projections, such as pulvinar projections to V1, at a disadvantage when it comes to controlling cortical output. This strong physiologically demonstrated control of V1 output by pulvinar appears to conflict with the proposal that thalamic input to layer 1 defines a modulatory input.

Layer 1 of cortex is dominated by axons and dendrites, with a few cells bodies that belong to GABAergic interneurons (Winer and Larue, 1989). Pyramidal cells residing in both layer 2/3 and layer 5 spread their apical dendrites in layer 1. Any projections onto such distal dendrites would need to have high spatial/temporal summation to reach the threshold of these cells (Rubio-Garrido et al., 2009). There are several ways pulvinar axons synapsing in layer 1 could interact with the apical dendrites of layer 2/3 pyramidal cells. In addition to direct synapses onto the dendritic arbor, the pulvinar projections to V1 layer 1 could recruit local GABAergic interneuronal networks in two different fashions. Metabotropic glutamate receptor 2 (mGluR2) has been shown to mediate glutamate triggered inhibitory postsynaptic potential in the primary sensory cortex (Lee and Maunsell, 2009). Since mGluR2 is heavily expressed in V1 layer 1 (Koo et al., 2013), the pulvinar projections, which are glutamatergic (Jones, 2007), could inhibit electrically coupled interneurons via mGluR2, and in turn disinhibit the layer 2/3 pyramidal cells. Neurogliaform cells (NGFC) are densely populated in V1 layer 1/2 and form large electrically coupled interneuronal networks (Wozny and Williams, 2011; Jiang et al., 2013). These networks are able to greatly amplify signals and enhance the disinhibitory effect of pulvinar projections if recruited. The NGFC network exerts strong inhibition on layer 2/3 cells (Wozny and Williams, 2011), and could be a prime target of any disinhibition effort from thalamocortical projections. Another potential pathway is through single bouquet cells (SBC), which were found in layer 2 and may have dendrites extending into layer 1. SBC have been reported to have net disinhibitory effect on pyramidal cells by inhibiting several other classes of interneurons (Jiang et al., 2013)

In this study, we provide a first description of the morphology of pulvinar projections to V1 layer 1 in a primate and compare that with pulvinar projections to extrastriate areas V2 and V3. Additionally, we compare the pulvinocortical projections to those known to drive the cortex from the lateral geniculate nucleus (LGN), which sends axons primarily in layer 4 of V1 (Florence and Casagrande, 1987). In examining the ultrastructure of the projections from pulvinar to V1 layer 1, we also examine several hypotheses on the anatomical circuitry that underlie the strong pulvinar control on V1 we discovered (Purushothaman et al., 2012).

Methods

Subjects

Eighteen Bush Babies (*Otolemur garnettii*) of both species ranging in age from 6 months to 10 years were used. These animals were cared for according to the National Institutes of Health Guide for the Care and Use of Laboratory Animals and according to a protocol approved by the Vanderbilt University Institutional Animal Care and Use Committee (IACUC). To reduce the number of these valuable primates used in experiments, some of these animals were used in a separate physiological study involving the other hemisphere.

Surgery and Tracer Injections

The animals were initially anesthetized with ketamine for intubation. Subsequently, they were anesthetized with propofol and nitrous oxide and with the muscle relaxant vecuronium bromide to control eye movements. The lateral (PL) and inferior (PI) pulvinar were carefully mapped with single tungsten electrodes (FHC, Inc., ME) using visually evoked potentials in response to simple stimuli such as light bars and dots. Tracer injections were made near the central vision representations of the maps in PI and PL. Only cases where the tracer remained within the pulvinar and where axons in V1 were well-labeled

were used in this study. Injections were made with in-house manufactured injectrodes that allowed extracellular recording while pressure injecting the tracer at the same locations. 300-450nl of 20kD 10% biotinylated dextran (BDA), or 20kD dextran conjugated to Alexa-fluor 488 (Invitrogen, Life Technologies, NY) were injected for light microscopic examination. 1500nl of 20kD or 3kD 10% BDA was injected into pulvinar for electron microscope examination. The animal was revived after the injection, and, after the appropriate survival time, was perfused transcardially with either a 0.5% glutaraldehyde and 4% paraformaldehyde fix or a 2% glutaraldehyde and 2% paraformaldehyde fix, after a survival period. The survival period was 9-10 days for the 3kD BDA injections, and 2-4 weeks for the other types of tracers. Details of the surgery and tracer injections were the same as used in our previous report (Marion et al., 2013).

Tissue processing and tracer visualization

The brain was stereotaxically blocked in the coronal plane before removal. For light microscopy, the tissue was sectioned frozen coronally to 30-52μm. BDA was visualized by incubating sections free-floating in 1:400 or 1:500 streptavidin Alexa-fluor 488 or streptavidin Alexa-fluor 568 (Invitrogen, NY) in tris buffered saline (TBS) for 2 hours. Alternate coronal sections were used for tracer examination and stained for cytochrome oxidase (CO) to reveal cortical areas and layers. The CO staining method was as described previously (Boyd and Matsubara, 1996).

Electron Microscopy

Eight of the eighteen cases were used for EM examination of pulvinar axons in V1. All of these cases showed tracer injections that were confined to pulvinar and did not spread to LGN. They also showed good tracer transport to V1 under LM examination. In these cases, after the perfusion and coronal blocking, the animal's brain was removed and immediately cut coronally at 80-120μm using a vibratome. The BDA labeled pulvinar axons were visualized with either streptavidin conjugated horseradish peroxidase (HRP) followed by tetramethylbenzidine (TMB) and diaminobenzidine (DAB) for 10kD BDA (Shostak et al., 2003), or a standard ABC kit followed by DAB reaction (Ichida et al., 2014). Sections showing BDA labeled axons in V1 were selected and postfixed in 1% osmium tetroxide, dehydrated in an ethanol series, and flat embedded in EPON or Durcupan resin between 2 sheets of Aclar plastic (Electron Microscopy Sciences, PA). Cortical layer 1 of selected areas of V1 were cut off and mounted on EPON resin blocks, and cut into ultrathin sections of 65-70nm, which were collected on carbon backed, Formvar coated nickel slot grids. Ultrathin sections near the surface of the original sections were selected, and immunostained for the presence of gamma amino butyric acid (GABA). The immunostaining was done by incubating the sections in 1:300 rabbit anti-GABA antibodies in tris-buffered saline with 0.1% Triton-X (TBST) of pH 7.6 overnight, and then incubating the sections in 1:20 goat anti-rabbit secondary conjugated to 15nm gold particles in TBST of pH 8.2 for 1 hour. The GABA stained sections were then stained with 2% uranyl acetate for 30min and 8% lead citrate and air dried.

Bouton size quantification

For bouton size quantification, sections were selected from the center of the pulvinar projection foci in V1 by eye. Due to the wide spread of pulvinar axons in V1, we selected sections with multiple layer 2/3 arbors from the pulvinar, under the assumption that such sections contain the center of projections, where the axons move radially from the white matter to the superficial cortical layers. The bouton size distributions we used to compare with the pulvinar to V1 boutons were taken from previous reports using similar methods (Marion et al., 2013, Marion et al. (2014)), where confocal stacks were taken partly from the center of projection foci, and partly from the periphery of these foci. However, no significant

difference was found between the bouton sizes at center and periphery of projection foci, and those two types of stacks were pooled together in our comparison.

High power confocal stacks of boutons were taken using a Zeiss 510 confocal microscope equipped with a 63x 1.4 NA objective. Once a stack had been acquired an observer naive to the origin of the stack was recruited to identify boutons in the stack. For each bouton, the areas at half maximum intensity on the image flattened across the Z axis was taken as its area. All bouton identified in this study were larger than the 2D resolution of the microscope ($0.07\mu m^2$). In rare cases, some boutons on the images contained saturated pixels, complicating the identification of half-peak contours. These boutons did not tend to be of a specific size, and were excluded from calculations. When a stack contained too many boutons, only boutons in a central column that occupied ~50% of the area of the stack or contained ~25% of the boutons in the stack were used.

Ultrastructural Analysis

Ultrathin sections were examined under the electron microscope (Tecnai 12, FEI, OR). All labeled pulvinar axons involved in a synapse were photographed, and synapses in the same section not involving labeled axons were randomly photograph to serve as controls. For synapses not involving labeled pulvinar axons, the pre- and post- synaptic profiles were determined on basis of the existence of presynaptic vesicles. The ultrastructural features of adjacent terminals also were noted. The areas of the presynaptic profiles involved in photographed unlabeled synapses, as well as those postsynaptic to labeled pulvinar axons, were measured and the number of gold particles in all of these profiles counted. The densities of gold particles in presynaptic profiles of asymmetric and symmetric synapses were used as negative and positive controls of GABA immunostaining, respectively.

Statistical Analysis

Since we did not find significant differences between the bouton sizes of the same projection type between samples taken from individual animals these data were pooled for all animal cases. Since the bouton sizes of some projection types involved in our comparison (pulvinar to V1 layer 1, and V1 to V2 layer 4) deviate strongly from a normal curve for some projection types involved (Shapiro-Wilk test, pulvinar to V1 layer 1, $p = 6.44E\text{-}7$; V1 to V2 layer 4, $p = 2.46E\text{-}7$). As a result, we used non-parametric methods for our comparisons. The bouton areas of different projection types were compared using a Kruskal Wallis test followed by a Bonferroni corrected Wilcoxon rank-sum test.

To establish the level of gold particle densities for positive and negative controls in sections immunostained to reveal the presence of GABA, we first calculated the distributions of gold particle density in the presynaptic profiles of asymmetric (presumed non-GABAergic) synapses and presynaptic profiles of symmetric (presumed GABAergic) synapses. The profiles to be quantified were outlined by hand, after an EM picture was taken and its contrast enhanced in GIMP (version 2.8.14, www.gimp.org). We approximated the membrane boundaries of these profiles as precisely as possible, and ran a straight line between the nearest visible membrane positions. After outlining the profiles, we compared the distribution of gold particle density in the postsynaptic profiles labeled pulvinar axons with the positive and negative controls with a Kolmogorov-Smirnov test.

Results

Tracer Injections

Injections of label in pulvinar were limited to PL. Some of these injections were described in detail previously in (Marion et al., 2013). Briefly, sixteen successful pulvinar injections were made in 13 cases.

Among these cases, 7 were treated for EM examination, of which 4 showed suitable morphology for data collection. Reconstructed injections consisted of tracks where injections were made at one or two points along the track. Injections tended to be widest in the dorsal ventral axis with the largest injection being approximately 1.1 mm in the dorsal ventral axis. Electrophysiological recordings from the tip of the injectrodes along with images of the sections (both CO and fluorescent) containing the injections were compared with the bush baby visuotopic maps of pulvinar (Li et al., 2013), confirming that the vast majority of all injections fell within the dorsal pulvinar map. Several injections, however, crossed the border between the dorsal and ventral retinotopic maps and covered the central vision representations of both. A typical tract in which two injections were made is presented in Figure 14.

Overview of the layer 1 projections from pulvinar

Projections from the pulvinar to the cortex were observed in areas V1, V2, V3, MT and a number of other areas lying in the occipital, parietal and temporal cortices (see also Rockland et al., 1999). Pulvinar axons that terminated in V1 (Figure 15) tended to ascend through the layers in a vertical, columnar manner, generally without branching in other layers and were only seen to arborize once they reached layer 1 (see below for exceptions). No pulvinar axons in V1 were observed to have boutons in layers 3 and 4. Typically these axons made a right angle turn in lower layer 1 and then arborized in the outer half of layer 1 (layer 1a). The axons then traveled for great distances forming *en passant* boutons and branching occasionally (Figure 16A). Although we could not fully reconstruct these axons it was clear that many of them arborized over a distance of more than ~800 μm, significantly more than the average width of a single column (530μm) in V1 (see Xu et al., 2005). The border between the upper and lower halves of layer 1 was also a common place for axons to branch where they would send collaterals off in opposite directions.

Less commonly observed were axons that ascended to the very top of layer 1 without turning at right angles, and only arborize locally. A few axons did produce boutons as they passed through the inner half of layer 1, but extensive arbors were never seen. Infrequently, axons were observed to form arbors in layers 2/3. These arbors had a different appearance, and like the LGN arbors ending in layer 4 (see Florence and Casagrande, 1987), these arbors tended to remain confined to an area smaller than a single vertical column (Figure 16B). Furthermore, these axons would continue to climb into layer 1 and arborize more broadly.

Pulvinar projections to V2 and V3 showed similar patterns -- we briefly describe them here. These projections mainly terminated in layer 3/4 with a small minority terminating in lower layer 2 and upper layer 1. Therefore, unlike in V1, the bulk of pulvinar projections in extrastriate areas was found in the middle layers, mainly layer 4. The axons extending to layer 1 branched in a similar manner as that described for axons terminating in V1, running in the outer half of layer 1 (Figure 17). The tangential spread of such axons, however, matched the spread of axons in layer 3/4 below them, which were confined within single columns. The branches found in layer 1 and layers 3/4 are likely from the same axons, as no axons were found without branches and boutons in layer 3/4.

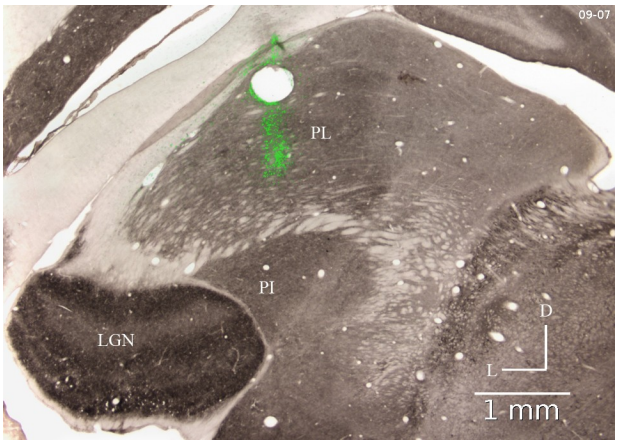

Figure 14: Tracer injection site in pulvinar

A coronal section stained for cytochrome oxidase (CO) overlaid on an adjacent section stained flourescently (green) for the injected tracer. The pulvinar injection was centered on the central vision representation in lateral pulvinar (PL). PI: inferior pulvinar; LGN: lateral geniculate nucleus; D: dorsal; L: lateral.

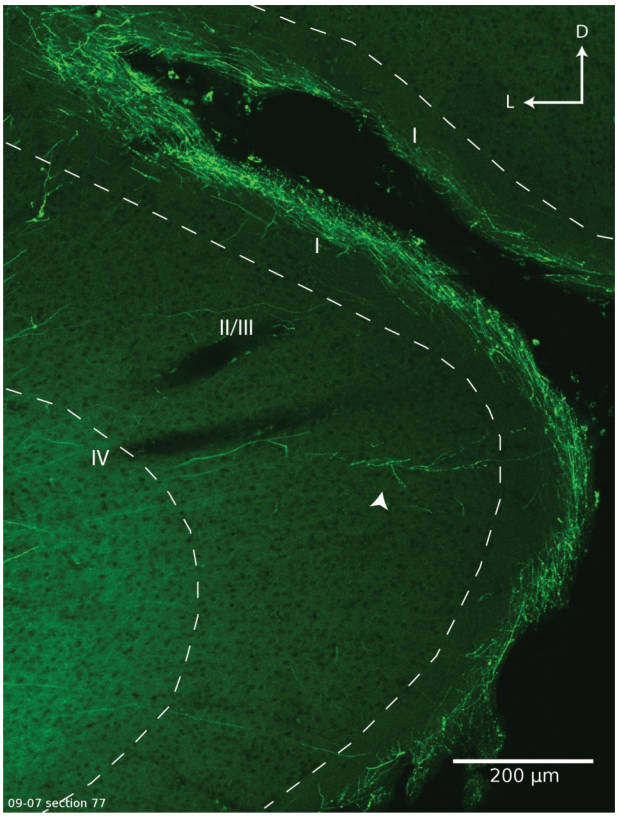

Figure 15: Pulvinar axon distribution in V1

Confocal photomicrograph of pulvinar projections (green) to the calcarine fissure in primary visual cortex (V1). Pulvinar axons can be seen to form arbors in a dense band in the outer half of layer 1. Occasional arbors are also observed in the upper part of layers 2-3 (arrow). D: dorsal; M: Medial.

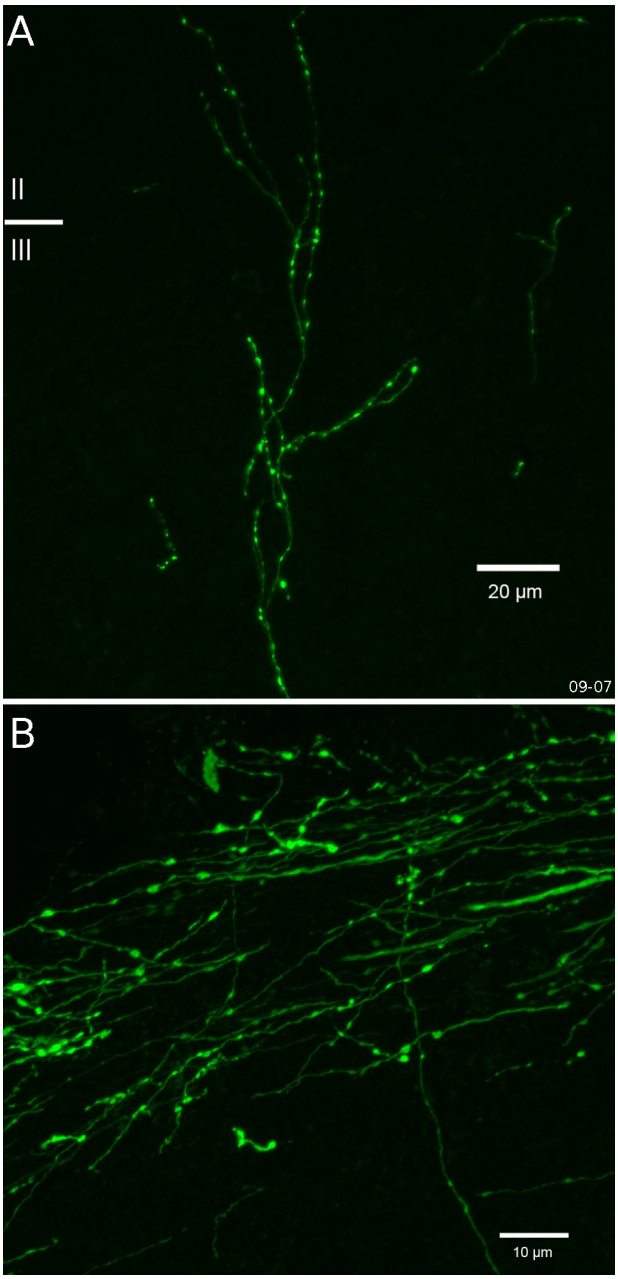

Figure 16: High power confocal images of pulvinar axons in V1

High power confocal photomicrographs of pulvinar projections to V1 layer 1 (**A**) and layer 2/3 (**B**). Axons in layer 1 tended to run within the upper single sub layer while axons in layer 2/3 tended to arborize oblique to the layer border. In panel **B** layer boundaries are not within the plain of the image and cortical surface lies above the top of the image.

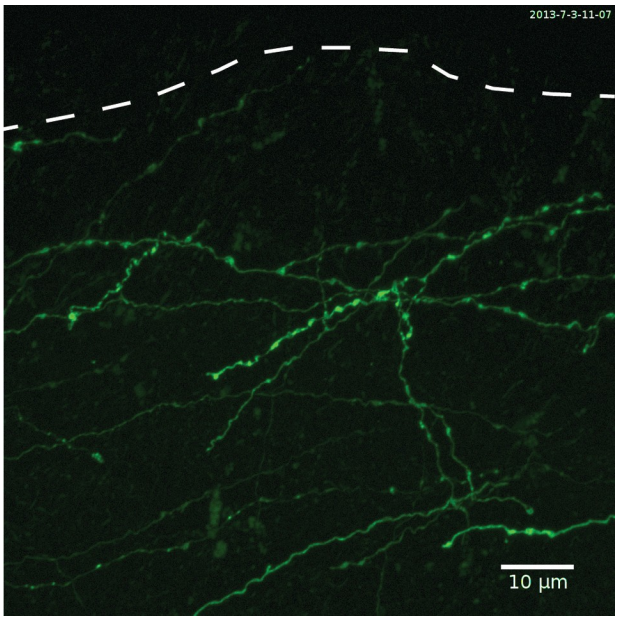

Figure 17: High power confocal image of pulvinar axons in V2

High power confocal photomicrograph of pulvinar projections (green) to layer 1 of the secondary visual cortex (V2). Axons forming terminals in layer 3 preceded to the outer part of layer 1, where they arborized similarly to the pulvinar axons in V1, but with a more limited tangential spread. The dashed line indicate the cortical surface.

Comparison of bouton sizes in V1 and V2

There is evidence that the size of presynaptic enlargements might act as a proxy measurement for functional impact or post synaptic strength (Pierce and Lewin, 1994; Sherman and Guillery, 1996; Marion et al., 2013). With this in mind we closely examined and quantified the boutons on pulvinar projections to layer 1 in V1 and V2. As described above, the vast majority of boutons observed were of the *en passant* type with only an occasional stalk like terminal. We subsequently compared these axons and boutons to those from the pulvinar to V2 layer 4 baby. The latter have bouton sizes comparable to other feedforward projections such as those from LGN to V1 (Marion et al., 2013). As presented in previous work (Marion et al., 2013), the layer 4 boutons in V2 have a median area of 0.48 μm^2 with a mean of 0.47 μm^2 (SEM = 0.002 μm^2, n = 87) (Marion et al., 2013). Boutons in layer 1 of V1 were measured in 4 samples in 4 cases and found to have median area of 0.33 μm^2 with a mean of 0.38 μm^2 (SEM = 0.001 μm^2, n = 97). Due to the sparseness of boutons in layer 1 of V2, only 2 samples in 2 cases could be quantified yielding median areas of 0.34 μm^2 with a mean of 0.33 μm^2 (SEM = 0.004 μm^2, n = 38).

These three projection types from the pulvinar have significantly different bouton sizes (Krusakl-Wallis test, H = 22.96, p = 1.03E-5). When compared pair-wise, pulvinar axons in the layer 1 of both V1 and V2 have similarly sized boutons, which are significantly smaller than pulvinar boutons in V2 layer 4 (Wilcoxon rank sum test; V1 layer 1 vs. V2 layer 1, T = 0.69, p = 0.49; V1 layer 1 vs. V2 layer 4, T = -4.14, p = 3.48E-5; V2 layer 1 vs. V2 layer 4, T = -4.00, p = 6.47E-5). A comparison is shown in Figure 18, together with measurements from three other typical "driving" projections in the early visual system. The distribution bouton sizes of pulvinar axons in V1 layer 1 showed a heavy and positive skew, much more so than what can be seen in the other two projection types (Non-parametric skew: V1 layer 1: 0.26, V2 layer 1: -0.048, V2 layer 4: -0.032).

Synapses and synaptic targets of pulvinar axons in V1 layer 1

We examined the ultrastructure of pulvinar axons in V1 to determine whether they synapsed with GABAergic interneurons or with the apical dendrites of pyramidal cells, and whether the post-synaptic density employed mGluR2.

Consistent with our light microscopy result, labeled pulvinar axons were only found close to the cortical surface. In three cases we were able to identify a large number of labeled pulvinar axons in their ultrathin sections. A segment of ~500μm of cortical surface at the center of the most dense projections was taken for EM examination. We sampled all the labeled pulvinar axon from the best ultrathin sections sectioned from these segments. A total of 83 synapses were analyzed. An example is shown in Figure 19A. The pulvinar axons in V1 layer 1 often formed multiple synapses with surrounding neurons. In some cases presynaptic profiles were also found adjacent to these pulvinar axons, however, any potential synapses they may form on the pulvinar axons were, unfortunately, obscured by the stain we used to label the pulvinar axons. Some of these adjacent pre-synaptic profiles were GABA positive (see below). One example of a pulvinar axon synapsing on a GABA negative profile, and surrounded by pre-synaptic profiles can be seen in Figure 19B.

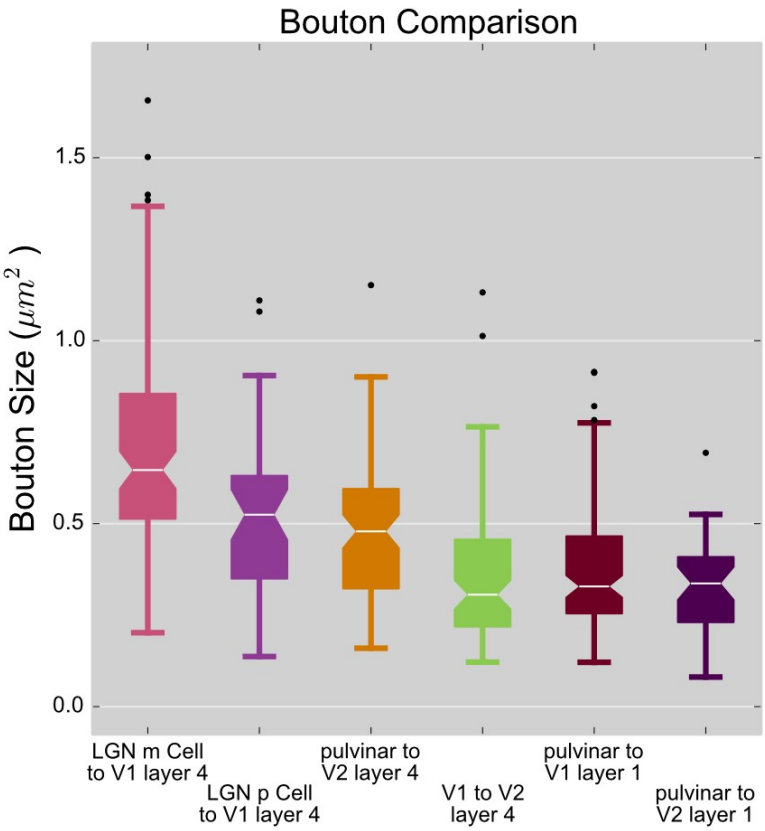

Figure 18: Bouton sizes of some projections in early visual system

Boxplot comparing the bouton sizes of different projection types in the early visual system. Columns from left to right represent projections 1) from LGN m cells to V1 layer 4; 2) from LGN p cells to V1 layer 4; 3) pulvinar to V2 layer 4; 4) V1 to V2 layer 4; 5) pulvinar to V1 layer 1; 6) pulvinar to V2 layer 1. Roughly, 3 tiers of bouton sizes can be found in the early visual system. LGN m cells have the largest boutons in V1. LGN p cells have boutons similar to those of pulvinar projections to V2 layer 4. V1 to V2 layer 4, pulvinar to layer 1 of both V1 and V2 have the smallest boutons among those compared here.

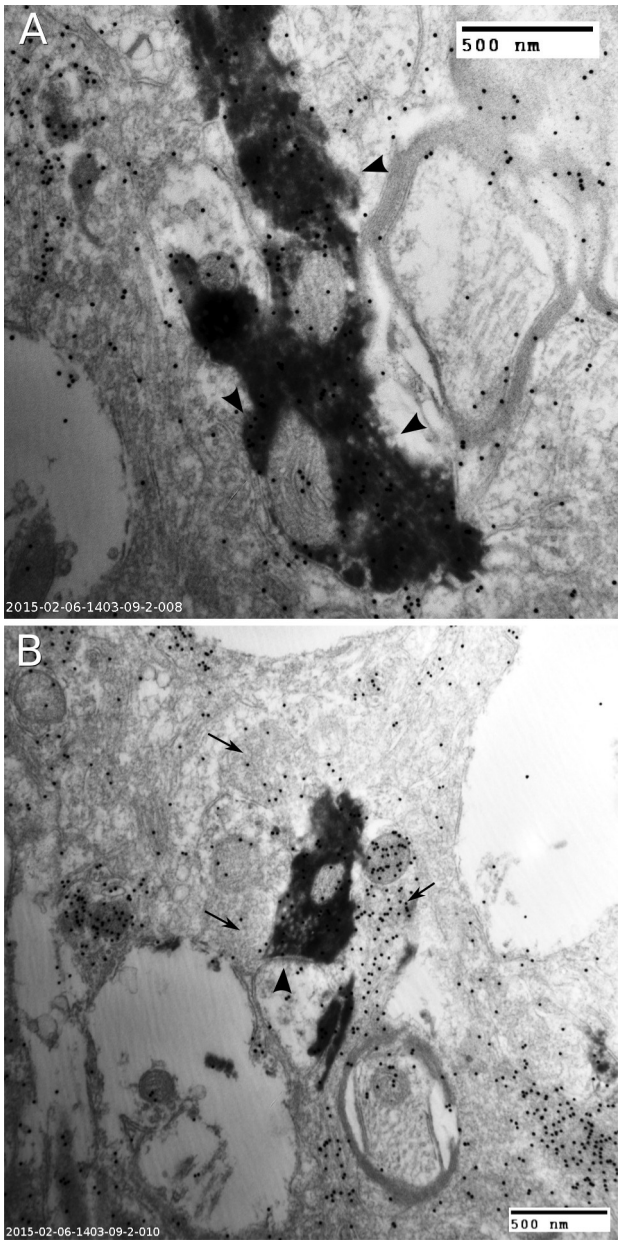

Figure 19: Example labeled pulvinar axons in V1 layer 1

Two examples of labeled pulvinar axons in V1 layer 1. **A**: a labeled pulvinar axon (black) synapsing with multiple post-synaptic profiles in V1 layer 1. All of these profiles show negative GABA immunostaining (black dots). Black arrowheads point to the synapses that can be clearly seen on this section. **B**: a pulvinar axon synapsing with a single post-synaptic profile. This axon terminal is surrounded at the same time by three pre-synaptic profiles filled with vesicles. One of these was stained GABA positive. The dark arrowhead points to the synapses formed by the pulvinar axon terminal on a GABA negative profile. Arrows with tails point to the pre-synaptic profiles adjacent to the pulvinar axon terminal.

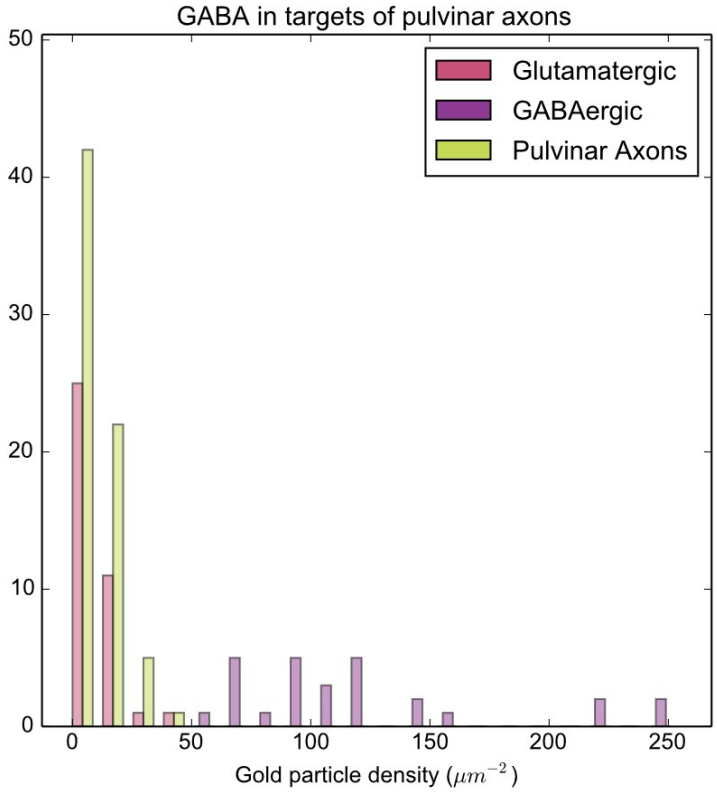

Figure 20: Pulvinar axons in V1 target non-GABAergic profiles

Density distributions of gold particles immunostained for GABA (see Methods) of post-synaptic targets of pulvinar axons in V1 layer 1 compared to positive (GABAergic) and negative (Glutamatergic) control. The gold particle distribution in the targets of pulvinar axons is not different from the negative control, and significantly different from the positive control (see text). The sample medians for these three types in particles per square micrometers were 29.51 for negative control, 334.17 for positive control, and 35.91 for pulvinar targets. There is no overlap between the sample distribution for pulvinar targets and the positive (GABA) control, and there medians are significantly different (35.91 vs. 334.17, p = 1.15E-16 Wilcoxon ranksum test). This result indicates that pulvinar axons synapse with apical dendrites of pyramidal cells in V1 layer 1 exclusively.

GABA immunostaining with small (15nm) gold particles was preformed on the ultrathin sections (see Methods). We quantified the gold particle densities in the pre-synaptic profiles of symmetric and asymmetric synapses in these stained sections as positive and negative controls for GABA staining, as described in the Methods. The gold particle density in the post-synaptic targets of pulvinar axons were then quantified and compared to the distribution of positive and negative controls. Figure 20 shows the distribution of gold particle densities in these three types of profiles. The positive and negative controls showed no overlap, and their medians were significantly different (Figure 20) (Wilcoxon rank sum test: $T = 8.9$, $p = 1.15E-16$), demonstrating a sufficient differentiating power of the GABA staining method. The distribution of gold particle densities in the profiles postsynaptic to the pulvinar axons was not any different from that of negative control (glutamatergic profiles), and was significantly different from the positive control (GABAergic profiles) (Kolmogorov-Smirnov test, pulvinar vs. GABA control: $D = 1.0$, $p = 1.07E-21$; pulvinar vs. non-GABA control: $D = 0.13$, $p = 0.66$). These comparisons (Figure 20) indicate that the pulvinar axons in V1 layer 1 synapse only with non-GABAergic apical dendrites of pyramidal cells.

Discussion

The goal of this study was to understand the anatomical basis of our previous result (Purushothaman et al., 2012), which showed that projections from pulvinar to V1 have a powerful impact on the responses of V1 output cells. Our key findings are that pulvinar axons terminate mainly in the outer half of layer 1 of V1, contrasting with the main terminations from pulvinar to extrastriate areas that target layers 3/4. Within layer 1 of V1, pulvinar boutons are smaller than those found in layer 4 of V2. Pulvinar axons in V1 layer 1 make multiple asymmetric synapses that appear to exclusively target the apical dendrites of pyramidal cells arising from the underlying cortical column and never appear to make synapses with GABAergic neurons. In the discussion below we consider the significance of these findings in light of results of others.

Axon distribution and morphology

Our findings are in accord with past results showing that the pulvinar projections to the cortex occur in the superficial layers in V1 (Ogren and Hendrickson, 1977; Rezak and Benevento, 1979), and layers 1, 3, and 4 in prestriate areas (Benevento and Rezak, 1976). Our results refined these previous findings by showing that the majority of pulvinar projections to V1 are focused on layer 1, with only minor branches in layer 3 (at least in bush baby), and that pulvinar projections to cortical layer 1 in V1, V2 and V3 are all confined in the upper half of layer 1, or layer 1a. The form of these projections fits with the general patterns shown by layer 1 thalamo-cortical projections from other nuclei in that they parallel the cortical surface, span more than one column, have *en passant* boutons and often have collaterals in layer 3/4 (Lachica and Casagrande, 1992; Rockland et al., 1999; Rubio-Garrido et al., 2009; Carey et al., 1979).

We identified at least two types of pulvinar projections to V1: those that terminate only in layer 1 and those that terminate in layers 1-3. Further, it appears that unlike those terminating in V1, projections to layer 1 of V2 and V3 may arise as collaterals of axons that primarily terminate in the middle layers. There is precedence for different types of thalamo-cortical layer 1 projections. At least two classes of K-cells exist in the bush babies and macaques (Lachica and Casagrande, 1992; Casagrande et al., 2007), and multiple classes of layer 1 terminating thalamic projections appear to exist in the rodent (Rubio-Garrido et al., 2009).

Bouton Sizes

It could be argued that the rank-sum test we used to make the pair-wise comparisons between the bouton sizes of the different projection types may not yield the correct significance level, due to different shapes of the bouton size distribution (Fagerland and Sandvik, 2009). The significance levels of these different bouton sizes, however, are high enough that they are unlikely to be caused by the difference in the shapes of these distributions alone (Fagerland and Sandvik, 2009). Furthermore, the distributions of bouton sizes from layer 1 and layer 4 projections, if indeed different enough to affect the significance level, would be significant enough to be classified as two types of projections, and distinguish the layer 1 projections from the typical driving projections such as those from LGN to V1 layer 4.

The sizes of boutons in a projection have been shown to correlate with the number and size of synapses and with post synaptic efficacy (Pierce and Lewin, 1994; Sherman and Guillery, 1996; Marion et al., 2013). By this criterion our quantitative data indicate that layer 1 projections may have less efficacious synapses than those terminating in layer 4. To our knowledge, no comparable measurements have been made comparing layer 1 bouton sizes with those in layer 4 elsewhere in the brain. The projections from LGN M and P cells are usually considered to be the typical feedforward and driving projections (Sherman and Guillery, 1998). And the pulvinar projections to V2 layer 4, as we argued in a previous report, also showed a lot of characteristics of a driving pathway (Marion et al., 2013). The fact that pulvinar axons in layer 1 of both V1 and V2 showed smaller boutons than the "driver" type projections to V2 layer 4 suggests that these layer 1 projections are different from typical driving projections. When projections from pulvinar to layer 1 and layer 4 co-exist in a cortical area, such as V2 and V3, the different bouton sizes of layer 1 and layer 4 axons also suggest that the projections to layer 4 dominate the pulvinar projection to that area.

Sherman and Guillery (1998) have laid out a straightforward set of criteria for classifying glutamatergic projections into two types: Drivers (class 1) and modulators (class 2). Among the properties they used to classify projections are bouton size and location of the synapse relative to the soma. Within Sherman and Guillery's framework our data suggest that layer 1 projections are modulators, and, as such, are involved in gain control and other processes that shape, but do not carry, the "main messages" being transmitted between areas. The idea that projections to layer 1 are modulatory has a long history and fits well with the idea of Jones (1998) that layer 1 projections from thalamus are distinct from those carrying the main message to layer 4. According to his theory layer 1 projections may be utilized to synchronize activity between cortical areas (Jones, 2001), an idea that also fits with a proposed role for pulvinar (Saalmann et al., 2012).

Anatomical Basis of pulvinar control of V1 output

We found that pulvinar projections arborize almost exclusively in upper layer 1 of V1, do not show bouton sizes typical of driving projections, and do not appear to directly recruit local interneuron networks. Thus the question of how pulvinar exerts such strong control over V1 output (Purushothaman et al., 2012) remains unanswered. It has been reported that layer 2/3 pyramidal cells can be made to fire with glutamate uncaging targeted to layer 1 in slice preparation (Dantzker and Callaway, 2000), and that calcium action potentials can be initiated from the dendritic tufts of cortical pyramidal cells (Schiller et al., 1997). A synchronized barrage of action potentials in the dendrites, therefore, may be able to amplify the pulvinar drive of the underlying output pyramidal cells of V1, though single dendritic action potentials are ineffective (Schiller et al., 1997). Indeed, based on slice physiology, layer 1 inputs have been reported to have a strong effect on pyramidal cells, and may in fact cause cells, with the synchronization effect of dendritic action potentials, to trigger pyramidal cells and would therefore qualify as a type of driving input (Larkum et al., 1999a; b; Schwindt and Crill, 1999). To explain our previous results demonstrating a

strong impact of pulvinar on V1 cells (Purushothaman et al., 2012), we would expect some mechanism to cause large scale simultaneous activity similar to hippocampal field sharp waves (Kamondi et al., 1998).

Among our proposed layer 1 models, the involvement of NGFC networks was most likely to initiate such a simultaneous activity. Since our results ruled out a direct recruitment of interneurons by pulvinar projections in V1 layer 1, there are two additional mechanisms that may contribute to this strong pulvinar control of V1 output. The extensive arbors branching from a single pulvinar axon may form a large number of synapses on the apical dendritic tufts of a single pyramidal cell. We observed multiple synapses on many pulvinar axons in V1, further increasing the potential number of dendrites that can be simultaneously activated by a single pulvinar axon. These simultaneous inputs from a single pulvinar axon to a single V1 pyramidal cell could be arranged to achieve optimal spatial integration and effectively drive axonal action potentials. The second possibility involves the layer 5 pyramidal cells in V1. V1 projects to the PL mainly through layer 5 pyramidal cells (Raczkowski and Diamond, 1981), and layer 5 pyramidal cells have apical dendrites extending into layer 1 (Rubio-Garrido et al., 2009). If pulvinar projections connect with both layer 5 and layer 2/3 pyramidal cells, those pulvinar projecting layer 5 pyramidal cells could form a recurrent loop with pulvinar's cells projecting to V1. This loop could be responsible for synchronizing neighboring pulvinar neurons, which, with their converging projections onto the apical dendrites, are able to sufficiently drive layer 2/3 pyramidal cells.

References

Bender D. 1981. Retinotopic organization of macaque pulvinar. *Journal of Neurophysiology* **46**:672–693.

Bender D. 1983. Visual activation of neurons in the primate pulvinar depends on cortex but not colliculus. *Brain Research* **279**:258–261.

Benevento L, Rezak M. 1976. The cortical projections of the inferior pulvinar and adjacent lateral pulvinar in the rhesus monkey (*macaca mulatta*): An autoradiographic study. *Brain Research* **108**:1–24.

Boyd J, Matsubara J. 1996. Laminar and columnar patterns of geniculocortical projections in the cat: Relationship to cytochrome oxidase. *Journal of Comparative Neurology* **365**:659–682.

Campos-Ortega J. 1968. Descending subcortical projections from the occipital lobe of *galago crassicaudatus*. *Experimental Neurology* **21**:440–454.

Carey R, Fitzpatrick D, Diamond I. 1979. Layer i of striate cortex of *tupaia glis* and *galago senegalensis*: Projections from thalamus and claustrum revealed by retrograde transport of horseradish peroxidase. *Journal of Comparative Neurology* **186**:393–437.

Casagrande V, Yazar F, Jones K, Ding Y. 2007. The morphology of the koniocellular axon pathway in the macaque monkey. *Cerebral Cortex* **17**:2334–2345.

Dantzker J, Callaway E. 2000. Laminar sources of synaptic input to cortical inhibitory interneurons and pyramidal neurons. *Nature neuroscience* **3**:701–707.

Fagerland MW, Sandvik L. 2009. The wilcoxon–mann–whitney test under scrutiny. *Statistics in medicine* **28**:1487–1497.

Felleman D, Van Essen D. 1991. Distributed hierarchical processing in the primate cerebral cortex. *Cerebral cortex* **1**:1–47.

Florence S, Casagrande V. 1987. Organization of individual afferent axons in layer iV of striate cortex in a primate. *The Journal of neuroscience* **7**:3850–3868.

Hollander H. 1974. Projections from the striate cortex to the diencephalon in the squirrel monkey (*saimiri sciureus*). a light microscopic radioautographic study following intracortical injection of h3 leucine. *Journal of Comparative Neurology* **155**:425–440.

Holmgren C, Harkany T, Svennenfors B, Zilberter Y. 2003. Pyramidal cell communication within local networks in layer 2/3 of rat neocortex. *The Journal of physiology* **551**:139–153.

Ichida J, Mavity-Hudson J, Casagrande V. 2014. Distinct patterns of corticogeniculate feedback to different layers of the lateral geniculate nucleus (lGN). *Eye and Brain* **In Press**.

Jiang X, Wang G, Lee A, Stornetta RL, Zhu J. 2013. The organization of two new cortical interneuronal circuits. *Nature neuroscience* **16**:210–218.

Jones E ed. 2007. The thalamus. 2nd ed. Cambridge University Press, UK: Cambridge.

Jones E. 1998. Viewpoint: The core and matrix of thalamic organization. *Neuroscience* **85**:331–345.

Jones E. 2001. The thalamic matrix and thalamocortical synchrony. *Trends in neurosciences* **24**:595–601.

Kamondi A, Acsady L, Buzsaki G. 1998. Dendritic spikes are enhanced by cooperative network activity in the intact hippocampus. *The Journal of neuroscience* **18**:3919–3928.

Koo M, Wenger A, Singh E, Li K, Mavity-Hudson J, Marion R, Casagrande V. 2013. Driving & modulatory pathways illuminated by immunostaining in primate cortex. In: Neuroscience meeting planner. San Diego, CA: Society for Neuroscience.

Kubota Y, Hatada S, Kondo S, Karube F, Kawaguchi Y. 2007. Neocortical inhibitory terminals innervate dendritic spines targeted by thalamocortical afferents. *The Journal of neuroscience* **27**:1139–1150.

Lachica E, Casagrande V. 1992. Direct w-like geniculate projections to the cytochrome oxidase (cO) blobs in primate visual cortex: Axon morphology. *Journal of Comparative Neurology* **319**:141–158.

Larkum ME, Kaiser K, Sakmann B. 1999a. Calcium electrogenesis in distal apical dendrites of layer 5 pyramidal cells at a critical frequency of back-propagating action potentials. *Proceedings of the National Academy of Sciences* **96**:14600–14604.

Larkum ME, Zhu J, Sakmann B. 1999b. A new cellular mechanism for coupling inputs arriving at different cortical layers. *Nature* **398**:338–341.

Lee J, Maunsell J. 2009. A normalization model of attentional modulation of single unit responses. *PLoS One* **4**:e4651.
Li K, Patel J, Purushothaman G, Marion R, Casagrande V. 2013. Retinotopic maps in the pulvinar of bush baby (otolemur garnettii). *Journal of Comparative Neurology* **521**:3432–3450.
Marion R, Li K, Mavity-Hudson J, Casagrande V. 2014. Morphological comparison of inputs to primate visual areas mT, v1 and v2. In: Neuroscience meeting planner. Washington, DC: Society for Neuroscience.
Marion R, Li K, Purushothaman G, Jiang Y, Casagrande V. 2013. Morphological and neurochemical comparisons between pulvinar and v1 projections to v2. *Journal of Comparative Neurology* **521**:813–832.
Ogren M, Hendrickson A. 1977. The distribution of pulvinar terminals in visual areas 17 and 18 of the monkey. *Brain Research* **137**:343–350.
Pierce J, Lewin G. 1994. An ultrastructural size principle. *Neuroscience* **58**:441–446.
Purushothaman G, Marion R, Li K, Casagrande V. 2012. Gating and control of primary visual cortex by pulvinar. *Nature Neuroscience* **15**:905–912.
Raczkowski D, Diamond I. 1978. Connections of the striate cortex in *galago senegalensis*. *Brain Research* **144**:383–388.
Raczkowski D, Diamond I. 1981. Projections from the superior colliculus and the neocortex to the pulvinar nucleus in galago. *Journal of Comparative Neurology* **200**:231–254.
Rezak M, Benevento L. 1979. A comparison of the organization of the projections of the dorsal lateral geniculate nucleus, the inferior pulvinar and adjacent lateral pulvinar to primary visual cortex (area 17) in the macaque monkey. *Brain Research* **167**:19–40.
Rockland K, Andresen J, Cowie R, Robinson D. 1999. Single axon analysis of pulvinocortical connections to several visual areas in the macaque. *Journal of Comparative Neurology* **406**:221–250.
Rockland K, Pandya D. 1979. Laminar origins and terminations of cortical connections of the occipital lobe in the rhesus monkey. *Brain research* **179**:3–20.
Rubio-Garrido P, Perez-De-Manzo F, Porrero C, Galazo MJ, Clasca F. 2009. Thalamic input to distal apical dendrites in neocortical layer 1 is massive and highly convergent. *Cerebral cortex* **19**:2380–2395.
Saalmann Y, Pinsk M, Wang L, Li X, Kastner S. 2012. The pulvinar regulates information transmission between cortical areas based on attention demands. *Science* **337**:753–756.
Schiller J, Schiller Y, Stuart G, Sakmann B. 1997. Calcium action potentials restricted to distal apical dendrites of rat neocortical pyramidal neurons. *The Journal of physiology* **505**:605–616.
Schwindt P, Crill W. 1999. Mechanisms underlying burst and regular spiking evoked by dendritic depolarization in layer 5 cortical pyramidal neurons. *Journal of Neurophysiology* **81**:1341–1354.
Sherman S, Guillery R eds. 2006. Exploring the thalamus and its role in cortical function. The MIT press.
Sherman S, Guillery R. 1996. Functional organization of thalamocortical relays. *Journal of Neurophysiology* **76**:1367–1395.
Sherman S, Guillery R. 1998. On the actions that one nerve cell can have on another: Distinguishing "drivers" from "modulators". *Proceedings of the National Academy of Sciences* **95**:7121–7126.
Sherman S, Guillery R. 2002. The role of the thalamus in the flow of information to the cortex. *Philosophical Transactions of the Royal Society of London. Series B, Biological Sciences* **357**:1695–1708.
Shostak Y, Ding Y, Casagrande V. 2003. Neurochemical comparison of synaptic arrangements of parvocellular, magnocellular, and koniocellular geniculate pathways in owl monkey *aotus trivirgatus* visual cortex. *Journal of Comparative Neurology* **456**:12–28.
Winer J, Larue D. 1989. Populations of gABAergic neurons and axons in layer i of rat auditory cortex. *Neuroscience* **33**:499–515.
Wozny C, Williams S. 2011. Specificity of synaptic connectivity between layer 1 inhibitory interneurons and layer 2/3 pyramidal neurons in the rat neocortex. *Cerebral Cortex* **21**:1818–1826.
Xu X, Bosking W, White L, Fitzpatrick D, Casagrande V. 2005. Functional organization of visual cortex in the prosimian bush baby revealed by optical imaging of intrinsic signals. *Journal of neurophysiology* **94**:2748–2762.

CHAPTER 5

THE MEDIAL INFERIOR PULVINAR INFLUENCES THE MIDDLE TEMPORAL AREA (MT) OUTPUT IN PRIMATE

Introduction

In the traditional view of the visual hierarchy, visual information flows from the retina to the lateral geniculate nucleus (LGN), then to the primary (V1) and secondary (V2) visual cortex, and either to the dorsal ("where") processing stream through the middle temporal area (MT) or to the ventral ("what") processing stream through V4 (Felleman and Van Essen, 1991). Despite being outside of this hierarchy (Felleman and Van Essen, 1991), the primate pulvinar connects extensively with areas near the root of the visual cortical hierarchy (Kaas and Lyon, 2007), and strongly regulates early visual cortical areas (Purushothaman et al., 2012; Soares et al., 2004). The pulvinar receives driving input from V1 (Bender, 1983; Raczkowski and Diamond, 1981) and proposed modulatory input from various higher visual areas including V2, V3, as well as large portions of the dorsal and ventral streams (Raczkowski and Diamond, 1981). The pulvinar projects to all visual cortical areas (Kaas and Lyon, 2007), and some of these pulvinocortical projections show characteristic anatomical features of driving projections (Marion et al., 2013, 2014).

Based on chemoarchitecture and connection patterns, the pulvinar can be roughly divided into lateral (PL), medial (PM), and inferior (PI) subdivisions, and PI can be further divided into central lateral (PIcl), central medial (PIcm), medial (PIm) and posterior (PIp) (Stepniewska and Kaas, 1997) subdivisions. PIm has a separate visual field representation (Ungerleider et al., 2014), and provides the main pulvinar input to MT (Lin and Kaas, 1980; Cusick et al., 1993).

MT is sensitive to the direction of motion (Baker et al., 1981) and serves as a gateway for the dorsal visual stream (Felleman and Van Essen, 1991). V1, LGN and the pulvinar all project to MT, but we know very little about how the pulvinar projections affect MT neural responses. V1 provides the main input to MT (Rockland, 1989; Anderson et al., 1998), but MT still shows direction selectivity after a V1 lesion (Rodman et al., 1989). The superior colliculus (SC) projects to the pulvinar (Glendenning et al., 1975; Benevento and Fallon, 1975), and a direct visual pathway from the retina to SC, then to MT via the pulvinar has long been proposed to mediate this residual MT visual response, as well as blind sight in patients with V1 lesions (Kaas, 2015). Although the majority of SC to pulvinar projections do not directly terminate on pulvinar cells projecting to MT (Stepniewska et al., 2000), PIm neurons directly relaying signals from SC to MT do exist (Berman and Wurtz, 2010) and SC has disynaptic projection to MT through the pulvinar (Lyon et al., 2010). PIm projections to MT end in layers 4 and 6 (Glendenning et al., 1975; Marion et al., 2014), showing a projection pattern typical for feedforward driving projections (Felleman and Van Essen, 1991). Compared to pulvinar projections to V1 (Li et al., 2014), which arrives mostly in layer 1, one might predict an even greater impact of pulvinar (Purushothaman et al., 2012) on the cortical target.

In this study, we injected glutamate in PIm to activate the pulvinar neurons, and electrophysiologically recorded from MT layer 2/3 neurons to determine the effect of increased pulvinar activity on MT output both while no visual stimulus was provided and while MT neurons were stimulated with a preferred stimulus, the random dot kinematograms (RDK). We also performed the same

experiment after inactivating the central vision representation of V1 and V2 to suppress any pathways relayed through these cortical areas and isolate the effect of the direct PIm to MT projections.

Methods

Animals and Anesthesia

Nine adult prosimian primates (bush babies *Otolemur garnettii*), of both sexes were used in these experiments according to approved protocols from the Institutional Animal Care and Use Committee (IACUC) at Vanderbilt University. Some of the animals involved in this study were used for a separate tracer study performed on the other hemisphere.

Anesthesia was first induced with 20-40mg/kg ketamine and 0.4-0.5mg/kg xylazine, and then maintained through the initial surgery with 1%-3% isoflurane in oxygen. During recording, we switched the anesthesia to 0.2-0.6mg/kg/hour propofol and 75%/25% nitrous oxide/oxygen (see Li et al., 2013). The anesthesia plane was monitored with EEG and ECG and periodically checked with toe pinch, and adjusted as needed. At the end of each sterile survival session, after closing all openings, first vecuronium bromide and then propofol/nitrous was withdrawn and the animal was monitored until it was fully awake. Animals were given the analgesic buprenorphine 0.01 mg/kg immediately after surgery, and twice a day for the following 3 days.

Electrophysiology

For each animal, a craniotomy and durotomy were first performed over LGN/pulvinar, and the retinotopic organization of PIm was mapped with single tungsten electrode (FHC) in a survival session. PIm was initially located by finding the central representation of the two lateral pulvinar maps based on our published maps (Li et al., 2013) and moving the electrode 0.5mm medially. Later in a terminal session, MT recordings were made using an electrode array while manipulations were performed in V1 or PIm. A craniotomy and durotomy were performed over MT guided by the skull marks over the Sylvian fissure, and the MT central vision representation was located with single electrode recording (also see **receptive field mapping**). A Utah 96 electrode array (Blackrock Microsystems) was pneumatically inserted over the central vision representation of MT and secured with 1.5% agarose in normal saline. Spikes were collected using Cerebus multichannel data acquisition system (Blackrock Microsystems) and sorted offline with primary component analysis using Offline Sorter (Plexon). To limit our analysis to visually responsive multi- and single- units, we first excluded all spike waveforms below 4.5 standard deviations of the baseline noise, as well as those with inter-spike interval histograms showing fixed frequency noise. We then excluded non-visually responsive units. Visually responsive units were defined as having average peak activity during the presentation random dot kinematograms of the preferred direction that is both more than 10 spikes per second, and exceeded the 95% confidence interval of their respective spontaneous activity, before manipulation to V1 and pulvinar.

Receptive field mapping

A monitor was placed 28.5cm from the animal's eyes and a thick sheet of paper was taped on the monitor during receptive field mapping to serve as a tangent screen. Pupils were dilated with 1% atropine drops and contact lenses with sufficient power were fitted to keep the monitor in clear focus. A blood vessel map was back reflected on the monitor, with which the optic discs were located and the *areae centrales* were inferred. Throughout the experiment, the positions of retinal landmarks were periodically checked for residual drifts of the paralyzed eyes. Light lines and spots were projected on the screen with a

hand held ophthalmoscope to test visual response. Receptive fields were hand mapped and plotted on the tangent screen relative to the *areae centrales*.

Visual stimuli

Visual stimuli used during MT recordings were generated with Psychophysics Toolbox 3 and presented on a 22-inch Sony CRT display at 60Hz refresh rate. 5% RDK with 100% coherence were presented at directions varying from 0° to 315° in steps of 45°. The dots were 0.2° in diameter, 114.7 cd/m^2 on a black background of 1.04 cd/m^2, and were moving at a uniform speed between 10°/s and 20°/s. The eight directions plus one static condition, were randomly presented in 1s trials spaced by 1s of black screen. RDK was shown in a circular patch covering MT receptive fields of interest and was kept as small as possible.

Drug application

The PIm map does not have a well-organized retinotopy nor a clear central vision representation. Therefore, we made injections that covered the ventral half of PIm, where most neurons had receptive fields close to the central vision representation. In the terminal session, before the array insertion in MT, a single electrode penetration was performed in PIm to confirm the location of PIm found in the previous survival session. After the array insertion, a homemade injectrode with a tungsten electrode attached to the side of a glass pipette was lowered into the located PIm, and its location electrophysiologically confirmed. During MT recordings, a pressure injection of 500-1000nl of 1M glutamate and 2% 10kD biotinylated dextran (BDA) in saline was made into PIm. In 3 of the animals, before array insertion, a craniotomy/durotomy was performed over V1, exposing V1 central vision as identified by blood vessel patterns (Purushothaman et al., 2012), and a piece of gelfoam soaked in saline was applied on the cortical surface. After injectrode insertion but before PIm injection, muscimol was applied by dripping 100µl of 100mM muscimol in saline on the gelfoam. This method has been used to effectively suppress the activity of V1 to MT projections in bush baby in less than 45 minutes (Collins et al., 2005).

Histology

Animals were put into deep anesthesia by infusing >10ml propofol, and then were perfused through the heart with a saline rinse followed by a fixative (2% paraformaldehyde and 2% glutaraldehyde or 4% paraformaldehyde and 1% glutaraldehyde in 0.1M phosphate buffer). The brain was blocked coronally at AP +8 and -2 in the Horsely-Clark coordinates. The cortex containing MT was separated from the thalamus and flattened in a petri dish with a weighted cover. Brain pieces were left in 0.1 M phosphate buffer with 30% sucrose for two days, then frozen and stored at -70 degrees. The flattened cortex was tangentially sectioned at 52µm, and stained for cytochrome oxidase (CO) to reveal MT and locate the electrode array relative to MT. The thalamus was cut coronally at 52µm, and the sections were examined under bright field. The sections containing PIm were alternately stained for CO (see Li et al., 2013) and BDA. Sections to be stained to reveal BDA were placed in 1:400 streptavidin Alexa-fluor 488 (Invitrogen) for 2 hours, then rinsed three times in Tris buffer saline (TBS, pH 7.6), mounted, and cover-slipped with Vectashield (Vector).

The tangential sections of MT were aligned by blood vessel patterns and other landmarks. The border of MT was identified by the darker CO stain in the sections containing layers 4/5, and compared to the electrode marks left in the sections containing layers 2/3. Coronal sections of the thalamus containing the injection site were similarly aligned. The extent of drug spread was identified on sections fluorescently stained for BDA, and compared to pulvinar subdivisions identified on adjacent CO sections.

Photomicrographs of tissue sections were taken under light and/or fluorescent illumination and then only the global contrast was manipulated to visualize histological features.

Data analysis

When statistically comparing the average neuron activity, we calculated the percentage change before and after each manipulation, then performed one-sample t tests on this percentage change against unity. The neuronal activity data used were all averaged across a large number of trials (N ~ 400, depending on the specific manipulation). Thus, the sample distributions of their means should be close to normal. Peristimulus time histograms (PSTH) were computed with fixed 50-ms windows then smoothed with a 150-ms-wide sliding Gaussian window. The ratio of peak-to-baseline response was estimated as the ratio of the post-stimulus peak of the PSTH to the pre-stimulus PSTH values averaged over the 600 ms before stimulus onset. The directionality index (DI) we calculated for MT neurons follow the formula used by Movshon and Newsome (1996), where DI = 1 - (visually evoked activity at anti-preferred direction - spontaneous activity before trials at anti-preferred direction) / (visually evoked activity at preferred direction - spontaneous activity before trials at preferred direction).

Results

Response properties of neurons in PIm

We explored the retinotopic organization of PIm with single tungsten electrode penetrations. Electrode penetrations in the more lateral part of the pulvinar encountered neurons with receptive fields consistent with the two well organized retinotopic maps reported before (Li et al., 2013). Previously we found a chemoarchitectonic area in the pulvinar we later named PIm that showed similar characteristics reported for the PIm and owl monkey, squirrel monkey and macaque monkey (Lin and Kaas, 1979; Stepniewska and Kaas, 1997). Based on this finding we consider the pulvinar area medial to the two retinotopic maps and ventral to the central representation to those two maps to be PIm. Most neurons encountered in this area were responsive to simple visual stimuli such as a flashing or moving light spot, and had localized receptive fields. Many of these neurons were selective to the direction of movement. The medial border of PIm was determined by the disappearance of neurons responsive to these simple stimuli, which is about 0.5mm from the lateral border of PIm. The dorsal border of PIm was determined by a decrease in direction selective neurons as well as the appearance of full field visual responsive neurons (Petersen et al., 1985). The receptive field sizes in PIm were similar to those in MT or the lateral pulvinar maps, and larger than reported for bush baby V1 and V2 (Debruyn et al., 1993; Allison and Casagrande, 1994).

Vertical electrode penetrations in PIm could be distinguished from those in the dorsal and ventral maps in PL and PIcl, as penetrations in PIm did not show smooth receptive field progression. Neighboring neurons in PIm would often show receptive fields that were far apart, especially near the ventral end of PIm. There is, however, a trend for more central neuron to be encountered near the ventro-posterior end of PIm. Near the dorso-anterior end of PIm, all the neurons had receptive fields in the periphery. Neighboring neurons in that area, however, did not seem to have receptive fields in neighboring places in the periphery. Neurons that were deeper or encountered in more posterior penetrations tended to have more central receptive fields. At the same time, however, neurons with receptive fields in the periphery (>40°) were still often encountered in these parts of PIm, suggesting a more complex topographic arrangement existing in this region. In spite of the fact that the PIm map did not appear to have a smooth and systematic spatial organization, once receptive fields were plotted together, there appeared to be fairly complete coverage of the contralateral visual field with no PIm neurons' receptive fields crossing the midline into the ipsilateral visual field.

Injections in PIm

We made 1M glutamate injections mixed with BDA 20kD into the PIm in areas with neurons having central receptive fields (<10°). When examined under the fluorescent microscope, we found these injections were approximately 2 by 4 mm on the coronal plane and centered in the posterior part of the pulvinar. The tip of the pipettes as indicated by the track left in the tissue, were in the ventral part of PIm. To some extent, the glutamate/BDA injections tended to leak back along the shaft of the pipette, and form an area of spread that is longer on the dorsal-ventral axis. Regardless, all these injections covered PIm, and partly extended into PM as well as the central vision representations of the two lateral pulvinar maps. On the dorsal side, these injections spread to the dorsal edge of the pulvinar, covering a part of the pulvinar potentially analogous to the dorsal medial pulvinar (Pdm) in macaque monkeys (Petersen et al., 1985). None of the injections spread into LGN based on fluorescent staining of BDA, and most were posterior to LGN. An example section showing the spread of an injection overlaid on an adjacent CO section is shown in Figure 21.

MT activity with PIm activation

With an electrode array implanted over the central vision representation of MT and electrode tips reaching layer 2/3 (500μm below surface), we injected 500-1000μl of 1M glutamate into ventral PIm over the course of ~5 min. Each appearance of the RDK stimulus lasted for 1 second and was spaced by a 1 second blank screen (see Methods). We collected neural activity within the 0.6 seconds before stimulus onset, defined as spontaneous activity, and the neural activity during the 1 second stimulus presentation, defined as visually evoked activity. Neural activity was measured for 400 seconds before and after the glutamate injection as the before and after conditions, respectively. After activation of the pulvinar, there was a significant increase in the spontaneous activity of MT layer 2/3 neurons (t test, $t = 3.01$, $p = 0.0043$). The visually evoked activity in MT was increased by a similar amount (t test, $t = 2.09$, $p = 0.042$). There was no evidence, therefore, that activation of pulvinar changed either the absolute difference or the ratio between evoked and spontaneous activity (absolute difference: $t = 1.10$, $p = 0.28$; ratio: $t = -1.24$, $p = 0.22$) (Figure 22C). There did seem to be an iceberg effect, however, when the transient response (calculated as the evoked activity during the first 0.5 seconds of stimuli presentation) showed a smaller signal to noise ratio due to the rising spontaneous activity ($t = -2.96$, $p = 0.049$) (Figure 22D).

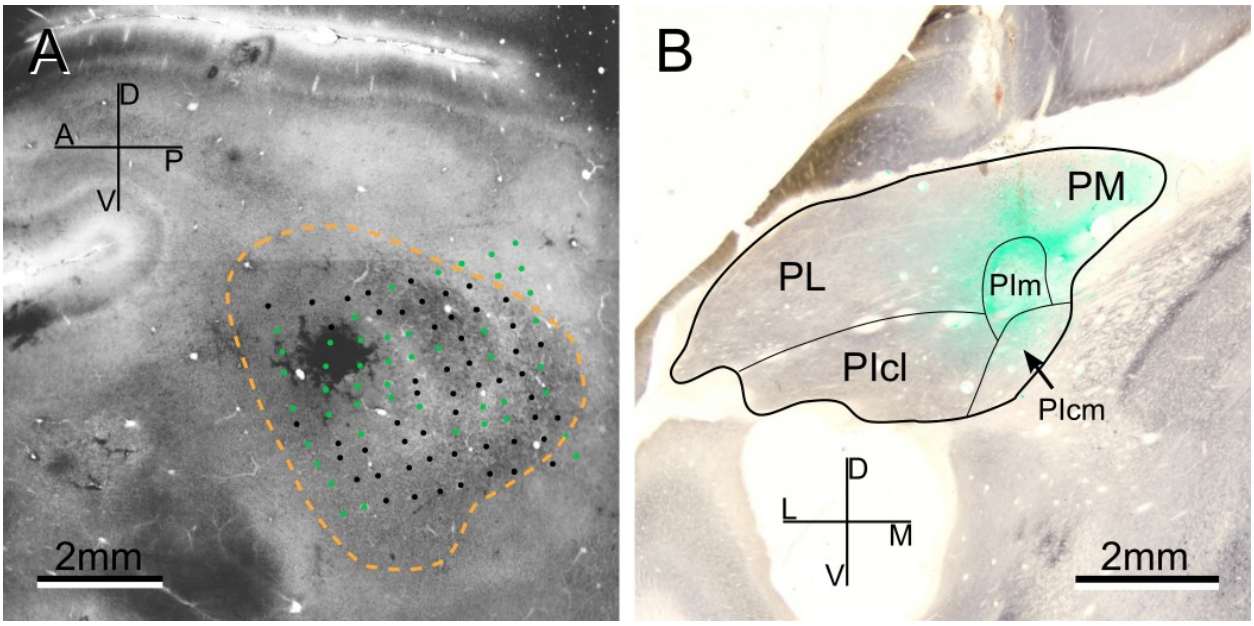

Figure 21: Injection and recording site

We recorded from MT with a 96 electrode Utah array while injecting glutamate in the medial inferior pulvinar. **A**: An example array implant site over MT. The array pins (black and green dots) and the MT site (dashed yellow circle) were reconstructed from serial tangential section of the cortex. MT were identified by dense staining for cytochrome oxidase (CO). The array was located by the electrode marks left in more superficial layers (black dots), and the green dots show inferred electrode sites. This diagram was overlaid on one of the CO sections near layer 4 showing the extent of MT. **B**: An example glutamate injection site. A coronal section of the left pulvinar fluorescently stained (green) for the biotinylated dextran mixed with glutamate injection, overlaid on an adjacent section stained for CO. The architectonic subdivisions of pulvinar are marked with solid black lines. The injection is spatially restricted in the medial part of pulvinar, centered in PIm, and spread into PL, PIcl and PM. There was no spread in either the lateral geniculate nucleus (LGN) or the superior colliculus (SC). D: dorsal; V: ventral; L: lateral; M: medial; A: anterior; P: posterior; PL: lateral pulvinar; PM: medial pulvinar; PIcl: central lateral inferior pulvinar; PIm: medial inferior pulvinar; PIcm: central medial inferior pulvinar.

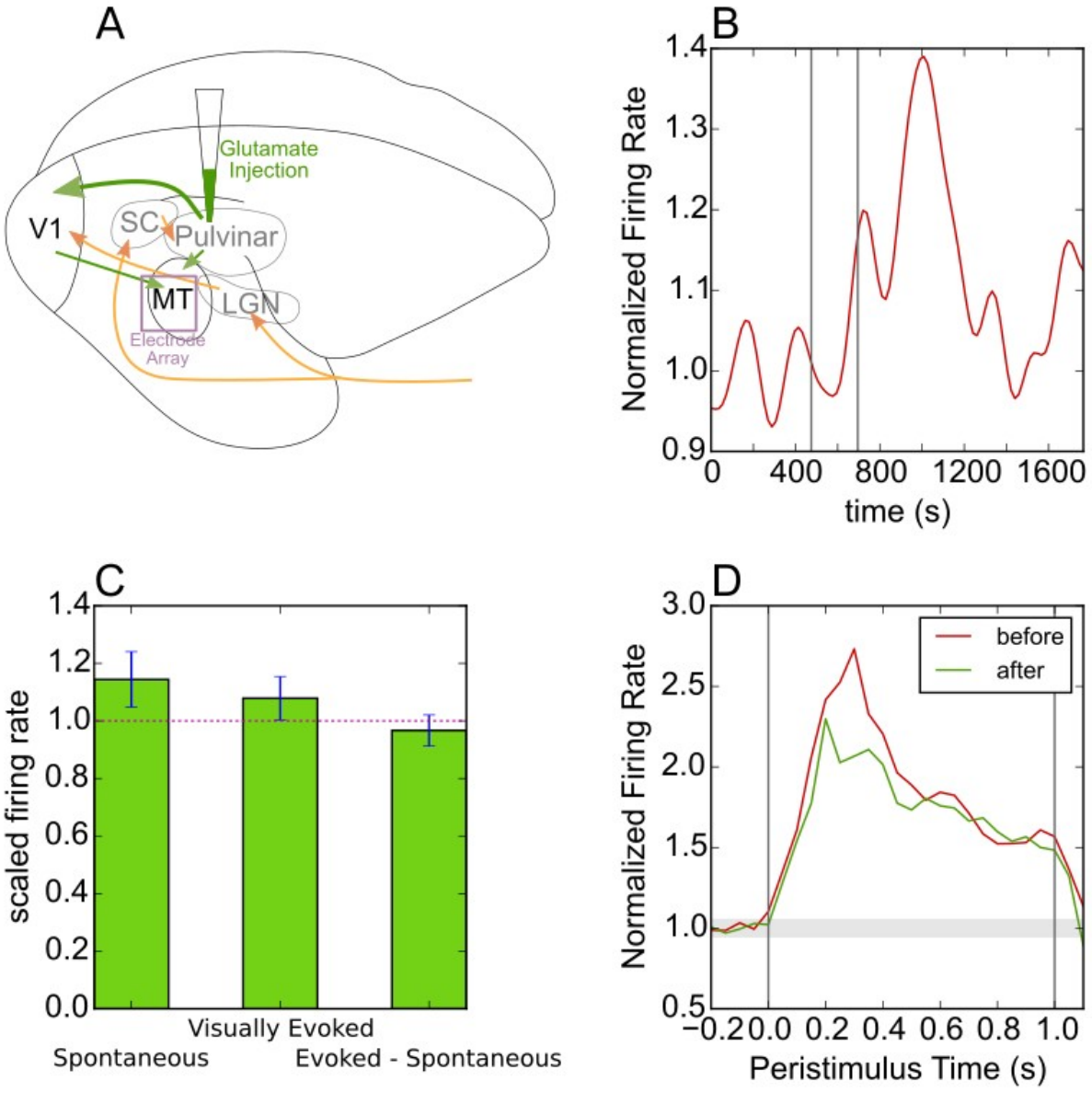

Figure 22: MT activity increases with pulvinar activation

MT neurons showed increase in spontaneous activity with pulvinar activation when V1 was intact. **A**: Connections in the early visual system and diagram for the experiment. Yellow: feedforward projections; Green: feedforward projections to be excited with pulvinar activation. LGN: the lateral geniculate nucleus; SC: the superior colliculus; V1: the primary visual cortex; MT: the middle temporal area. **B**: Time course of the normalized spontaneous activity of an example MT cell. Vertical lines mark the start and end of glutamate pressure injection. **C**: The mean percentage change of the spontaneous activity, visually evoked activity of MT cells, and the difference between visually evoked and spontaneous activity, or the visual signal in MT cell responses. Red line is at 1.0, showing a level with no change. Error bar shows a 95% confidence interval of the percentage change. There are increases in both spontaneous firing rate and visually evoked firing rate at the MT neuron population level after pulvinar activation, but there is no significant differential change between them. **D**: Averaged peri-stimulus time histogram normalized by each cells background activity. Shaded area

mark the 3 standard deviation around the averaged background activity. After pulvinar activation, the MT neurons showed a smaller peak to background ratio but no other difference, consistent with a increase in spontaneous activity without a comparable increase in visual response.

MT activity after V1 inactivation

The method we used to inactivate V1 was identical to that reported to greatly reduce MT activity measured with intrinsic signal optical imaging, and in that study the drugs were shown to not spread to other nearby cortical areas (Collins et al., 2005). We recorded MT activity 25-40 minutes after muscimol application on V1, and observed that both the spontaneous and visually evoked activity decreased significantly (spontaneous: $t = -4.46$, $p = 3.8e-5$; evoked: $t = -5.09$, $p = 4.1e-6$) (Figure 23A). In spite of the decrease of activity, MT cells still showed clear visual responses to the RDK stimuli after V1 inactivation. We calculated the visual responsiveness of MT neurons by calculating their PSTHs during a 400 second window before V1 inactivation and again during a 400s window before pulvinar glutamate activation but after V1 inactivation (see Methods). Of the 51 significantly responsive MT neurons as calculated before V1 inactivation, 47 were still visually responsive after V1 inactivation. We calculated the directionality index (DI) of MT neurons before and after V1 inactivation. The mean DI for MT neurons before V1 inactivation was 1.18, clustered near 1 ($t = 0.45$, $p = 0.65$), reflecting unidirectional response commonly seen in MT (Rodman et al., 1990). After V1 inactivation, the mean DI did not change significantly ($t = -0.55$, $p = 0.58$).

MT activity with PIm activation with V1 inactivation

We waited 25 to 40 min after muscimol application on V1 before injecting glutamate into the pulvinar. To our surprise, MT neuron activity showed a sharp decrease after pulvinar activation with an inactivated V1 (Figure 24A), in contrast to the excitatory effect of the same manipulation with intact V1. Both spontaneous and visually evoked neural activity in MT showed a significant decrease (Figure 24B) (t test; spontaneous: $t = -5.48$, $p = 9.53e-7$; evoked: $t = -6.58$, $p = 1.45e-8$). No significant change in either the ratio or the absolute difference of evoked to spontaneous activity, however, was found after pulvinar activation (absolute difference: $t = -1.21$, $p = 0.23$; ratio: -0.31, $p = 0.76$), nor did the directionality index change ($t = 0.089$, $p = 0.93$). One factor to consider, however, is that muscimol may continue to spread in V1, affect more neurons, and have increased its suppressive effect on MT even after 25-40 minutes of application on the V1 surface. To control for this potential effect of the continuously intensifying suppression of MT by muscimol in V1, we calculated a predicted neural activity for each recorded MT neuron, based on its activity just before muscimol application and just before glutamate injection, assuming a linear change of muscimol effect over time. Essentially we made a prediction about the changes in neural activity after glutamate injection, based on the assumption that the injection had no effect, and compared it with the actual recorded neural activity. The recorded spontaneous neuron activity in MT after pulvinar activation was significantly lower than the predicted activity ($t = -2.06$, $p = 0.044$), showing that pulvinar activation had a suppressive effect on MT activity that is significantly below that predicted suppression from muscimol inhibition of V1.

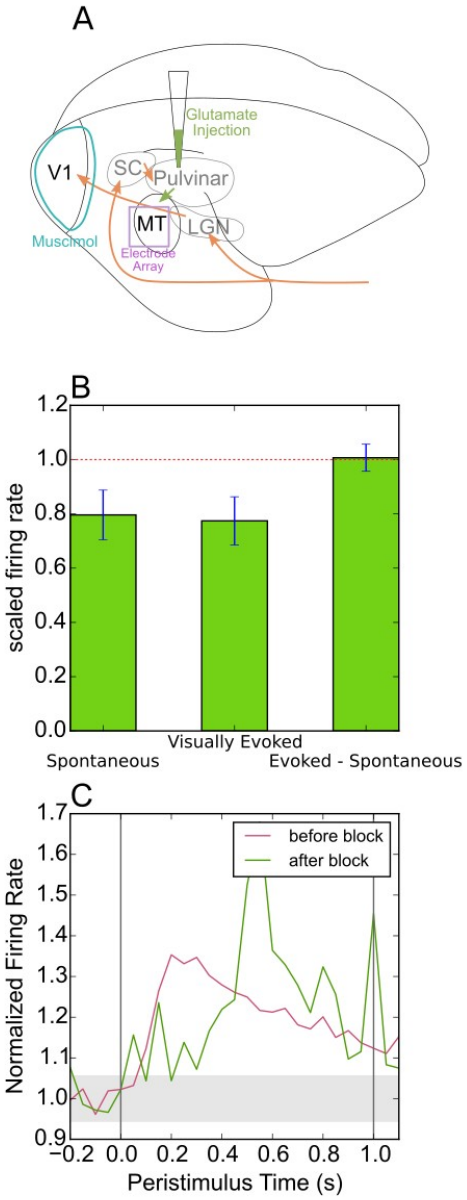

Figure 23: MT suppression with V1 blockade

Both spontaneous and visually stimulated neuron activity decreased in MT after V1 inactivation, but visual response to random dot kinematograms was still present. **A**: Connections in the early visual system and diagram for the experiment with V1 inactivation. Yellow: feedforward projections; Green: feedforward projections to be excited with pulvinar activation. With V1 inactivated, The loop from pulvinar to MT via V1 is blocked. LGN: the lateral geniculate nucleus; SC: the superior colliculus; V1: the primary visual cortex; MT: the middle temporal area. **B**: The mean percentage change of the spontaneous activity, visually evoked activity of MT cells, and the difference between visually evoked and spontaneous activity, or the visual signal in MT cell responses. Red line is at 1.0, showing a level with no change. Error bar shows a 95% confidence interval of the percentage change. Both spontaneous firing rate and visually evoked firing rate showed decrease at the MT neuron population level after V1 blockade, but there is no significant differential change between them. **C**:

Averaged peri-stimulus time histogram normalized by each cells background activity before and after V1 inactivation. Shaded area mark the 3 standard deviation range around the background activity. With V1 blocked, the initial peak immediately after stimulus onset disappeared and the visual response came much slower.

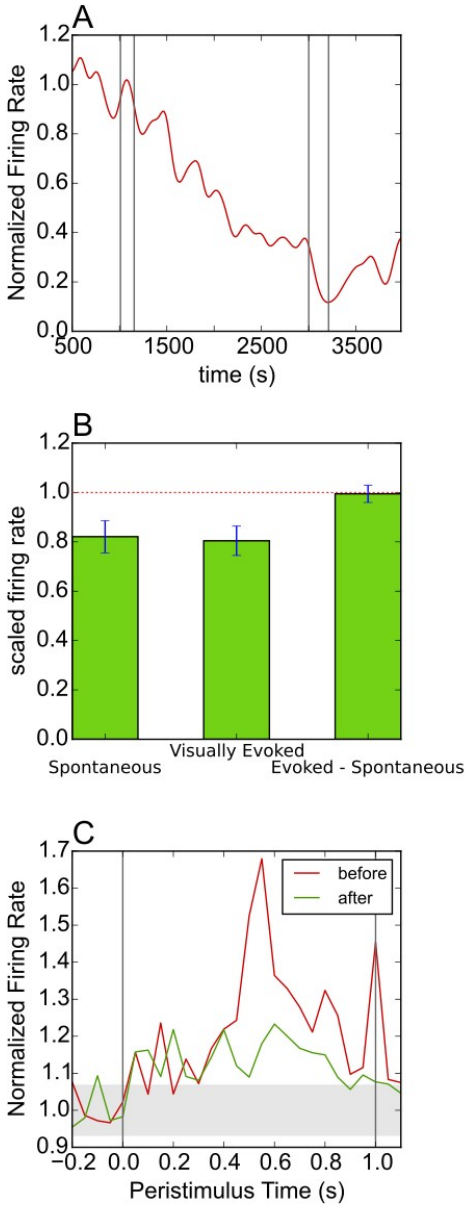

Figure 24: MT activity decreases after pulvinar activation with V1 blockade

Activity changes of MT neurons with pulvinar activation with V1 inactivation. **A**: Time course of the normalized spontaneous activity of an example MT cell. The first pair of vertical lines mark the start and end of muscimol application and the second pair mark the glutamate pressure injection. **B**: The mean percentage change of the spontaneous activity, visually evoked activity of MT cells, and the difference between visually evoked and spontaneous activity, or the visual signal in MT cell responses. Red line is at 1.0, showing a level with no change. Error bar shows a 95% confidence interval of the percentage change. After glutamate injection in PIm after V1 blockade, both spontaneous firing rate and visually evoked firing rate of MT neurons showed further decrease beyond that can be predicted from continued V1 suppression from muscimol application, but there is no significant differences between the changes in spontaneous and visually evoked response. **C**: Averaged peri-stimulus time histogram normalized by each cells background activity pulvinar activation.

Shaded area mark the 3 standard deviation around the background activity. The late onset visual response seemed to be suppressed in MT after pulvinar activation.

Discussion

In this study, we examined the visually responsive neurons in the medial inferior pulvinar (PIm) of bush baby, found directionally selective neurons in this area, and confirmed that the area did not have a well organized retinotopic but a trend for neurons representing paracentral vision to cluster near the posterior-ventral end of the nucleus. In subsequent experiments, we recorded from the cortical target of PIm, area MT. In the layer 2/3 neurons of MT, we found that PIm activation with glutamate increased activity (both spontaneous and evoked) when input to MT from V1 was intact, but that activation of PIm when V1 was suppressed actually had the opposite effect on MT activity, which was suppressive. Below we consider the implications of these results in the context of previous findings.

The medial inferior pulvinar

We qualitatively examined the response properties of PIm neurons, and found them to be more directionally selective than those in the lateral pulvinar maps (Li et al., 2013). Receptive field sizes, however, were comparable between the PIm map and the ventral map in PIcl (Li et al., 2013). Given that Berman and Wurtz (2011) reported higher directional selectivity for macaque PIm neurons that receive MT input than those that project to MT, the high proportion of directionally selective neurons we find in bush baby may also reflect a denser or stronger MT input in PIm compared to other pulvinar subdivisions.

The two general features of PIm organization we identified are consistent with previous reports on PIm organization. Its crude retinotopy has been reported in macaque monkey both anatomically and electrophysiologically (Bender, 1981; Adams et al., 2000; Berman and Wurtz, 2010). Our findings in bush baby confirmed this lack of a smooth, well organized retinotopy in PIm. Despite this lack of a well-organized retinotopy, we observed a general trend for a clustering of neurons representing paracentral vision near the ventroposterior boundary of PIm. This trend is similar to that reported in macaque monkeys (Standage and Benevento, 1983). In macaque PIm, ventroposterior PIm projects to posterior MT, where central vision is represented, and dorsoanterior PIm projects to anterior MT, where the peripheral visual field is represented (Standage and Benevento, 1983; Van Essen et al., 1981). Therefore, this arrangement of the bush baby PIm map is similar to that of macaque without significant rotation. As such, this arrangement can be contrasted to the relative rotation found between the arrangements of the lateral pulvinar maps in bush baby and macaque monkey (Li et al., 2013). This difference likely results from the physical location of PIm which lies deep inside the thalamus, farther from the dorsal surface of the thalamus, which appears to have seen a significant expansion in primates (Chalfin et al., 2007). The retinotopic organization of bush baby PIm we report here could also be explained as two populations of neurons coexisting in PIm, one of which is retinotopically organized following the trend we had observed, and the other consisting entirely of neurons that have peripheral receptive fields. Such an organization could provide the cortical targets of PIm with simultaneous input from the center and the periphery of the visual field, which may facilitate detection of fast moving objects or aid in making appropriate saccades.

The impact of V1 suppression on MT activity

After application of muscimol on V1, we observed a decrease of both spontaneous and visually evoked activity in MT layer 2/3 neurons. Most of these neurons, however, retained visual responses to moving random dots. Based on a previous report using the same V1 inactivation method (Collins et al., 2005), when we recorded in MT 25-45 minutes after muscimol application, V1 had already started to be suppressed but the suppression likely had not reached its maximum level. Thus, our results cannot be interpreted as either supporting or refuting the existence of residual MT activity after total V1 inhibition or a V1 lesion (Rodman et al., 1989; Rosa et al., 2000; Collins et al., 2003). If V1 were indeed the only source of visual information for MT, however, one might expect a decrease in V1 activity would first

impact either the ratio or absolute difference between signal and noise in MT visual response, a result that we did not see.

Different effects of direct and indirect pulvinar projections to MT

In this study we also were interested in understanding the impact of pulvinar on MT responses, especially given that lateral pulvinar has a major impact on the response of V1 neurons (Purushothaman et al., 2012). As mentioned in the introduction, V1 provides the main input to MT (Rockland, 1989; Anderson et al., 1998), but PIm also provides a substantial input and both input end in layer 3/4 (Glendenning et al., 1975; Lin and Kaas, 1980; Dick et al., 1991; Rockland, 1989; Anderson et al., 1998).

In the present study we recorded from layer 2/3 neurons in MT, which were one step removed from the input layer 4. Our results showed that, with V1 intact, pulvinar activation with glutamate increased both spontaneous and visually evoked activity in MT, but did not alter the direction selectivity or differentially increase the evoked over spontaneous activity. Therefore, activation of pulvinar can significantly impact the output cells of area MT. This effect, without V1 manipulation, represents the combined effect of all pulvinar projections, direct and indirect, into MT. They pulvinar projections to V1 and V2 stand out as the major indirect pathways. The pulvinar has strong regulation over V1 output (Purushothaman et al., 2012), and has a projection to V2 with features of driving input (Marion et al., 2013) that affects V2 output in a subtle way (Soares et al., 2004). These two indirect pathways, together with the direct projections from PIm to MT, all can contribute to this excitatory effect of pulvinar on MT.

Our much more puzzling result came after we silenced V1 with muscimol. In the latter case increasing pulvinar activity with glutamate had the exact opposite effect with both spontaneous and evoked activity decreasing in the superficial output layers of MT. Our activation of the pulvinar was clearly performed after the muscimol inactivation of V1 was starting to take effect. First, as mentioned earlier, we used the same method and time frame as (Collins et al., 2005) where optically imaged activity in MT dropped dramatically. More importantly, our data clearly show that MT activity dropped following blockade of V1 but before we activated pulvinar with glutamate. As discussed in the results, this further decrease of MT activity after pulvinar activation was also in addition to, and could not explained by, a gradually increasing effect of the muscimol on V1.

What might explain this counterintuitive result? When we suppressed the central representation of both V1 and V2, we blocked the pathways from pulvinar to MT that are relayed by these two areas. PIm has relatively dense projections to MT (Standage and Benevento, 1983; Berman and Wurtz, 2010, 2011), and both PIm and MT are close to the bottom of the visual hierarchy (Benevento and Davis, 1977; O'Brien et al., 2001; Anderson et al., 1998). With V1/V2 blocked, the effect of direct PIm to MT projections likely outweighed the effect of indirect projections relayed by other higher order visual areas, and our results showing the inhibitory effect of pulvinar activation on MT likely reflect these direct projections. The axons of these projections in MT layer 4 could contact a significant percentage of inhibitory interneurons whose influence is not evident when there is a strong drive from V1.

This inhibitory effect has two possible functional implications. First, the direct pulvinar to MT pathway may be excitatory in awake animals viewing natural visual stimuli. A disruption of the natural excitatory/inhibitory circuit recruitment of an excitatory thalamocortical pathway under an artificially induced (pharmacological) pattern of PIm activation could lead to suppression of the cortical target (Logothetis et al., 2010, Figure S5). PIm projections to MT could also serve as a modulatory input that has a net inhibitory effect in awake animals in response to natural visual stimuli. The modulatory role of pulvinar input to MT is consistent with reports showing a driving projection from LGN K layers to MT (Schmid et al., 2010), and reports showing that PIm is not responsible for direction selectivity in MT (Berman and Wurtz, 2011).

Taken together, these results suggest a complex role for pulvinar axons in area MT.

References

Adams M, Hof P, Gattass R, Webster M, Ungerleider L. 2000. Visual cortical projections and chemoarchitecture of macaque monkey pulvinar. *Journal of Comparative Neurology* **419**:377–393.

Allison J, Casagrande V. 1994. Receptive field structure of v2 neurons in the prosimian primate *galago crassicaudatus*. In: Society of neuroscience annual meeting.

Anderson J, Binzegger T, Martin K, Rockland K. 1998. The connection from cortical area v1 to v5: A light and electron microscopic study. *The Journal of neuroscience* **18**:10525–10540.

Baker J, Petersen S, Newsome W, Allman J. 1981. Visual response properties of neurons in four extrastriate visual areas of the owl monkey (aotus trivirgatus): A quantitative comparison of medial, dorsomedial, dorsolateral, and middle temporal areas. *Journal of Neurophysiology* **45**:397–416.

Bender D. 1981. Retinotopic organization of macaque pulvinar. *Journal of Neurophysiology* **46**:672–693.

Bender D. 1983. Visual activation of neurons in the primate pulvinar depends on cortex but not colliculus. *Brain Research* **279**:258–261.

Benevento L, Davis B. 1977. Topographical projections of the prestriate cortex to the pulvinar nuclei in the macaque monkey: An autoradiographic study. *Experimental Brain Research* **30**:405–424.

Benevento L, Fallon J. 1975. The ascending projections of the superior colliculus in the rhesus monkey (*macaca mulatta*). *Journal of Comparative Neurology* **160**:339–361.

Berman R, Wurtz R. 2010. Functional identification of a pulvinar path from superior colliculus to cortical area mT. *Journal of Neuroscience* **30**:6342–6354.

Berman R, Wurtz R. 2011. Signals conveyed in the pulvinar pathway from superior colliculus to cortical area mT. *Journal of Neuroscience* **31**:373–384.

Chalfin B, Cheung D, Muniz J, De Lima Silveira L, Finlay B. 2007. Scaling of neuron number and volume of the pulvinar complex in new world primates: Comparisons with humans, other primates, and mammals. *Journal of Comparative Neurology* **504**:265–274.

Collins C, Lyon D, Kaas J. 2003. Responses of neurons in the middle temporal visual area after long-standing lesions of the primary visual cortex in adult new world monkeys. *The Journal of neuroscience* **23**:2251–2264.

Collins C, Xu X, Khaytin I, Kaskan P, Casagrande V, Kaas J. 2005. Optical imaging of visually evoked responses in the middle temporal area after deactivation of primary visual cortex in adult primates. *Proceedings of the National Academy of Sciences of the United States of America* **102**:5594–5599.

Cusick C, Scripter J, Darensbourg J, Weber J. 1993. Chemoarchitectonic subdivisions of the visual pulvinar in monkeys and their connectional relations with the middle temporal and rostral dorsolateral visual areas, mT and dLr. *Journal of Comparative Neurology* **336**:1–30.

Debruyn E, Casagrande V, Beck P, Bonds A. 1993. Visual resolution and sensitivity of single cells in the primary visual cortex (v1) of a nocturnal primate (bush baby): Correlations with cortical layers and cytochrome oxidase patterns. *Journal of Neurophysiology* **69**:3–18.

Dick A, Kaske A, Creutzfeldt O. 1991. Topographical and topological organization of the thalamocortical projection to the striate and prestriate cortex in the marmoset (callithrix jacchus). *Experimental Brain Research* **84**:233–253.

Felleman D, Van Essen D. 1991. Distributed hierarchical processing in the primate cerebral cortex. *Cerebral cortex* **1**:1–47.

Glendenning K, Hall J, Diamond I, Hall W. 1975. The pulvinar nucleus of *galago senegalensis*. *Journal of Comparative Neurology* **161**:419–457.

Kaas J, Lyon D. 2007. Pulvinar contributions to the dorsal and ventral streams of visual processing in primates. *Brain Research Reviews* **55**:285–296.

Kaas J. 2015. Blindsight: Post-natal potential of a transient pulvinar pathway. *Current Biology* **25**:R155–R157.

Li K, Patel J, Purushothaman G, Marion R, Casagrande V. 2013. Retinotopic maps in the pulvinar of bush baby (otolemur garnettii). *Journal of Comparative Neurology* **521**:3432–3450.

Li K, Purushotham G, Mavity-Hudson J, Jiang Y, Yampolsky D, Casagrande V. 2014. Mechanisms of pulvinar control of the primary visual cortex (v1). In: Neuroscience meeting planner. Washington, DC: Society for Neuroscience.

Lin C, Kaas J. 1979. The inferior pulvinar complex in owl monkeys: Architectonic subdivisions and patterns of input from the superior colliculus and subdivisions of visual cortex. *Journal of Comparative Neurology* **187**:655–678.
Lin C, Kaas J. 1980. Projections from the medial nucleus of the inferior pulvinar complex to the middle temporal area of the visual cortex. *Neuroscience* **5**:2219–2228.
Logothetis N, Augath M, Murayama Y, Rauch A, Sultan F, Goense J, Oeltermann A, Merkle H. 2010. The effects of electrical microstimulation on cortical signal propagation. *Nature neuroscience* **13**:1283–1291.
Lyon D, Nassi J, Callaway E. 2010. A disynaptic relay from superior colliculus to dorsal stream visual cortex in macaque monkey. *Neuron* **65**:270–279.
Marion R, Li K, Mavity-Hudson J, Casagrande V. 2014. Morphological comparison of inputs to primate visual areas mT, v1 and v2. In: Neuroscience meeting planner. Washington, DC: Society for Neuroscience.
Marion R, Li K, Purushothaman G, Jiang Y, Casagrande V. 2013. Morphological and neurochemical comparisons between pulvinar and v1 projections to v2. *Journal of Comparative Neurology* **521**:813–832.
Movshon J, Newsome W. 1996. Visual response properties of striate cortical neurons projecting to area mT in macaque monkeys. *Journal of Neuroscience* **16**:7733–7741.
O'Brien B, Abel P, Olavarria J. 2001. The retinal input to calbindin-d28k-defined subdivisions in macaque inferior pulvinar. *Neuroscience Letters* **312**:145–148.
Petersen S, Robinson D, Keys W. 1985. Pulvinar nuclei of the behaving rhesus monkey: Visual responses and their modulation. *Journal of Neurophysiology* **54**:867–886.
Purushothaman G, Marion R, Li K, Casagrande V. 2012. Gating and control of primary visual cortex by pulvinar. *Nature Neuroscience* **15**:905–912.
Raczkowski D, Diamond I. 1981. Projections from the superior colliculus and the neocortex to the pulvinar nucleus in galago. *Journal of Comparative Neurology* **200**:231–254.
Rockland K. 1989. Bistratified distribution of terminal arbors of individual axons projecting from area v1 to middle temporal area (mT) in the macaque monkey. *Visual Neuroscience* **3**:155–170.
Rodman H, Gross C, Albright T. 1989. Afferent basis of visual response properties in area mT of the macaque. i. effects of striate cortex removal. *The Journal of neuroscience* **9**:2033–2050.
Rodman H, Gross C, Albright T. 1990. Afferent basis of visual response properties in area mT of the macaque. iI. effects of superior colliculus removal. *The Journal of neuroscience* **10**:1154–1164.
Rosa M, Tweedale R, Elston G. 2000. Visual responses of neurons in the middle temporal area of new world monkeys after lesions of striate cortex. *The Journal of Neuroscience* **20**:5552–5563.
Schmid M, Mrowka S, Turchi J, Saunders R, Wilke M. 2010. Blindsight depends on the lateral geniculate nucleus. *Nature* **466**:373–377.
Soares J, Diogo A, Fiorani M, Souza A, Gattass R. 2004. Effects of inactivation of the lateral pulvinar on response properties of second visual area cells in cebus monkeys. *Clinical and Experimental Pharmacology and Physiology* **31**:580–590.
Standage G, Benevento L. 1983. The organization of connections between the pulvinar and visual area mT in the macaque monkey. *Brain Research* **262**:288–294.
Stepniewska I, Kaas J. 1997. Architectonic subdivisions of the inferior pulvinar in new world and old world monkeys. *Visual Neuroscience* **14**:1043–1060.
Stepniewska I, Qi H, Kaas J. 2000. Projections of the superior colliculus to subdivisions of the inferior pulvinar in new world and old world monkeys. *Visual Neuroscience* **17**:529–549.
Ungerleider L, Galkin T, Desimone R, Gattass R. 2014. Subcortical projections of area v2 in the macaque. *Journal of Cognitive Neuroscience*.
Van Essen D, Maunsell J, Bixby J. 1981. The middle temporal visual area in the macaque: Myeloarchitecture, connections, functional properties and topographic organization. *Journal of Comparative Neurology* **199**:293–326.

CHAPTER 6

SUMMARY AND CONCLUSIONS

In the previous chapters we described the results of several studies on the organization of the pulvinar and its projections to V1 and MT. In this chapter, we provide a summary of these studies and discuss their broader implications when these results are considered together.

The structure of primate pulvinar

In chapter 3, we identified 3 subdivisions of PI that are likely analogous to macaque central PIcl, PIm and PIcm, based on stains for CO and AChE. Electrophysiologically, we found two retinotopic maps in the lateral pulvinar and studied their organization. We correlated the electrophysiologically identified maps with the chemoarchitectonically delineated subdivisions of the bush baby pulvinar, and the lateral retinotopic maps were found to occupy the same space as PL and PIcl. In chapter 5, we also electrophysiologically examined neurons in bush baby PIm and found a separate visual map without precise retinotopy. With these results we confirmed and extended the original chemoarchitectonic and connectional studies in bush baby pulvinar (Symonds and Kaas, 1978; Carey et al., 1979; Raczkowski and Diamond, 1981; Wong et al., 2009), and further elucidated the organization of its lateral and inferior subdivisions.

In our review of the macaque pulvinar literature described in chapter 2, we were able to document a consensus on the organization of macaque PLvl/PI where two retinotopic maps exist in ventral PL and PIcl, with a third and more medial map in PIm that has only coarse retinotopy. As discussed in chapter 3 and chapter 5, the electrophysiologically identified maps in PL, PIcl and PIm in bush baby are very similar to those described in macaque, both in terms of the spatial relationships between the maps and in the retinotopic organization of the individual maps, assuming that a geometric rotation of the pulvinar complex took place during the evolution of simians from prosimians. This spatial shift of pulvinar submodules between primate species is likely a result of the marked expansion of the pulvinar in macaque compared to bush baby pulvinar. In chapter 3 we also suggested that the currently available data on cebus pulvinar retinotopy can be interpreted to delineate two retinotopic maps with an organization very similar to those described in both macaque and bush baby pulvinar. Therefore, all 3 branches of the primate family (prosimian, New World and Old World) appear to share a common pattern of ventrolateral pulvinar organization.

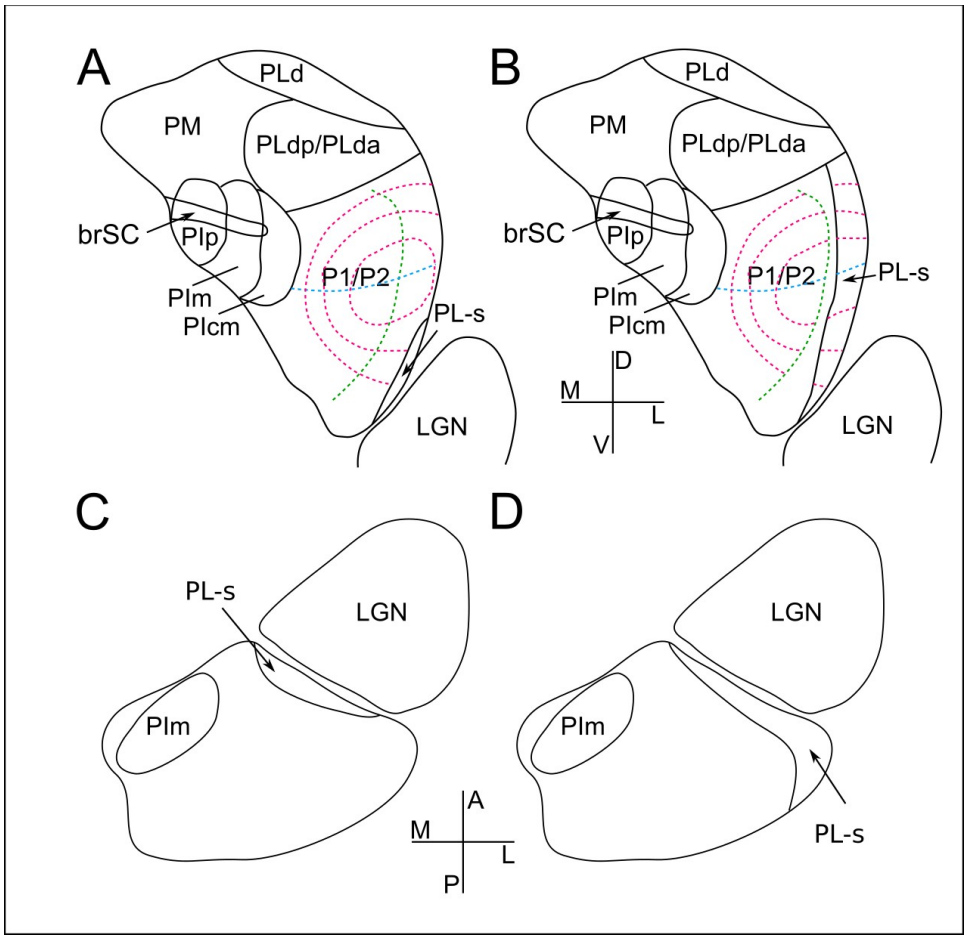

Figure 25: Comparisons of two interpretations of the parcellation of lateral pulvinar

The diagrams show coronal views in panels **A** and **B**, and horizontal views in panels **C** and **D**. **A, C**: The "small PL-s" scheme. PL-s is only on the anterior-ventral edge of the pulvinar. **B, D**: The "large PL-s" scheme. The lateral shell region extends dorsally and posteriorly compared to the small version, and features a retinotopic map on its lateral surface. It is unclear what retinotopic organization exists between the P1 map and PL-s. In one case Bender (1981) identified a border between the lateral and ventral map (Bender, 1981 Figure 8) that correlates with the medial border of the large version of PL-s (Gutierrez et al., 1995 Figure 4); these borders do not coincide at different anterior-posterior levels, however.

There are, however, some species differences in the detailed organization of pulvinar maps, as briefly mentioned in chapter 3, and here we provide some further discussion. One difference is the split HM representation reported for the macaque inferior map (or P2) (Bender, 1981), which was not found in our examination of the bush baby pulvinar. Bender (1981) observed that instead of sitting in the vicinity of each other, pulvinar neurons representing the part of visual field just above and below the horizontal meridian outside of the central 3 degrees of the visual field sit on the ventral and dorsal half of the lateral P2 map surface in macaque. The existence of a lateral shell region located in ventral PL (PL-s) that borders LGN and has connections with MT (as we discussed in chapter 2), is consistent with this organization of P2. The small version of PL-s only covers the anterior-ventral surface of the pulvinar, allowing P2 to extend to the lateral pulvinar surface elsewhere (See Figure 25A, C)(Shipp, 2001). Anterograde tracer injections in V1 and in V2 have sometimes been reported to reveal projection sites only as a lateral shell in PLvl (Ogren and Hendrickson, 1976; Wong-Riley, 1977). These shell-like projection zones could result from the cortical injections in these studies that cover the paracentral HM representation in V1 or V2, as a split-HM P2 map would represent the paracentral HM on its lateral surface. There exists an alternative interpretation, however, of these observations on the macaque lateral pulvinar surface. Some investigators refer to a subdivision roughly in the same area as PL-s but larger and covering the posterolateral surface of the pulvinar (named PIl or PIl-s, see Figure 25B, D) (Cusick et al., 1993; Gutierrez et al., 1995; Gutierrez and Cusick, 1997). The larger version of PL-s would occupy a large part of the lateral map as identified by Bender (1981), and would behave similarly to a retinotopic map with split HM if PL-s has a full retinotopic representation of the contralateral visual field on its lateral surface, with a ventral upper field representation and a dorsal lower field representation. This alternative interpretation assuming the larger version of PL-s, would consider the shell-like projection zones to be the result of denser V1/V2 projections to PL-s compared to their projections to P2 (Gutierrez and Cusick, 1997). Due to the difficulty in sampling in such a small area for extracellular recordings, we expect that future connection studies with rigorous reconstruction of V1/V2/MT projections to ventral PL will help us evaluate the 2 proposals for this lateral shell region: 1) a restricted PL-s area bordering LGN and including the peripheral visual representation of P2, or 2) a larger version of PL-s that extends posteriorly to wrap around P2 plus a P2 that has a visual field representation on its lateral surface.

According to Shipp (2003), the lateral retinotopic maps of P1 and P2 in macaque pulvinar have submodules, and the maps can be divided into slabs perpendicular to the iso-representation axis that runs from its anterolateral end to its posteromedial end, with each slab having a full contralateral visual field representation. In this scheme, the more anterolateral slabs would connect with early visual cortical areas, and the more posteromedial slabs would connect with higher order cortical areas in the ventral visual stream (Shipp, 2003). The projection zones of cortical areas in the P1/P2 maps then would partially overlap with each other, and these overlap regions would then allow one submodule to connect to multiple cortical areas and mediate thalamic relays between them (Shipp, 2003). In chapter, 3 we discussed how our findings in the bush baby pulvinar do not support such a structure for this primate, and how the difference between the shapes of the iso-representation curves between bush baby and macaque pulvinar may reflect a simpler organization in bush baby pulvinar. There is a further implication of this specific retinotopic map organization in the bush baby pulvinar. The maps that do not allow submodules also limit the types of visual information that can be provided to the cortex. The macaque P1/P2 involved in the model of Shipp (2003) have connections with V1, V2, MT and all of the ventral visual stream areas. Not all combinations of these cortical areas, however, are strongly connected. V4 and inferior temporal areas, for example, share the strongest connections only with their respective neighboring cortical areas (Felleman and Van Essen, 1991). By having multiple submodules in the P1/P2 maps, and having each submodule connect only to some of these cortical areas, this organization would allow the relay of visual information at different stages of processing or refinement between small sets of cortical areas. For example, the most anterior portion of P1/P2 connects only V1 and V2 (Shipp, 2001), and could relay simple edge detection results from V1 to V2. In contrast, the more posterior portion of P1/P2 that

connects P4, TEO and TE (Shipp, 2001) could relay simple shape information between these ventral visual stream areas. The bush baby P1/P2 maps cannot be divided into similar submodules yet are connected with a similarly large set of cortical areas (Glendenning et al., 1975; Raczkowski and Diamond, 1981). A direct result of this organization is that cells relaying between different combinations of cortical areas, and cells relaying different types of information would be spatially mixed. One also would expect less variety in the types of information provided by the bush baby maps, compared to the combined variety provided by multiple submodules inside the macaque P1/P2 maps. Since cortico-pulvinar projections have diffuse axons (Rockland, 1998), without spatial segregation P1/P2 cells are more likely to receive input from a large set of cortical areas, reflecting a higher level of integration. These facts suggest that the visual processing in prosimian P1/P2 maps may require the input from many visual cortical areas, while the messages it provides to these multiple cortical areas would be similar. In comparison, each submodule of the macaque P1/P2 receives only from a few cortical areas, and pulvinar-cortical inputs to different cortical areas are from different submodules that could potentially carry out different types of computation in parallel. The different submodules also could provide different types of visual information to different cortical targets.

Pulvinar modulation of the cortex

In chapter 4 we examined the distribution, morphology and targets of the pulvinar projections to V1, in an attempt to find the anatomical basis of the strong control of pulvinar on V1 output cells (Purushothaman et al., 2012). We found that projections from the lateral pulvinar maps (P1/P2) end mostly in layer 1 of V1, with very few axonal endings in layers 2/3 just below the main projection site in layer 1. These axons make *en passant* boutons that are smaller than either LGN to V1 boutons or pulvinar to V2 boutons, which are considered to be responsible for feedforward driving pathways. The pulvinar axons in V1 layer 1 were found to only synapse with non-GABAergic dendrites, most likely the apical dendrites of layers 2/3 and layer 5 pyramidal neurons in V1. These results ruled out the possibility of pulvinar projections having typical features of feedforward driving projections, which usually arrive in cortical layers 3/4 and have larger boutons. Another possible mechanism for strong pulvinar control, the inhibition of large interneuron networks that heavily suppress the layers 2/3 output neurons, either through inhibitory glutamatergic receptors, or through a second layer of interneurons, was also ruled out. Given these conclusions, a high level of synchronization appears to be necessary for pulvinar projections to V1 to effectively trigger responses in V1 pyramidal neurons, either through dendritic action potentials, or some other means.

Most pulvinar cells that project to V1 also project to V2 at least in macaque (Kennedy and Bullier, 1985). Despite the large differences in layer distributions of pulvinar axons in V1 and V2, it appears that the same axons provide the projection terminations in layer 1 and layers 3/4 in both V1 and V2 (Marion et al., 2013, 2014). With this connection pattern, regardless of how many types of pulvinar neurons provide projections to V1 and V2, each type of neuron would provide similar signals to V1 and V2 but have a different impact on the local cortical circuits in these two cortical areas due to the different axon morphologies and local connections. Although this connection pattern appears similar to that of the corticothalamic collaterals of layer 5 corticofugal neurons that send out motor commands, both V1 and V2 are early sensory areas and it is hard to imagine a need for pulvinar-cortical collaterals that serve feedback control purposes. A more likely functional reason of these duplicated projections is the synchronization between V1 and V2, or more broadly, the priming of V1 to V2 projections so they can interact effectively with pulvinar to V2 projections. The idea that the pulvinar works as an oscillator that synchronizes cortical interactions has been proposed by many investigators (Steriade, 1997; Shipp, 2003), and has been partially confirmed for pulvinar projections to V4 and TEO, two ventral visual stream areas (Saalmann et al., 2012). The collaterals of the pulvinar-cortical projections that go to V1 could modulate the V1 output so V1 to V2 projections would have certain features adapted to fit those of pulvinar to V2

projections. In the case of the pulvinar serving as a simple oscillating clock, the two projections into V2 could have the same carrying frequency and phase because of the modulation by pulvinar collaterals to V1 layer 1. Other signal modulations could be carried out in the same way as the synchronization of oscillating clocks (Shipp, 2004; also see the "short term memory" in Crick and Koch, 1990). For example, a spatially focused enhancement of V1 output, which could serve as a mechanism for spatial attention, would ensure that the pulvinar output and V1 output refer to the same spatial target, and their interactions in higher order cortical areas that receive both inputs then would make sense. This potential functional role is consistent with the fact that projections to these different cortical areas arise from the same neurons but the axonal arbors take different forms. That is because one of the pathways (e.g., the pulvinar projections to V1) would only need to send synchronizing signals and not the actual visual information, and would not need the elaborate and specific connections seen in the pulvinar projections to the other cortical areas (e.g., V2).

In chapter 5 we compared the neuron activity in the output layer of MT when the pulvinar was at different pharmacologically manipulated states. When V1 was not manipulated, increasing pulvinar activity by injecting glutamate increased both spontaneous and visually evoked activity in MT, but did not affect them differentially. After blocking V1 with muscimol, a potent $GABA_a$ agonist, increasing pulvinar activity reduced activity in MT, both spontaneous and visually evoked. These results indicate that the excitatory impact of pulvinar on MT relayed by V1 outweighs the impact of the direct pulvinar projections to MT, and the direct pulvinar projections to MT have an inhibitory effect if triggered with unstructured pharmacological activation. This inhibitory effect with glutamate activation of the pulvinar could reflect either an inhibitory pathway, or an excitatory pathway that is able to recruit inhibitory cortical circuits and behaves in an inhibitory manner given unstructured activation (see Logothetis et al., 2010). The impact of pulvinar on MT, including both the excitatory effect relayed by V1, and the inhibitory effect of the direct pulvinar projection, appear to function in an approximately linear fashion. There are two aspects of this linear impact: the pulvinar input to MT and the V1 input to MT are not combined in a supralinear fashion that would selectively enhance visual responses over spontaneous activity; and the increased pulvinar input is not able to saturate V1 output neurons responsible for relaying this excitatory effect.

Strength and Diversity

The pulvinar projections to V1 and to MT represent the two main types of pulvinar-cortical projections. These two types of projections arise from different regions of the primate pulvinar, V1 projections from the ventral lateral maps (P1/P2), and MT projections from PIm. The sources of these projections in the pulvinar have different types of organization at the level of the pulvinar: 1) the PLvl and PIcl maps have precise retinotopy, while 2) the PIm map has a mixture of two cell populations with different coarse retinotopic organizations (see chapter 5). Since both V1 and MT have a single well organized retinotopic representation of the visual field (Xu et al., 2004, 2005), we expect both projections from P1 to V1 and from P2 to V1 should have a smooth one-to-one mapping, while the projections from PIm to MT would map the mixed retinotopy in PIm to the retinotopically organized but coarse map in MT (Xu et al., 2004). The laminar distribution of the terminals from these pulvinar subdivisions in the cortex also differ, with pulvinar to MT projections having a similar layer distribution as pulvinar to V2 projections. Both projections strongly modulate the activity in their target cortical areas. In V1 we reported a differential increase of visually evoked responses after pulvinar activation (Purushothaman et al., 2012), which is different from the type of activation we observed in MT. That difference, however, might be the explained by the different ways we pharmacologically activated pulvinar. In the previous report (Purushothaman et al., 2012), we used bicuculline to increase the activity in the pulvinar, which may combine supralinearly with the activity in pulvinar, differentially increasing visually evoked responses. The observation we made in V1 after pulvinar activation did not necessarily require a

supralinear combination between pulvinar input and geniculate input to V1. Our observation that pulvinar activation did not differentially increase MT visual responses when the major effect was relayed through V1 also supports the idea that pulvinar input has an approximately linear effect on both V1 and MT.

There are likely other types of pulvinar-cortical projections, one of which being the pulvinar projections to V2. Although the pulvinar projections to V2 have the same laminar distribution and bouton sizes as those of the pulvinar projections to MT, pulvinar projections to V2 are distinct from those to MT since they share the same origin and retinotopic organization as the pulvinar projections to V1 (Marion et al., 2013, 2014). Furthermore, although the pulvinar projections to MT and V2 both appear to have characteristics of driving connections, there is a key difference between them in relation to how they compare to the other cortical inputs to their respective target areas. In both areas the pulvinar input and V1 input have the same layer distributions [Marion et al. (2013); Marion et al. (2014); also see chapter 5], but in MT the V1 projections have focused terminal clusters and large boutons (Anderson et al., 1998), while in V2 the V1 projections feature smaller boutons compared to the pulvinar input (Marion et al., 2013). It is not yet clear whether the pulvinar projections to V2 bear different functional relevance compared to the pulvinar projections to MT, as there has only been one ambiguous report to date that observed both excited and suppressed neurons in V2 after pulvinar inactivation (Soares et al., 2004). The pulvinar projections to V1 appear to be unique, but we expect that more instances of the other two types of pulvinar-cortical projections will be found from other pulvinar subdivisions to other cortical visual areas.

Pulvinar's modulation of the cortex is an essential component of the visual processing in the primate brain. The exploration of the pathways, information coding, and computations involved has generated very interesting results, but also will require great continued effort in the future. This thesis represents but a few tiny first steps in this grand journey. We started with the visual pulvinar subdivisions that occupy the earliest levels of the visual hierarchy, P1/P2 and PIm (see chapter 2), and explored their projections to the earliest visual cortical areas, V1 and MT. At least two different types of pulvinar-cortical projections were examined, and although with vastly different anatomical features, both types showed strong regulation of visual information in the cortex. More pulvinar subdivisions and their projections to more cortical targets, however, should be examined in the future. Will pulvinar projections to higher order visual areas continue to show strong regulation of their cortical targets? What kind of projections will higher order pulvinar subdivisions, such as the dorsal posterior lateral pulvinar, or even some portion of the medial pulvinar, have on their cortical targets? Some cortical areas receive projections from multiple pulvinar subdivision (i.e.: P1/P2, P3 and PLdp all project to V4, PL-s and PIm both project to MT). How do these projections differ, how do they interact, and what distinguishes them functionally? In our studies we only tested the impact of the pulvinar in the context of cortical responses to simple visual stimuli. This choice was constrained, in part, by our lack of understanding of the full range of pulvinar neurons' visual response properties, as well as our inability to provide structured manipulation of pulvinar activity. With a better understanding of visual response properties in the various subdivisions of the primate pulvinar, in the future we should be able to design structured manipulation schemes of the pulvinar and other inputs to cortical target areas to better probe the complex interactions occurring in the cortex, and reveal how the pulvinar input functions to alter the cortical responses to different features of visual stimuli. Overall, we expect that future studies of the functional role played by pulvinar-cortical projections will bring more interesting insights to the field of visual neuroscience.

References

Anderson J, Binzegger T, Martin K, Rockland K. 1998. The connection from cortical area v1 to v5: A light and electron microscopic study. *The Journal of neuroscience* **18**:10525–10540.

Bender D. 1981. Retinotopic organization of macaque pulvinar. *Journal of Neurophysiology* **46**:672–693.

Carey R, Fitzpatrick D, Diamond I. 1979. Layer i of striate cortex of *tupaia glis* and *galago senegalensis*: Projections from thalamus and claustrum revealed by retrograde transport of horseradish peroxidase. *Journal of Comparative Neurology* **186**:393–437.

Crick F, Koch C. 1990. Towards a neurobiological theory of consciousness. In: Seminars in the neurosciences. Vol. 2. Saunders Scientific Publications.

Cusick C, Scripter J, Darensbourg J, Weber J. 1993. Chemoarchitectonic subdivisions of the visual pulvinar in monkeys and their connectional relations with the middle temporal and rostral dorsolateral visual areas, mT and dLr. *Journal of Comparative Neurology* **336**:1–30.

Felleman D, Van Essen D. 1991. Distributed hierarchical processing in the primate cerebral cortex. *Cerebral cortex* **1**:1–47.

Glendenning K, Hall J, Diamond I, Hall W. 1975. The pulvinar nucleus of *galago senegalensis*. *Journal of Comparative Neurology* **161**:419–457.

Gutierrez C, Cusick C. 1997. Area v1 in macaque monkeys projects to multiple histochemically defined subdivisions of the inferior pulvinar complex. *Brain Research* **765**:349–356.

Gutierrez C, Yaun A, Cusick C. 1995. Neurochemical subdivisions of the inferior pulvinar in macaque monkeys. *Journal of Comparative Neurology* **363**:545–562.

Kennedy H, Bullier J. 1985. A double-labeling investigation of the afferent connectivity to cortical areas v1 and v2 of the macaque monkey. *Journal of Neuroscience* **5**:2815–2830.

Logothetis N, Augath M, Murayama Y, Rauch A, Sultan F, Goense J, Oeltermann A, Merkle H. 2010. The effects of electrical microstimulation on cortical signal propagation. *Nature neuroscience* **13**:1283–1291.

Marion R, Li K, Mavity-Hudson J, Casagrande V. 2014. Morphological comparison of inputs to primate visual areas mT, v1 and v2. In: Neuroscience meeting planner. Washington, DC: Society for Neuroscience.

Marion R, Li K, Purushothaman G, Jiang Y, Casagrande V. 2013. Morphological and neurochemical comparisons between pulvinar and v1 projections to v2. *Journal of Comparative Neurology* **521**:813–832.

Ogren M, Hendrickson A. 1976. Pathways between striate cortex and subcortical regions in *macaca mulatta* and *saimiri sciureus*: Evidence for a reciprocal pulvinar connection. *Experimental Neurology* **53**:780–800.

Purushothaman G, Marion R, Li K, Casagrande V. 2012. Gating and control of primary visual cortex by pulvinar. *Nature Neuroscience* **15**:905–912.

Raczkowski D, Diamond I. 1981. Projections from the superior colliculus and the neocortex to the pulvinar nucleus in galago. *Journal of Comparative Neurology* **200**:231–254.

Rockland K. 1998. Convergence and branching patterns of round, type 2 corticopulvinar axons. *Journal of Comparative Neurology* **390**:515–536.

Saalmann Y, Pinsk M, Wang L, Li X, Kastner S. 2012. The pulvinar regulates information transmission between cortical areas based on attention demands. *Science* **337**:753–756.

Shipp S. 2001. Corticopulvinar connections of areas v5, v4, and v3 in the macaque monkey: A dual model of retinal and cortical topographies. *Journal of Comparative Neurology* **439**:469–490.

Shipp S. 2003. The functional logic of cortico-pulvinar connections. *Philosophical Transactions of the Royal Society of London. Series B, Biological Sciences* **358**:1605–1624.

Shipp S. 2004. The brain circuitry of attention. *Trends in Cognitive Sciences* **8**:223–230.

Soares J, Diogo A, Fiorani M, Souza A, Gattass R. 2004. Effects of inactivation of the lateral pulvinar on response properties of second visual area cells in cebus monkeys. *Clinical and Experimental Pharmacology and Physiology* **31**:580–590.

Steriade M. 1997. Synchronized activities of coupled oscillators in the cerebral cortex and thalamus at different levels of vigilance. *Cerebral Cortex* **7**:583–604.

Symonds L, Kaas J. 1978. Connections of striate cortex in the prosimian, *galago senegalensis*. *Journal of Comparative Neurology* **181**:477–511.

Wong P, Collins C, Baldwin M, Kaas J. 2009. Cortical connections of the visual pulvinar complex in prosimian galagos (*otolemur garnettii*). *Journal of Comparative Neurology* **517**:493–511.
Wong-Riley M. 1977. Connections between the pulvinar nucleus and the prestriate cortex in the squirrel monkey as revealed by peroxidase histochemistry and autoradiography. *Brain research* **134**:249–267.
Xu X, Bosking W, White L, Fitzpatrick D, Casagrande V. 2005. Functional organization of visual cortex in the prosimian bush baby revealed by optical imaging of intrinsic signals. *Journal of neurophysiology* **94**:2748–2762.
Xu X, Collins C, Kaskan P, Khaytin I, Kaas J, Casagrande V. 2004. Optical imaging of visually evoked responses in prosimian primates reveals conserved features of the middle temporal visual area. *Proceedings of the National Academy of Sciences* **101**:2566–2571.